

N75-14796



**Calspan**

STUDY OF THE DETAIL CONTENT OF  
APOLLO ORBITAL PHOTOGRAPHY

Submitted by: Robert E. Kinzly

Calspan Report No. YB-5224-M-1


Prepared For:  
HEADQUARTERS  
NATIONAL AERONAUTICS AND SPACE  
ADMINISTRATION  
WASHINGTON, D.C.

15 AUGUST 1974  
CONTRACT NO. NASW-2434  
FINAL REPORT

Prepared By:

  
R.E. Kinzly, Head  
Electro-Optical Systems Section

Approved By:

  
A.D. O'Connor, Head  
Systems Research Department

## ABSTRACT

This final report documents the results achieved during a study of the Detail Content of Apollo Orbital Photography under contract NASW-2434 with NASA Headquarters. This study spanned an 18 month period and was composed of three tasks whose objectives were to assess the effect of anomalous V/H (Velocity to Height ratio) sensor operation or photoreproduction processes upon the detail content of lunar surface photography obtained from the orbiting Command Module. This report includes data and conclusions obtained from the Apollo 15, 16 and 17 missions.

The specific tasks undertaken included (1) an evaluation of the residual motion smear in Apollo 15 panoramic photography due to intermittent V/H sensor operation and (2) intercomparison of the detail content of multiple generations of Apollo 16 and 17 photography.

During the Apollo 15 mission the panoramic camera V/H sensor did not operate properly and resulted in anomalously high or pre-set nominal command V/H rates. In some cases a transition between the anomalous rate and the nominal rate occurred during the exposure of a frame. Two such frames (316 and 360) were examined to determine the subsequent effect on the detail content. The evaluation showed that a loss in resolution due to image motion blur and exposure differences within a frame could occur due to the intermittent V/H sensor operation. The lack of correct compensation reduced the resolution by 1/3 (to about 6 meters on the lunar surface). Only when the commanded V/H is equal to the nominal value can the full resolution potential of the panoramic camera be realized; but this may not always occur. Consequently it is concluded that a significant portion of the Apollo 15 panoramic imagery may have lower resolution than the nominal 2 meter value. The user of this imagery should refer to the telemetry data to determine the V/H command situation for the frames he is exploiting and account for the effects of poor resolution if necessary.

An assessment of the detail content of multiple generations of Apollo 16 and 17 photography was made to determine the degradation, if any, in the quality of the photographic products furnished to various users. The original flight film is copied to produce a Master Positive (2P) or Direct Negative (2N) copy. These are the earliest generations which the user may exploit and only a limited number of such copies are produced. Most investigators are likely to use 3rd Generation or 4th Generation Positive copies. Unfortunately 3P and 4P copies of the same type of photography were not available thus preventing a direct comparison of the most likely user products. The evaluation showed that the tone quality of the Master Positive is superior to that of the Direct Negative for the panoramic photography. This superiority results from a greater dynamic range which means that the 2P photography contains higher contrast images over a wider range of average exposure levels than the 2N photography. The data indicates that this difference is preserved in the higher generation products which the user is likely to employ. Tonal quality differences were also present in 2nd Generation copies of metric photography, however, it is not clear that these differences are preserved in the user products. MTF measurements were made in order to compare the fine detail content of the various generations of photography evaluated. Approximately half of these frames showed some loss in fine detail content which is attributed to the reproduction process. An increase in the ground resolution element by a factor of 1.5 was observed; 3 meters for the panoramic photography and 30 meters for the metric photography.

This study successfully demonstrated the development and application of image evaluation methods for orbital photography of the lunar surface. Descriptions of the various elements of software used in this study are included in this report. It is recommended that the development of these techniques be continued for application to future manned and unmanned spacecraft involved in planetary exploration.

## FOREWORD

The research reported herein is the result of a series of tasks performed over an 18 month period under Contract Number NASW-2434 with NASA Headquarters and monitored by Mr. Leon Kosofsky (Code: MAL).

The author is grateful to Mr. Kenneth Hancock of the NASA Johnson Space Center and Mr. Daniel Kinsler of the Lunar Science Institute for furnishing the Apollo orbital photography needed to perform the study. The telemetry data used in the evaluation of the Apollo 15 panoramic photography was obtained from Mr. Bernard Moleburg of the NASA Johnson Space Center while other auxiliary data were obtained from the microfilm files at the Lunar Science Institute. Contributions by others at Calspan Corporation include Mr. Timothy Gallagher who performed the microdensitometry required for the evaluation of the Apollo 16 and 17 photography and Mr. Larry Perletz for assistance in the microdensitometry and analysis associated with the evaluation of the Apollo 15 photography.

## TABLE OF CONTENTS

<u>Section</u>		<u>Page</u>
	ABSTRACT . . . . .	iii
	FOREWORD . . . . .	v
1	INTRODUCTION . . . . .	1
2	EVALUATION TECHNIQUES . . . . .	3
	2.1 Frame Selection . . . . .	4
	2.2 Calculating the MTF from Edges . . . . .	4
	2.3 Tone Quality Evaluation Methods . . . . .	10
3	EVALUATION OF APOLLO 15 PANORAMIC CAMERA V/H ANOMALY .	13
	3.1 Residual Blur Estimation . . . . .	16
	3.2 Modulation Transfer Function Estimation . . . . .	30
4	COMPARISON AMONG MULTIPLE GENERATIONS OF APOLLO 16 AND 17 PHOTOGRAPHY . . . . .	34
	4.1 Product Tonal Quality . . . . .	34
	4.2 Fine Detail Content . . . . .	43
5	CONCLUSIONS . . . . .	49
	REFERENCES . . . . .	51
Appendix	SOFTWARE DESCRIPTIONS . . . . .	53

## LIST OF FIGURES

<u>Figure No.</u>		<u>Page</u>
1	APOLLO ORBITAL PHOTOGRAPHY REPRODUCTION SEQUENCE . . . . .	2
2	DATA FLOW FOR MTF DETERMINATION FROM EDGE TRACES . . . . .	6
3	MACRO FLOW DIAGRAM FOR EGSA MAIN PROGRAM . . . . .	7
4	EFFECT OF D-LOG E RESPONSE CURVE UPON OBJECT CONTRAST AND TONE QUALITY . . . . .	10
5	TYPICAL APOLLO 15 PANORAMIC PHOTOGRAPHS WITH V/H ANOMAL- IES . . . . .	14
6	STRIP CHART RECORDS OF TELEMETRY DATA . . . . .	15
7	PAN PHOTO GEOMETRY . . . . .	18
8	ERRORS RESULTING FROM ASSUMPTION OF A FLAT LUNAR SURFACE	21
9	MEASURED AND EXPECTED MTF's FOR APOLLO 15 FRAME 316 WITH V/H ANOMALY . . . . .	31
10	MEASURED AND EXPECTED MTF's FOR APOLLO 15 FRAME 360 WITH V/H ANOMALY . . . . .	32
11	SENSITOMETRIC CALIBRATION - APOLLO 16 PANORAMIC PHOTO- GRAPHY . . . . .	36
12	SENSITOMETRIC CALIBRATION - APOLLO 17 PANORAMIC PHOTO- GRAPHY . . . . .	37
13	SENSITOMETRIC CALIBRATION - APOLLO 17 METRIC PHOTOGRAPHY	38
14	GAIN FOR LOW AND MID-CONTRAST OBJECTS - APOLLO 16 2nd GENERATION PANORAMIC PHOTOGRAPHY . . . . .	39
15	GAIN FOR LOW AND MID-CONTRAST OBJECTS - APOLLO 17 2nd GENERATION PANORAMIC PHOTOGRAPHY . . . . .	40
16	GAIN FOR LOW AND MID-CONTRAST OBJECTS - APOLLO 17 2nd GENERATION METRIC PHOTOGRAPHY . . . . .	41
17	MODULATION TRANSFER FUNCTIONS - APOLLO 17 METRIC PHOTOGRAPHY . . . . .	45

<u>Figure No.</u>		<u>Page</u>
18	MODULATION TRANSFER FUNCTIONS - APOLLO 17 PANORAMIC PHOTOGRAPHY . . . . .	47
19	MODULATION TRANSFER FUNCTIONS - APOLLO 16 PANORAMIC PHOTOGRAPHY . . . . .	48
20	SOURCE AND CROSS REFERENCE LISTINGS FOR MAIN PROGRAM DTAPE . . . . .	54
21	TYPICAL DTAPE PROGRAM INPUT DATA SET . . . . .	57
22	SOURCE AND CROSS REFERENCE LISTINGS FOR EXPOS FUNCTION SUBPROGRAM (3 pages) . . . . .	60
23	SOURCE AND CROSS REFERENCE LISTINGS FOR MAIN PROGRAM EGSA (12 pages) . . . . .	64
24	TYPICAL EGSA PROGRAM INPUT DATA CARD . . . . .	78
25	EXAMPLE OF INDIVIDUAL FUNCTION PLOTS FROM THE EGSA PROGRAM . . . . .	80
26	EXAMPLE OF AN AVERAGE MTF PLOT FROM THE EGSA PROGRAM . . . . .	81
27	SOURCE AND CROSS REFERENCE LISTINGS FOR SUBROUTINE CONVLV (4 pages) . . . . .	83
28	SOURCE AND CROSS REFERENCE LISTINGS FOR SUBROUTINE FORINV (4 pages) . . . . .	90
29	SOURCE AND CROSS REFERENCE LISTINGS FOR SUBROUTINE FOURTR (4 pages) . . . . .	97
30	SOURCE AND CROSS REFERENCE LISTINGS FOR MAIN PROGRAM TONEQ (4 pages) . . . . .	105
31	TYPICAL TONEQ PROGRAM INPUT DATA SET . . . . .	110
32	EXAMPLE OF TONEQ PROGRAM PRINTED OUTPUT . . . . .	112

LIST OF TABLES

<u>Table No.</u>		<u>Page</u>
1	APOLLO FRAMES SELECTED AND ANALYZED . . . . .	4
2	OBJECT CONTRASTS USED IN TONE QUALITY EVALUATIONS . . . . .	12
3	NUMERICAL VALUES USED TO COMPUTE UNCOMPENSATED ANGULAR BLUR RATE . . . . .	22
4	NUMERICAL VALUES USED TO ESTIMATE EXPOSURE TIMES . . . . .	26
5	EXPOSURE TIME ESTIMATES . . . . .	27
6	RESIDUAL IMAGE BLUR . . . . .	28
7	TONE QUALITY COMPARISON (Low and Mid Contrast Objects) . . . . .	42
8	TONE QUALITY COMPARISON (High Contrast Objects) . . . . .	43
9	EDGE DATA COLLECTED AND PROPOSED FOR APOLLO 16 AND 17 PHOTOGRAPHY . . . . .	44



## 1. INTRODUCTION

This final report documents the results achieved during a study of the Detail Content of Apollo Orbital Photography under Contract NASW-2434 with NASA Headquarters. This study was composed of three tasks whose objectives were to assess the effect of a V/H anomaly or photo reproduction process upon the detail content of lunar surface photography obtained from the orbiting Command Module. The report includes results from the photo evaluation of the Apollo 15, 16 and 17 missions. An earlier report<sup>(1)</sup> presented the results of a similar study of photography from the Apollo 8, 12, 14 and 15 missions. This report also contains a detailed description of the Edge Gradient Spectral Analyses (EGSA) computer program that was employed extensively during these studies.

The specific tasks completed include (1) an evaluation of the residual motion smear in several Apollo 15 panoramic photographs due to intermittent V/H sensor operation and (2) intercomparison of the detail content of multiple generations of Apollo 16 and 17 photography.

Before proceeding we will briefly review the photography obtained during these Apollo missions and its reproduction sequence. In all these missions the Scientific Instrument Module (SIM) Bay contained two cameras; an Optical Bar Panoramic Camera and a Mapping (or Metric) Camera. The Panoramic Camera had a 610 mm (24 inch) focal length lens and employed EK Type 3414 film yielding an approximate resolution capability of 130 cycles/mm. The Mapping Camera had a 76 mm (3 inch) focal length lens and employed EK Type 3400 film. Its resolution capability was about 90 cycles/mm. Both cameras contained internal image motion compensation (IMC) mechanisms. The effect of erratic operation of the Apollo 15 panoramic IMC was assessed in the study.

The original flight film is reproduced for distribution to potential users. Figure 1 shows the reproduction sequence and terminology used. The

flight film is copied to produce a Second Generation or Master Positive (2P) copy. Only a limited number of such copies are generated. They are subsequently copied twice to produce a Fourth Generation (4P) copy which many investigators are likely to use. The flight film is also copied on to reversal film to obtain a Second Generation Direct (2N) Negative. This is copied once to produce a Third Generation (3P) Positive which is also available to investigators. This sequence eliminates one copy step in the hope of improving product quality and reducing production time. An assessment was made of the effect of both reproduction sequences on the detail content of Apollo 16 and 17 photography.

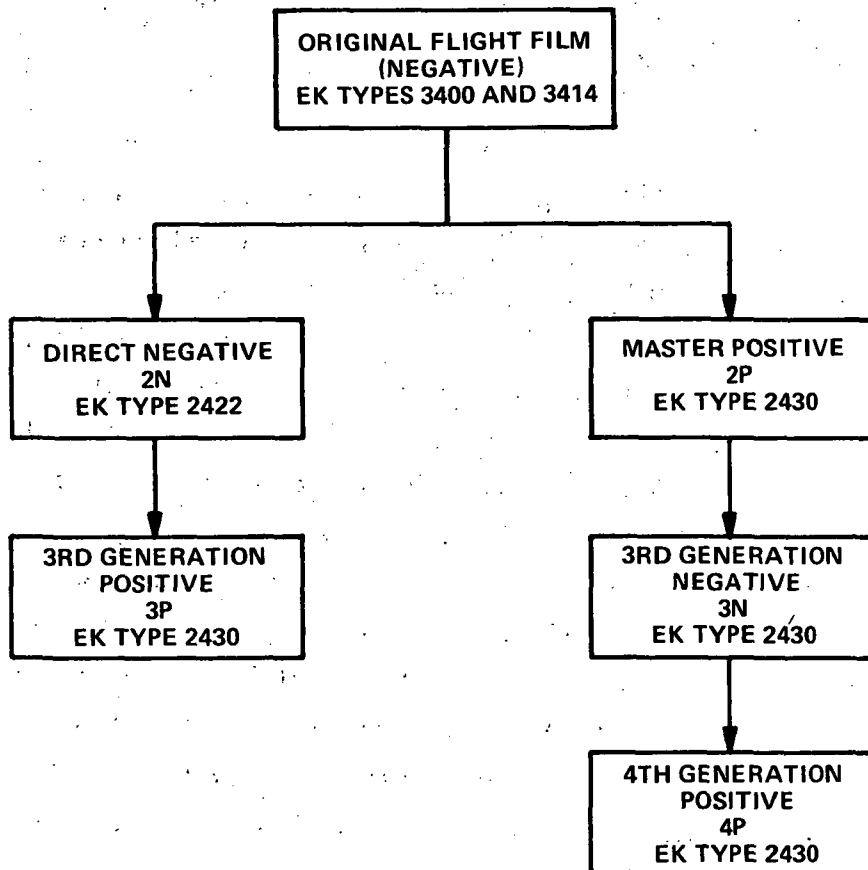


Figure 1 APOLLO ORBITAL PHOTOGRAPHY REPRODUCTION SEQUENCE

## 2. EVALUATION TECHNIQUES

All of the methods used in this study to evaluate the Apollo orbital photography were developed during previous contracted studies for NASA and others. These methods are briefly described in this section of the report. In some cases complex computer programs are required. Their operation is discussed and the software detailed in the appendix.

The evaluation of the quality of Apollo Orbital photography can require the measurement of various properties of the imagery. The properties which define image quality can be divided into four general categories: (1) "resolution" or fine detail content, (2) contrast or tone quality, (3) noise level and (4) metric quality. Overall performance can be based upon a composite measure which includes several (or all) of the categories but must be determined with the intended use of the imagery in mind.

The modulation transfer function (MTF) is often used as a measure of image resolution or fine detail content. In this study we used this image quality measure to determine the image blur resulting from erratic operation of the Apollo 15 panoramic camera IMC and to evaluate the nominal resolution in multiple generations of Apollo 16 and 17 metric and panoramic photography.

Contrast or tonal quality can be described as the fluctuation in density due to large area intensity differences in the scene (i.e. low frequency brightness variations). Such fluctuations are frequently used to classify areas or delineate regional boundaries. The most common measure of tonal quality is the Hurter-Driffield or D-Log E response curve. It describes how the apparent scene brightness is reproduced as density in the photograph. The D-Log E response curve was measured for each generation of Apollo 16 and 17 imagery evaluated to assess the effect of the reproduction sequence on tonal quality or large scale detail content.

2.1 Frame Selection - In selecting the frames to be analyzed the primary consideration is the availability of test targets for estimating the MTF. A shadow-to-sunlight edge inside craters will occur in the low sun angle photography. If the sun angle is too high this edge either does not exist or is too close to the rim of the crater to be useful. Similarly at extremely low sun angles the edge will be sufficiently close to the far rim of the crater to make edge analyses impractical. Sun elevation angles between 10° to 15° yield the most satisfactory shadow-to-sunlight edge. Table 1 indicates the frames analyzed during the study.

**Table 1**  
**APOLLO FRAMES SELECTED AND ANALYZED**

MISSION NO.	CAMERA	FRAME NO.	GENERATIONS ANALYZED	OBJECTIVE
15	PANORAMIC	316	4P	V/H ANOMALY
		360	4P	
16	PANORAMIC	4127	2P, 2N, 3P	REPRODUCTION EVALUATION
		5460	2P, 2N, 3P	
17	PANORAMIC	1633	2P, 2N, 3P	
		3111	2P, 2N, 3P	
	MAPPING	180	2P, 2N, 4P	
		2923	2P, 2N, 4P	

2.2 Calculating the MTF from Edges. It is common practice to use edges to calculate the MTF of an optical imaging system both in the laboratory and operationally. The MTF can be calculated using any target by dividing the measured image spectrum by the known spectrum of the object. In the case of an edge gradient analysis no correction for the target is necessary. The derivative of a sharp edge (i.e. gradient) is a narrow pulse (Dirac delta function) whose Fourier transform or spectrum is a constant proportional to the peak-to-peak amplitude of the edge. In selecting the edge for analysis we only require that it be much sharper than the degradation introduced by the optical system being evaluated. In the present case the shadow-to-sunlight edge sharpness is determined by the penumbra effect produced by the finite angular size of the sun. This effect is proportional to the diameter of the

crater. To insure sufficient sharpness we selected craters about 10 resolution elements wide (about 80 microns on panoramic imagery).

The edges are scanned using a microdensitometer and recorded on a strip chart or magnetic tape. The edge sharpness requirement produces targets that are short and curved. Consequently the microdensitometer scanning aperture must be small in both dimensions. If the edges were long, a long but narrow slit could be used to minimize the noise in the edge trace. Since this is not possible the density traces on the strip chart were hand-smoothed and digitized using a Calma digitizer. The data flow is summarized in Figure 2. A special software package, not shown in the figure, supports the Calma to generate a card deck containing the edge traces. The Edge Gradient Spectral Analyses (EGSA) software package shown in the figure consists of two major programs. The initial program reads the digitized density trace, converts it to exposure (illuminance trace) and writes an output tape for subsequent processing by the EGSA program itself. The latter is composed of a main program and several subprograms whose linkage is shown in the macro-flow diagram in Figure 3. In the discussion below we identify the purpose of each of these programs while detailed information is presented in the appendix. This was included in this report for those readers who may be interested in evaluating the detail content of other NASA imagery.

The first major step in the EGSA main program is the input of user data on punched cards in format 2F10.0, 7A4, F10.0. The following variables or arrays are specified for each data set to be processed:

- FINV - spatial frequency interval desired for output OTF data in cycles/mm
- FMAX - maximum spatial frequency of output OTF data in cycles/mm
- OPTION (7) - alpha-numeric array identifying the types of output data desired by user
- FCO - cutoff spatial frequency in cycles/mm used in smoothing the line spread

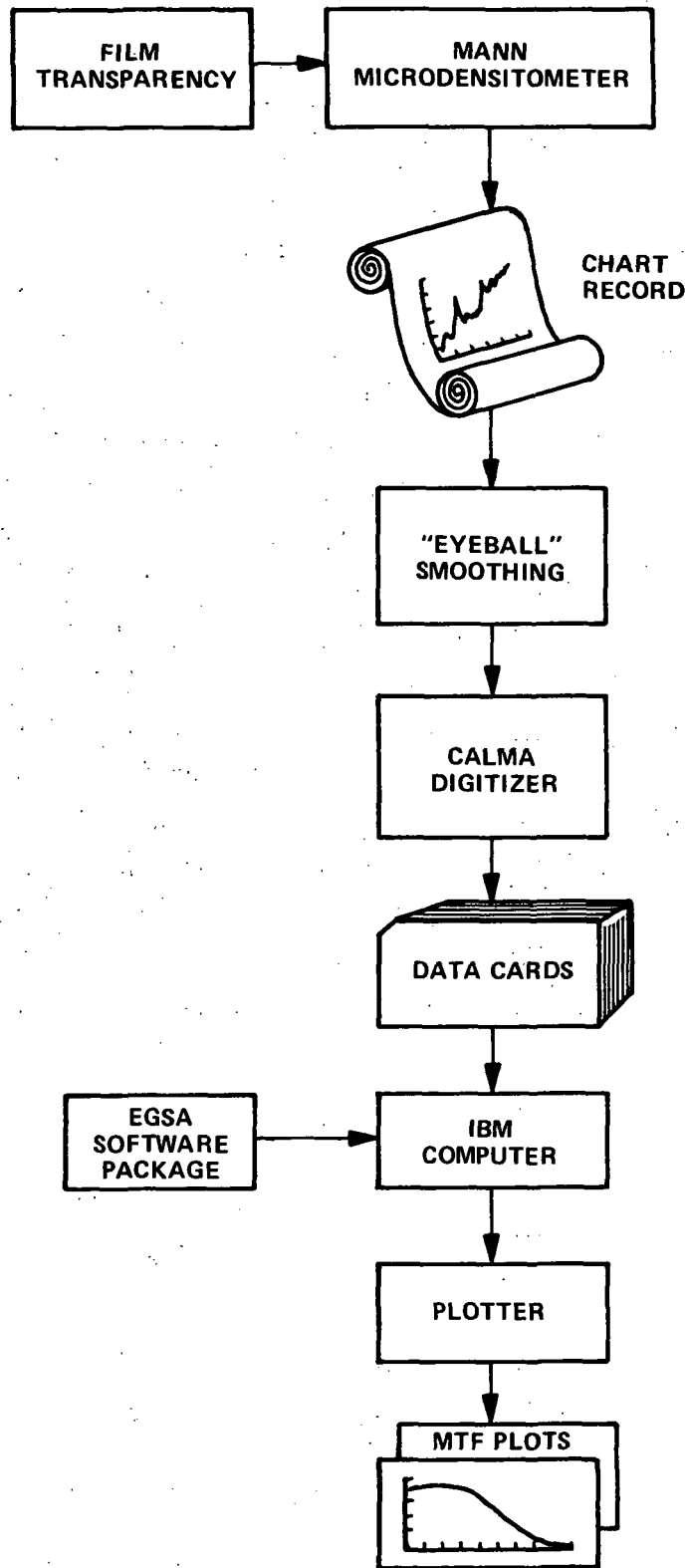


Figure 2 DATA FLOW FOR MTF DETERMINATION FROM EDGE TRACES

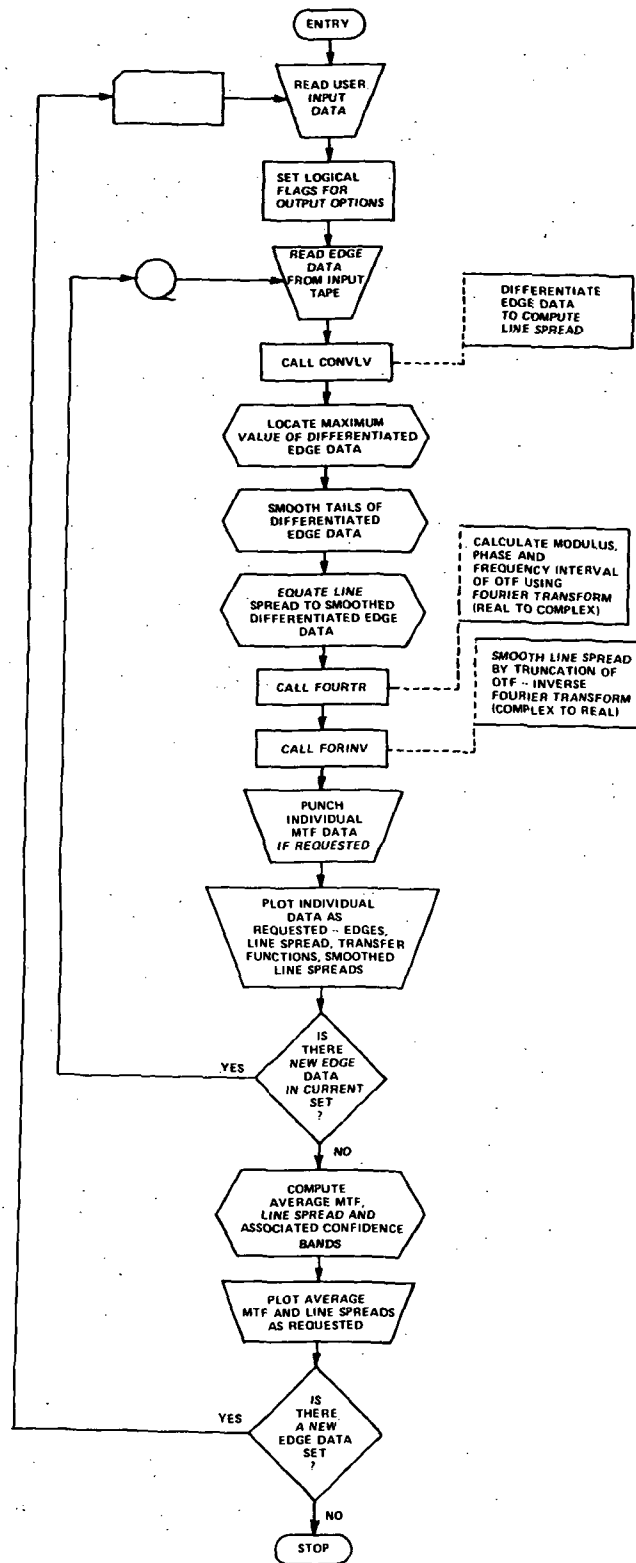


Figure 3 MACRO FLOW DIAGRAM FOR EGSA MAIN PROGRAM

The edge data is read from an unformatted input data tape and differentiated by Subroutine CONVLV. A special Fourier transform algorithm is employed in Subroutine FOURTR to compute the modulus (MTF) and phase of the Optical Transfer Function (OTF). If requested by the user as an option a smoothed Line Spread is computed using truncation of the OTF at frequency "FCO." The remainder of the main program provides plotted, printed or punched card output data depending upon the options identified by the user. The options available include: plots of the individual edge data, line spreads, smoothed line spreads and transfer functions (MTF only); plots of the average line spreads and MTF; and punched values of the individual and average MTFs.

Provision is made for processing multiple edge data sets under multiple options. The input data tape is read until a null record is encountered indicating the end of the current data set. The output requirements are then completed for that edge data set. The input data tape is read a second time for the next edge data set. If one exists it is processed under the same user specified data and options as the previous set. If a second null record is encountered, however, the program recycles to read new user input data. If no input is provided execution is terminated. For a single edge data set the null records may be deleted and execution will be terminated by the same sequence of operations through recognition of the end of identified files on the data tape and the main stream input.

In order to exercise the EGSA main program sixteen subprograms are required in addition to the standard FORTRAN I/O subprogram. Four of these programs are user supplied and their listings are included in the Appendix. CONVLV performs the convolution between two input functions or an input function and an internally specified function. These include an 11-point smoothing function and an 11-point differentiating function. DXSCAL computes the increment or scale factor (inches/point) for the x-axes of the individual function plots (edges, line spreads and smoothed line spreads). FORINV performs an inverse Fourier transform based upon a special algorithms for



transforming a complex function, inputed as modulus and phase, to a real output functions (i.e. OTF to Line Spread). FOURTR performs a Fourier transform of a real inputed function providing a complex output function as modulus and phase (i.e. Line Spread to OTF). The restrictions on the type of functions permits the use time saving algorithms in both FORINV and FOURTR without restricting the number of points in the input function as the more popular Fast Fourier Transform (FFT) algorithms does.

Ten of the required subprograms are part of the Calspan Corporation Program Library; all but one are used to generate graphic output. AXIS draws an axis with tick marks at one inch intervals, annotates the value of the variable at each of these marks, and provides an identification label. CLEAR fills each byte of a specified block of storage with zeros. This operation could be accomplished, less efficiently, by a sequence of do loops in the EGSA program. EFLOT is used to close the plot output file after all plot output is completed. LINE actually causes a plot to be drawn, consisting of line segments connecting specified data point coordinates expressed in inches through two data arrays. MGRID provides a grid of variable dimensions and interval size in the X and Y directions independently. NUMBER converts a floating point number and draws the resulting alphanumeric characters on a plot. In the EGSA program it is used to place identification data and scale factors on the output plots. PLOT is a basic plotting routine used to control pen position. In the EGSA program it is used to reset the plotter origin. PLOTTER is used to specify the plotting instrument, lined or unlined paper and the type and color of pen desired. SCALE scan the elements in a data array to find maximum and minimum values, computes a optimum scale value based upon plot dimensions (inches) and then changes the array values to corresponding "plotter inches." SYMBOL draws selected symbols or special special characters on a plot. In the EGSA program it is used to title some of the plots.

The remaining two subprograms are IBM supplied FORTRAN IV LIBRARY Subprograms. AMAX1 locates the largest value in an array of real variables. SQRT is a mathematical function that computes the square root of a real argument.

Listings of the first group of subprograms are included in the appendix. The subprograms in the remaining two groups are not included since the user is likely to have access to the same or equivalent programs within his computing facility. The appendix also includes examples of the user supplied input data cards, description of the record sequence for the unformatted input data tape and examples of the output data generated.

2.3 Tone Quality Evaluation Methods - Tone quality is related to density differences of large objects in an image. As the object area decreases in size the OTF reduces the density differences achieved between the object and background. Tone quality is expressed by the net D-Log E response curve which determines the density difference between a large object and the background as illustrated by the sketch in Figure 4. If we assume that apparent scene

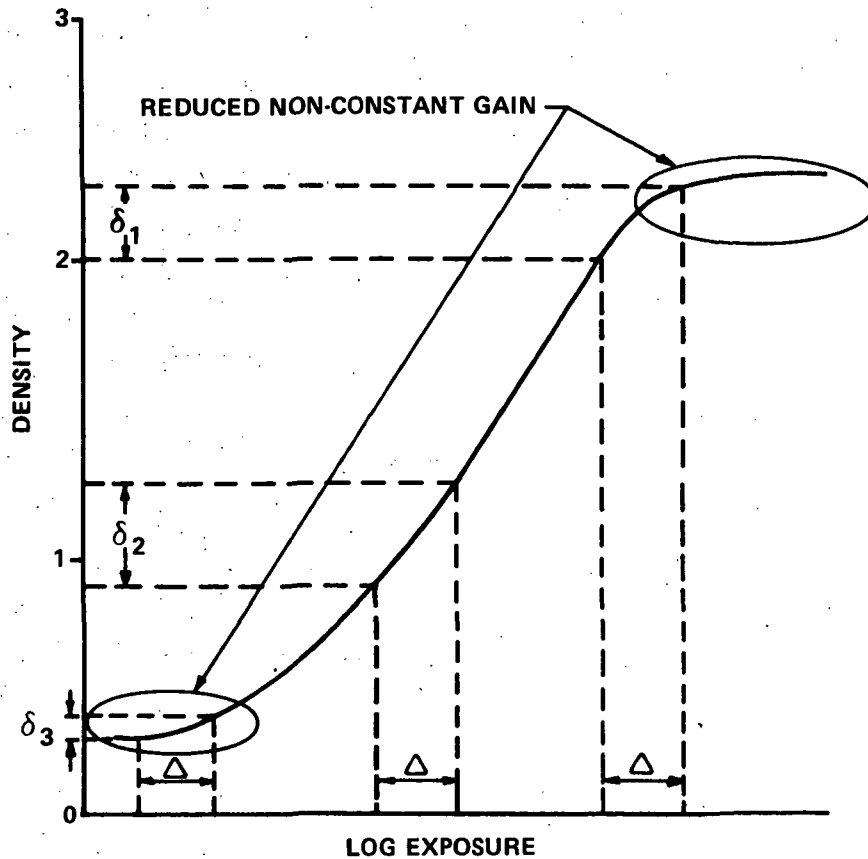


Figure 4 EFFECT OF D-LOG E RESPONSE CURVE UPON OBJECT CONTRAST AND TONE QUALITY

brightness is such that the difference in log exposure between the object and background is

$$\Delta \equiv \log \frac{E_o}{E_B} \quad (1)$$

then the average exposure level ( $= \frac{E_o + E_B}{2}$ ) influences the density difference. This average exposure level includes the camera parameters (f-number, shutter speed, lens transmission, etc.) as well as the exposure settings used to copy the original film. If the level is too high or too low the density difference (i.e.  $\delta_1$  or  $\delta_3$  indicated in the Figure) is less than  $\delta_2$  achieved by exploiting the middle portion of the D-Log E response curve. This portion is nearly linear and is customarily represented by a straight line equation, namely

$$D = \gamma \log E + k \quad (2)$$

where  $\gamma$  is the net film gamma and represents a constant gain between log exposure and density. At the higher and lower exposure levels the response curve departs from linearity; the gain is reduced and no longer is constant.

Differences in log exposure,  $\Delta$ , can be related to object contrast,

$$C = \frac{E_o - E_B}{E_B} \quad (3)$$

namely,

$$\Delta = \log(C+1) \quad (4)$$

and the resulting density difference,  $\delta$ , in the constant gain portion of the curve determined by using Eqs. (2) and (4);

$$\delta = \gamma \Delta = \gamma \log(C+1) \quad (5)$$

The ability of the eye to detect an object is approximately proportional to its density difference. In this case the density difference depends only on

the object contrast and the net film gain. In the non-constant gain regions the density difference is reduced and also depends upon the exposure levels. Therefore an appropriate measure of tone quality is the gain achieved as a function of object contrast and average exposure level, namely

$$\tau(C, E_A) = \delta(C, E_A) / \Delta \quad (6)$$

This quality parameter was calculated in this study using a spline interpolation between the measured step wedge densities (sensitometric calibration). The reader should be made aware that the step wedge densities and resulting response curve can depend upon the type of instrument used in measurement. In general macro-densities measured by a densitometer (such as a MacBeth Model TD102) are not always equal to micro-densities measured by a microdensitometer. The first instrument measures "diffuse" density while the latter generally measures "specular" density. The data in this study were obtained using a microdensitometer and our tone quality evaluation is more appropriate to the use of magnifications (i.e. microscope) when viewing the image rather than unaided viewing.

Calculations of gain factors, Eq. (6), were made at three levels of object/background contrast indicated in Table 2. The high contrast object would represent shadow/sunlight boundaries in Apollo imagery; the mid-contrast, albedo variations associated with bright rays; while the low contrast represents albedo changes caused by 1% reflectance variation about a 10% background reflectance.

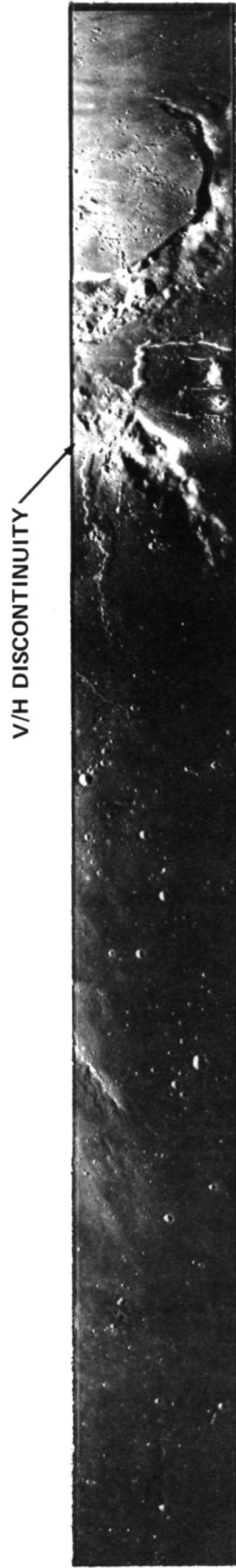
**Table 2**  
**OBJECT CONTRASTS USED IN TONE QUALITY EVALUATION**

CONTRAST LEVEL	$E_o/E_B$	C	$\Delta$	TYPICAL LUNAR OBJECT
HIGH	6:1	5.0	0.778	SUNLIGHT/SHADOW BOUNDARY
MID	1.3:1	0.30	0.114	BRIGHT RAY
LOW	1.1:1	0.10	0.041	1% ALBEDO CHANGE

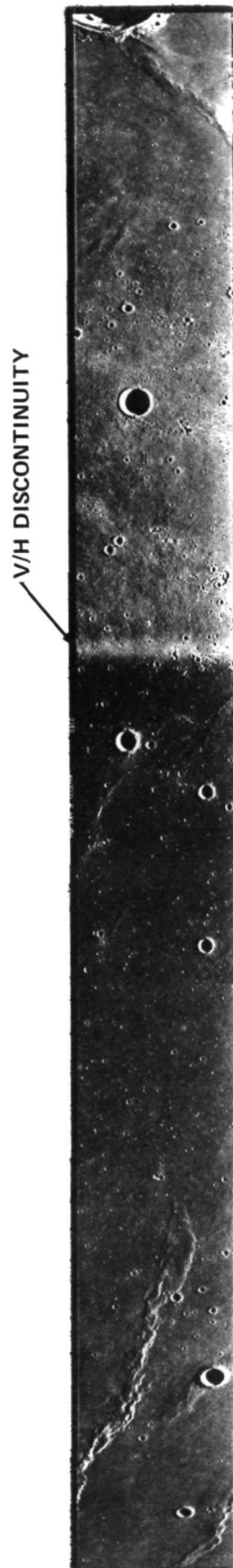
### 3. EVALUATION OF APOLLO 15 PANORAMIC CAMERA V/H ANOMALY

The Panoramic Camera flown on several Apollo missions was a modified Itek KA-80A camera. During operation its lens system is rotated about the velocity axis of the Command Module at a rate related to the apparent ground speed. When a photograph was taken a capping shutter opened while the lens scanned a  $108^\circ$  arc below the spacecraft producing a frame about 45 inches long. A variable width slit located next to the film acted as a scanning shutter. Its velocity (scanning rate) and width determined the instantaneous exposure time. Image motion compensation (IMC) is provided by a complex electro-mechanical subsystem. Forward motion is compensated by a gimbal that rocks a lens group to stabilize the image. A V/H (velocity/height) sensor measures the apparent ground motion to determine the rate of rocking needed. This sensor also controls the speed of lens system rotation and consequently the rate of film advance which is perpendicular to the flight direction. A second sensor, an exposure meter, measures the brightness of the lunar scene which is combined with the V/H data to control the width of the scanning slit.

During the Apollo 15 mission intermittent operation of the V/H sensor produced an anomaly in a number of the panoramic photographs. One of the tasks undertaken was to assess the effect of these anomalies on the detail content. In the photographs examined they resulted in (1) a loss of resolution due to image blur from uncompensated motion and (2) exposure differences within the frame. The latter effect is clearly visible in Figure 5 which shows Frames 316 and 360 evaluated in this task. These frames were taken at low sun elevation angle and selected to provide shadow-to-sunlight edges for evaluation. The exposure differences are thought to be a direct consequence of the low sun angle. Telemetry data shows that the camera exposure meter estimated the average lunar surface brightness to be about 200 foot-Lamberts for Frame 316 and less than 100 foot-Lamberts for Frame 360. In both cases the telemetry data reproduced in Figure 6(c) shows that the focal plane or scanning slit remained at maximum width (0.3 inches) during the complete exposure of both frames due to the low surface brightness. Thus the abrupt change in the V/H rate



(a) FRAME 316



(b) FRAME 360

Figure 5 TYPICAL APOLLO 15 PANORAMIC PHOTOGRAPHS WITH V/H ANOMALIES

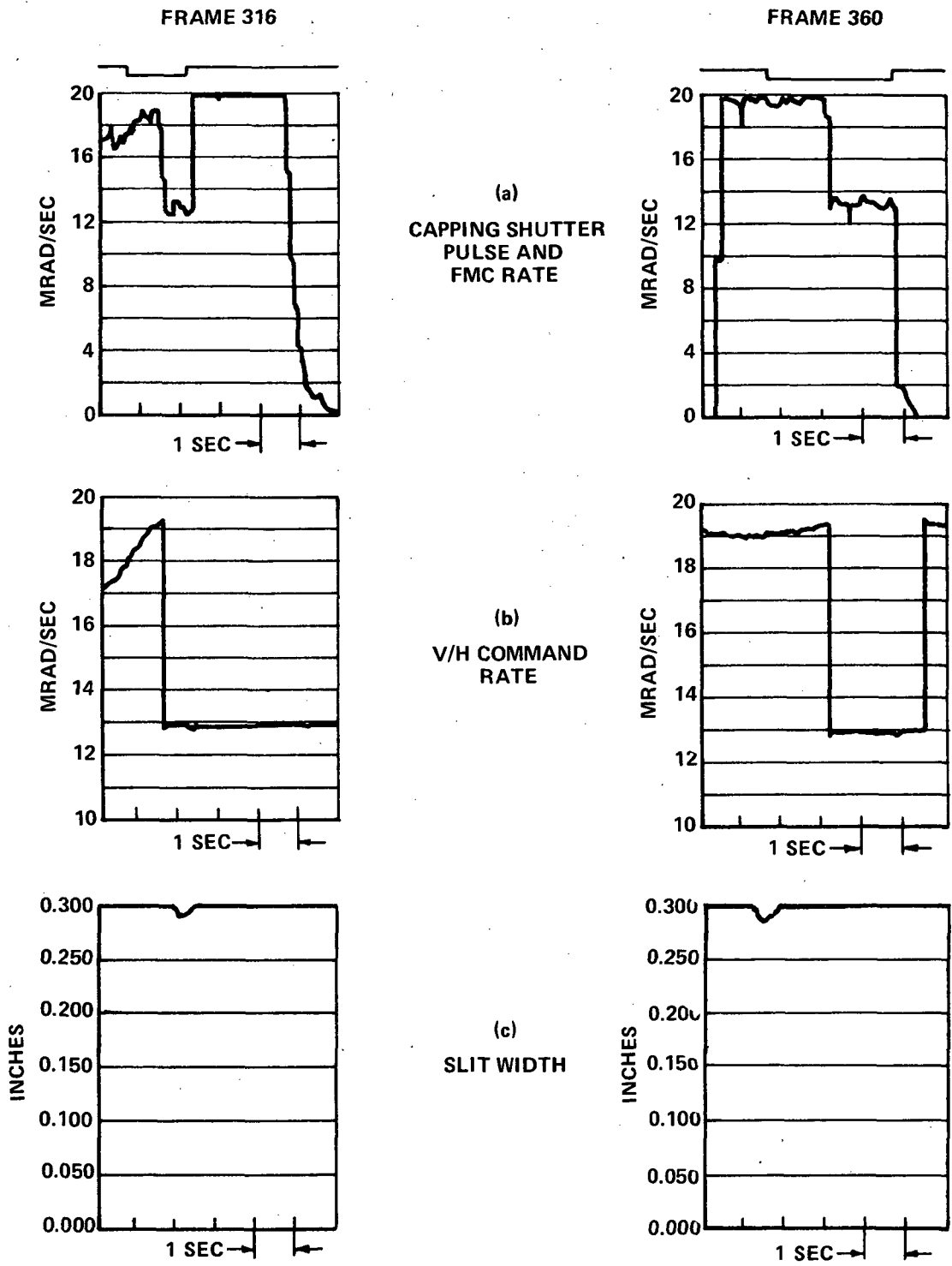


Figure 6 STRIP CHART RECORDS OF TELEMETRY DATA

indicated in 6(b) produced a corresponding change in lens rotation and the velocity of the slit relative to the film without a compensating change in slit width. This resulted in the exposure differences. In frames taken at higher sun angles or brighter lunar surfaces the slit width could be adjusted permitting reduction or elimination of these exposure changes.

The abrupt change in the commanded V/H rate was produced by the V/H sensor signal "going into" or "coming out of" saturation. When the signal exceeded 19.5 mrad/sec (established as the maximum rate that could be encountered in the Apollo missions) the commanded V/H rate was automatically reset to 13.0 mrad/sec (a nominal value) producing the abrupt changes shown in Figure 6(b). When these changes occurred while the capping shutter was open, Figure 6(a), the detail content of the photography was reduced.

To estimate the amount of residual motion blur produced by this V/H rate anomaly, microdensitometer traces were made of the shadow-to-sunlight edges on both sides of the abrupt change in commanded V/H rate. From the telemetry data presented in Figure 6 we see that the V/H sensor signal reached the saturation value and the V/H command was set to the nominal value for both of the frames evaluated. The first portion of Frame 316 is dark and has a commanded V/H rate varying from 17.6 to 19.3 mrad/sec and the latter portion is light with a V/H rate of 13.0 mrad/sec. Similar conditions exist for Frame 360 except that the commanded V/H rate is nearly constant equal to 19.2 mrad/sec in the dark portion of the frame. None of the commanded V/H rates resulted in full compensation of the image motion. The residual blur was measured using the EGSA program and also calculated directly from telemetry and auxiliary data. The results of both of these estimates are compared in this section.

3.1 Residual Blur Estimation - Telemetry and auxiliary data was used to estimate the residual blur in both the dark and light portions of each of the frames evaluated. This was achieved by calculating the difference between the uncompensated angular blur and the amount of compensation provided. In performing these calculations, estimates of the angular blur rates and



exposure times were made using the available data sources and measurements of the photographs themselves. We discuss the calculations of the uncompensated angular blur rate, the compensation rate, the exposure time and the residual blur separately in the subsections below.

3.1.1 Uncompensated Angular Blur Rate - In order to compute the angular blur rate due to the velocity of the Command Module provision must be made for the curvature of the lunar surface. In a previous study<sup>(1)</sup> expressions for the angular blur near the principal point in vertical and forward or aft oblique photography were developed. The expression for the ground blur at the lunar surface is

$$B_G = \frac{Vt_e}{1 + h/r_m} \quad (7)$$

where  $V$  is the velocity of the Command Module,  $t_e$  is the exposure time,  $h$  is the altitude of the Command Module and  $r_m$  is the nominal lunar radius (= 1738.1 kilometers). As the altitude decreases, this expression is asymptotic to the more familiar expression in which the blur is proportional to the product of the platform velocity and the exposure time. For Apollo orbital photography, the reduction in the blur due to the interaction of the Command Module altitude and the lunar surface curvature is approximately 6%.

In our earlier study, all assessments were made near the principal point in each photograph and the theoretical expressions developed are only valid under these conditions. In order to evaluate the Apollo 15 V/H nominally, our assessments had to be made away from the principal point in order to evaluate the MTF and residual blur on both sides of the V/H anomaly. Figure 7 shows a sketch where a point in a forward oblique pan photograph is under evaluation. The point is specified by a pitch angle,  $\phi$ , and a roll angle,  $w$ . In general the pitch angle would be the sum of the camera pitch angle plus an additional term due to the location of the point across the width of the photograph. In the present case however, all assessments were made near the optical axis ground track where the additional term is negligible. The pitch

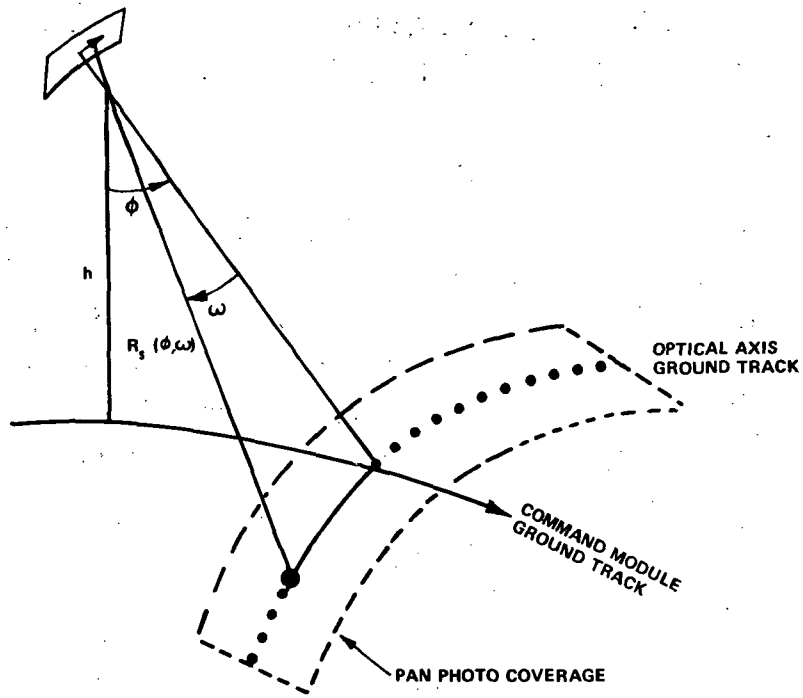


Figure 7 PAN PHOTO GEOMETRY

angle will result in a decrease in the apparent ground blur due to foreshortening as discussed below. The roll angle, on the other hand, being perpendicular to the Command Module **ground track** does not produce any foreshortening effects, however, the ground blur distance will be decreased from that expressed by Eq. (7) due to the fact that the point under assessment is away from the principal point by an amount expressed through the roll angle. For a vertical photograph an additional reduction factor,  $\cos \theta$ , must be included in Eq. (7) so that

$$B_G = \frac{Vt_e \cos \theta}{1 + h/r_m} \quad (8a)$$

where

$$\theta = \sin^{-1} \left[ \frac{R_s \sin \omega}{r_m} \right] \quad (8b)$$

and  $R_s$  is the slant range from the Command Module to the point under evaluation. The altitude of the Command Module is sufficiently small

compared to the lunar radius in this case so that this reduction factor is negligible in vertical panoramic photography. For oblique photography, the pitch and roll angles interact producing a more complicated expression for the reduction factor, however, its effect remains negligible.

The next step is the computation of the apparent ground blur by including the effects of foreshortening on the actual ground blur given by Eq. (7). Both the roll and the pitch angle can contribute to the foreshortening effect through the tilt angle given by

$$\cos t = \cos \phi \cos w \quad (9)$$

When the pitch angle is zero, however, the roll angle produces no foreshortening effect since all of the ground blur is perpendicular to the line of sight. The foreshortening factor,  $\cos \phi$ , was included in the expressions presented in our previous study. In the presence of a roll angle the foreshortening factor is  $\cos t$  as presented by Eq. (9). However, this factor should only be applied to the portion of the blur in the viewing direction. This requires knowledge of the azimuth angle between the direction of flight and the direction of tilt. Kawachi<sup>(3)</sup> presents the required transformation equations permitting us to write the apparent blur as

$$B_A = \frac{Vt_e (\sin^2 \alpha + \cos^2 \alpha \cos^2 t)^{1/2}}{1 + h/r_m} \quad (10a)$$

where the azimuth angle,  $\alpha$ , is given by,

$$\alpha = \tan^{-1} \left[ \frac{\sin w}{\tan \phi} \right] \quad (10b)$$

For the values of roll angles which we are considering, however, this expression can be approximated by the original on-axis equation, namely

$$B_A \approx \frac{Vt_e \cos \phi}{1 + h/r_m} \quad (10c)$$

This expression is a valid approximation because of two opposing effects; although the foreshortening factor is smaller, i.e.  $\cos t$  compared to  $\cos \phi$ , it is only applied to a smaller portion of the actual ground blur. These two facts compensate for each other, allowing the foreshortening effect to be approximated by  $\cos \phi$  with an error less than 0.1%.

The foreshortening effects, including the geometrical equations developed by Kawachi, assume a flat planetary surface. As a result of this assumption, the apparent ground blur will be slightly overestimated. Figure 8a shows the percentage error by which the blur is overestimated for two representative Command Module altitudes. For the present case, the error is less than 0.5% since the pitch angle will be either  $0^\circ$  or  $12.5^\circ$  determined by the mode of camera operation.

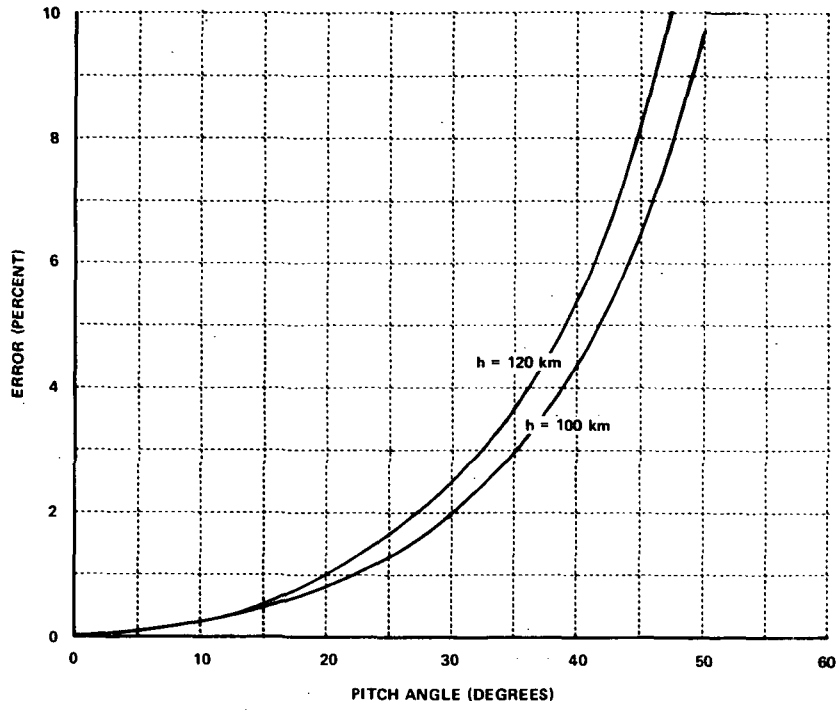
The next step in the calculation of the uncompensated angular blur rate is the conversion of the apparent ground blur to an apparent angular blur by the use of the slant range from the Command Module to the ground point under evaluation. In our earlier study, the expression for slant range employed was

$$R_s \approx \frac{h}{\cos t} \quad (11)$$

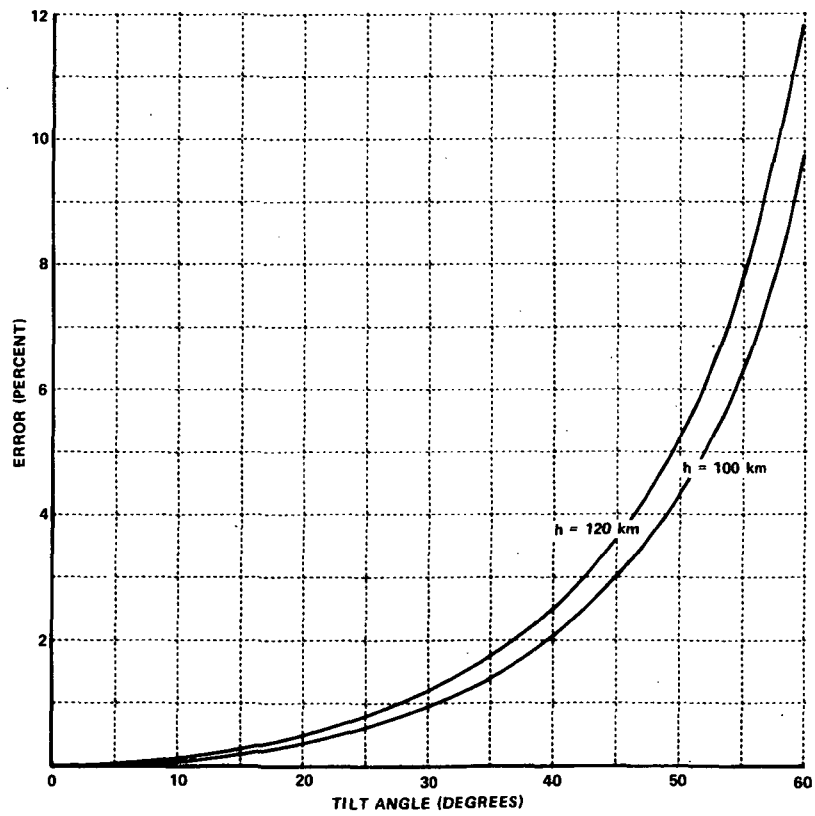
which is based upon the assumption of a flat planetary surface. The actual slant range is larger due to the curvature of the lunar surface and is given by

$$R_s = (h + r_m) \cos t - \left[ r_m^2 - (h + r_m)^2 \sin^2 t \right]^{1/2} \quad (12)$$

Figure 8b shows the error produced in the estimation of slant range by assuming a flat lunar surface. The net effect of the assumption is to overestimate the angular blur similar to the effect on foreshortening. In this case, however, errors on the order of 1% are expected since tilt angles can become as high as  $30^\circ$ . Finally, the uncompensated angular blur rate is determined by taking the apparent ground blur of Eq. (10c) and dividing by the slant



(a) FORESHORTENING EFFECT ERROR



(b) SLANT RANGE ERROR

Figure 8 ERRORS RESULTING FROM THE ASSUMPTION OF A FLAT LUNAR SURFACE

range expressed by Eq. (12) and the exposure time,  $t_e$ . The uncompensated angular blur rate,  $\dot{\beta}$ , is

$$\dot{\beta} = \frac{V \cos \phi}{(1+h/r_m) \left\{ (h+r_m) \cos t - \left[ r_m^2 - (h+r_m)^2 \sin^2 t \right]^{1/2} \right\}} \quad (13)$$

This expression was employed with the numerical values shown in Table 3 to calculate the blur rate for both the dark and light portions of the frames under evaluation. The values of the Command Module velocity and altitude and the pitch angle were obtained from auxillary data furnished by Mr. K. Hancock at the NASA Johnson Space Center. The roll angles were estimated by measuring the distance of the dark and light evaluation regions from the center of the frame which is directly proportional to the roll angle. The tilt angles are subsequently calculated from Eq. (9).

**Table 3**  
**NUMERICAL VALUES USED TO COMPUTE**  
**UNCOMPENSATED ANGULAR BLUR RATE**

VARIABLE	SYMBOL	VALUES	
		FRAME #316	FRAME #360
CM VELOCITY	V	1.6279 km/sec	1.6305 km/sec
CM ALTITUDE	h	109.22 km	106.14 km
LUNAR RADIUS	$r_m$	1738.1 km	1738.1 km
PITCH ANGLE	$\phi$	12.45°	0
ROLL ANGLES	$w_D$	20.4°	6.0°
	$w_L$	25.2°	10.8°
TILT ANGLES	$t_D$	23.8°	6.0°
	$t_L$	27.9°	10.8°

The following values resulted; Frame 316

$$\begin{aligned} \dot{\beta}_D &= 12.45 \text{ mrad/sec} \\ \dot{\beta}_L &= 11.99 \text{ mrad/sec} \end{aligned} \quad (14a)$$

and for Frame 360

$$\begin{aligned}\dot{\beta}_p &= 14.39 \text{ mrad/Sec} \\ \dot{\beta}_L &= 14.20 \text{ mrad/Sec}\end{aligned}\tag{14b}$$

An expression equivalent to Eq. (13) could also have been developed by employing the work of Kawachi<sup>(3,4)</sup>. He derives expressions for the image velocity for an oblique frame camera and notes<sup>(4)</sup> that "the image velocity for the panoramic photograph is the same as for a frame photograph tangent to it at the point in question." If we are interested in evaluating the velocity near the center of the width of the panoramic frame we can set the transformed film coordinates equal to zero, i.e.  $x' = y' = 0$ , in Eqs. (7) and (8) of Ref. 4 and obtain the net image velocity as

$$V_I = \frac{VF}{h} \cos t \left[ \sin^2 \alpha + \cos^2 \alpha \cos^2 t \right]^{1/2}\tag{15}$$

where  $F$  is the focal length of the camera and  $\alpha$  is defined by Eq. (10b). The uncompensated angular blur rate is determined by dividing by the product of the focal length and the factor  $1 + h/r_m$  included previously in Eq. (7). This factor is the principal correction for the curvature of the lunar surface. The resulting expression can also be obtained from Eqs. (10a) and (11) and is therefore equivalent to Eq. (13) except for the neglect of the effect of surface curvature upon slant range.

3.1.2 Blur Compensation Rate - The next step in computing the residual blur is the determination of the compensation rate applied by the camera. In the case of a panoramic camera<sup>(2)</sup> the blur compensation rate is proportional to the instantaneous rotation angle of the lens, namely,

$$\dot{\beta}_C = \left( \frac{V}{H} \right)_C \cos w\tag{16}$$

This reflects the decrease in angular blur due to the slant range assuming a flat planetary surface. It is not known whether the panoramic camera IMC computer was reprogrammed for the more complex effect of the slant range due

to the curvature of the lunar surface (c.f. Eq. (12)). If so, the compensation rate would be

$$\dot{\beta}_c = \frac{\left(\frac{V}{H}\right)_c}{\left\{ \left(1 + \frac{r_m}{h}\right) \cos w - \left[ \left(\frac{r_m}{h}\right)^2 \left(1 + \frac{r_m}{h}\right)^2 \sin^2 w \right]^{1/2} \right\}} \quad (17)$$

where  $r_m/h \sim 16$  can be assumed to be constant. Referring back to Figure 8b, we see that the effect is less than 1% for the rotation or roll angles we are considering. However, near the edge of the frame where the rotation angle approaches  $54^\circ$  the error would be as large as 7%. Conversely, the uncompensated blur rate is considerably less in this portion of the panoramic frame and the need for an accurate compensation rate diminished. Consequently, it is assumed that such a modification of the IMC computer was **not** undertaken since it would offer little advantage. Using Eq. (16), the roll angles presented in Table 3 and the V/H command values from the telemetry data presented in Figure 6, the compensation estimates were estimated for Frame 316 to be

$$\dot{\beta}_{cD} = 18.00 \text{ mrad/sec} \quad (18a)$$

$$\dot{\beta}_{cL} = 11.76 \text{ mrad/sec}$$

and for Frame 360

$$\dot{\beta}_{cD} = 19.09 \text{ mrad/sec} \quad (18b)$$

$$\dot{\beta}_{cL} = 12.77 \text{ mrad/sec}$$

We note that these results are only an approximation since the compensation rate is proportional to the instantaneous rotation angle and a given point in the panoramic frame will receive a varying amount of image motion compensation due to the finite width of the scanning slit. Consequently, Eq. (16) should be integrated over the exposure time of the point under evaluation to determine an average compensation rate, namely

$$\langle \dot{\beta}_c \rangle = \frac{1}{t_e} \int_{t_e} \dot{\beta}_c(t) dt \quad (19)$$



This procedure was executed and the resulting average compensation rates were less than those presented in Eqs. (18a and 18b) by approximately 0.6%. In this case, therefore, the dynamic effect of the motion compensation can be neglected.

3.1.3 Exposure Time Estimation - Three different methods were used to estimate the exposure time of the dark or light portions of each frame under evaluation. As noted previously, the abrupt change in the average density across the V/H anomaly was attributed to a change in exposure time between these two portions of the frames. One method for determining the exposure times is based upon this fact, that is, the density difference is related to the ratio of the exposure times by the expression

$$\mathcal{R} = \frac{t_{eD}}{t_{eL}} = 10^{\delta/r} \quad (20)$$

where  $\delta$  is the density difference and  $r$  is the gain of the D-Log E response curve. The length of time that the capping shutter is open,  $t_c$  is equal to the sum of the times required to expose each portion of the frame, that is,

$$\begin{aligned} t_c &= \frac{L_D}{V_D} + \frac{L_L}{V_L} \\ &= \frac{L_D V_L + L_L V_D}{V_L V_D} \end{aligned} \quad (21)$$

where  $L_D$  is the length of the dark portion of the exposed frame,  $L_L$  is the length of the light portion of the exposed frame, and  $V_D$ ,  $V_L$  are the velocities of the scanning slit in the respective portions of the frame. Since the width of the scanning slit,  $W_S$ , is constant these velocities are inversely proportional to the exposure time and consequently we can equate the variable  $\mathcal{R}$  of Eq. (20) to the ratio of the velocities, namely

$$\mathcal{R} = V_L/V_D \quad (22)$$

Combining Eqs. (21) and (22) and eliminating the velocity of the scanning slit

in favor of the ratio of the slit width to the exposure time, we can derive an equation for the exposure in the light portion of the frame

$$t_{eL} = \frac{W_s}{R L_D + L_L} t_c \quad (23a)$$

as well as an expression for exposure in the dark portion

$$t_{eD} \approx t_{eL} \quad (23b)$$

These equations were employed with the numerical values shown in Table 4 to calculate the exposure times for both the dark and light portions of the frames under evaluation. The density difference was measured directly from the frames under evaluation while the gain of the response curve was obtained from Figure 31 of Reference 1 using the curve labeled "4th GEN POS (4P)". The capping shutter time and the scanning slit width were obtained from telemetry data shown previously in Figure 6. The values of the exposure time obtained using these expression are presented in Table 5 along with error estimates derived from first order analyses.

Table 4  
NUMERICAL VALUES USED TO ESTIMATE EXPOSURE TIMES

VARIABLE (UNITS)	SYMBOL	VALUE	
		FRAME # 316	FRAME # 360
DARK-LIGHT DENSITY DIFFERENCE	$\delta$	0.42	0.36
RESPONSE CURVE GAIN	$\gamma$	-2.0	-2.0
EXPOSURE TIME RATIO	$R$	0.61660	0.66069
SECTION LENGTHS (INCHES)	$L_D$	32	26
	$L_L$	13	19
CAPPING SHUTTER TIME (SECONDS)	$t_c$	1.5	3.1
SCANNING SLIT WIDTH (INCHES)	$W_s$	0.3	0.3

**Table 5**  
**EXPOSURE TIME ESTIMATES**

SOURCE	FRAME #316		FRAME #360	
	DARK	LIGHT	DARK	LIGHT
EQS (23a) AND (23b)	8.5 msec ± 9.3%	13.7 msec ± 7.7%	17.0 msec ± 5.3%	25.7 msec ± 4.2%
MOLEBURG EQ. (25)	9.2 msec ± 2.9%	13.6 msec ± 2.6%	17.6 msec ± 2.3%	26.0 msec ± 2.6%
ADJACENT FRAME	N/A	14.0 msec ± 5.0%	N/A	25.3 msec ± 3.2%

The second method used to estimate the exposure times is based upon an approximate formula which was furnished by Mr. B. Moleburg at the NASA Johnson Space Center, namely

$$t_e = \frac{KWs}{(V/H)_C} \quad (24)$$

where  $K = 0.59$  for the stereo mode and  $1.127$  for the mono mode. The  $V/H$  factor in the denominator of this expression is the command  $V/H$  rate obtained from telemetry data;  $19.2$  milliradians/second for the dark portion and  $13.0$  milliradians/second for the light portion. The exposure times obtained using this expression are also presented in Table 5 with their associated error estimates.

The final method used to estimate the exposure time is only applicable to the light portion of each frame under evaluation. In both cases, the adjacent frame had an exposure level equivalent to the light portion of the frames under evaluation and consequently the exposure time in the light portion is equal to the exposure time of either adjacent frame. The equation for calculating the exposure time for a frame with a constant  $V/H$  command rate is obtained by setting  $\mathcal{Q} = 1$ ,  $L_D = 0$  and  $L_L = L = 45$  inches in Eq. (23a), namely

$$t_e = \frac{W_s}{45} t_c \quad (25)$$

The results obtained using this method are also included in Table 5, and we note that the results from all three methods are in excellent agreement. In subsequent evaluations, results obtained from Eqs. (23a) and (23b) are employed.

3.1.4 Residual Blur - It is a straightforward procedure to combine the results derived above in order to determine the residual motion blur at the film plane. The equation for the residual image blur is

$$\delta_r = |\dot{\beta} - \dot{\beta}_c| t_e F \quad (26)$$

where  $F$  is the focal length of the camera (=610 millimeters). This blur produces a Modulation Transfer Function described by the equation

$$\tau(\nu) = \frac{\sin(\pi \nu / \nu_0)}{\pi \nu / \nu_0} \quad (27)$$

which degrades the nominal fine detail content of the photograph. The parameter  $\nu_0$  is simply the reciprocal of the residual image blur in cycles/mm. Values obtained for both the residual image blur and the "cutoff" spatial frequency are presented in Table 6.

Table 6  
RESIDUAL IMAGE BLUR

VARIABLE (UNITS)	FRAME #316		FRAME #360	
	DARK	LIGHT	DARK	LIGHT
RESIDUAL IMAGE BLUR (mm)	.0288 ± 12%	.0020 ± 44%	.0224 ± 7%	.0488 ± 17%
CUTOFF FREQUENCY (CYCLES/mm)	34.7 ± 4.2	512 ± 230	44.5 ± 3.1	20.5 ± 3.5

The expected value of the net MTF can be determined by multiplying the values obtained from Eq. (27) by the product of the MTF for the flight and subsequent copy films and the camera lens. Unfortunately, an MTF for the panoramic camera lens was not available, however, such lenses are noted for their high quality performance and it is very likely that the net MTF is dominated by the performance of the flight and copy films and any residual blur. Consequently, in determining the expected MTF the lens MTF was assumed to be 1.0 at all spatial frequencies evaluated.

A final comment is required concerning the precision of the approximations used in the expressions for the uncompensated angular blur rate and the compensation rate. In both cases only those approximations whose errors were less than 1% were retained. However, since we are employing difference between these two quantities in Eq. (26) a small error can be magnified when a small difference occurs. Eq. (13) for the uncompensated angular blur rate employs two approximations for the inclusion of foreshortening effects; the assumption of a flat planetary surface and equivalence between the off-axis and on-axis reduction factors. For vertical photography, these approximations introduce no errors. However, for oblique photography, the net effect is to over estimate the blur rate by about 0.5%. Eq. (16) for the blur compensation rate neglects the dynamic effects of motion compensation and over estimates by 0.6% compared to the average compensation rate. This occurs for both the oblique and vertical photography. In the case of oblique photography, since both the blur rate and compensation rate are over estimated by about the same percentage, the effect upon the residual image blur is negligible (i.e., about 0.6%) even when there are small differences between the rates. In the case of the vertical photography, only the compensation rate is in error and this is subsequently magnified by the differencing operation resulting in an under estimate of the residual image blur by 5% in the light portion of Frame 360 and an over estimate of the residual image blur by 3% in the dark portion of Frame 360. These errors are still less than the net accuracy of the residual blur estimates shown in Table 6.

3.2 Modulation Transfer Function Estimation - As noted previously in Section 2, a net MTF was estimated for each photo under evaluation. This was accomplished by tracing shadow-to-sunlit edges interior to craters using a microdensitometer and subsequently processing this edge data using the Edge Gradient Spectral Analysis (EGSA) software package described in Section 2.2.

A Mann microdensitometer was used to obtain the required edge data. For this purpose the microdensitometer was used in an improved but unconventional mode of operation. A  $41\mu\text{m}$  by  $41\mu\text{m}$  source aperture was employed with a 0.4 N.A. influx objective. This offered a magnification of approximately 40x producing a  $1.0\mu\text{m}$  square geometric image at the film plane. This image is subsequently broadened by the diffraction effects of the objective whose airy disc has a diameter of  $1.5\mu\text{m}$ . Consequently, the image of the source aperture will be a gaussian-like light distribution with a diameter of several micrometers. A 0.25 N.A. objective was used for the efflux optics and the subsequent sensor aperture chosen to minimize stray light and not further define the scanning aperture. In this mode of operation the distorted image of the source aperture is the scanning aperture and the spatial frequency response of the microdensitometer determined accordingly. The over filling of the efflux optics by the influx optics offers an improvement in instrument performance.

Edge data was collected in both the dark and light portions of each of the frames about 1 inch on either side of the suspected V/H discontinuity. This edge data was then hand smoothed and digitized for processing by the EGSA software. The average MTFs resulting from these measurements are presented in Figures 9 and 10 along with the expected MTF determined by the procedures described in Section 3.1.4. In estimating the average MTF through modulus averaging, 10 edges were measured in the dark portion of Frame 316 while 7 edges were measured in the light portion. Similarly, 11 edges were measured in the dark portion of Frame 360 and 10 edges in the light portion.

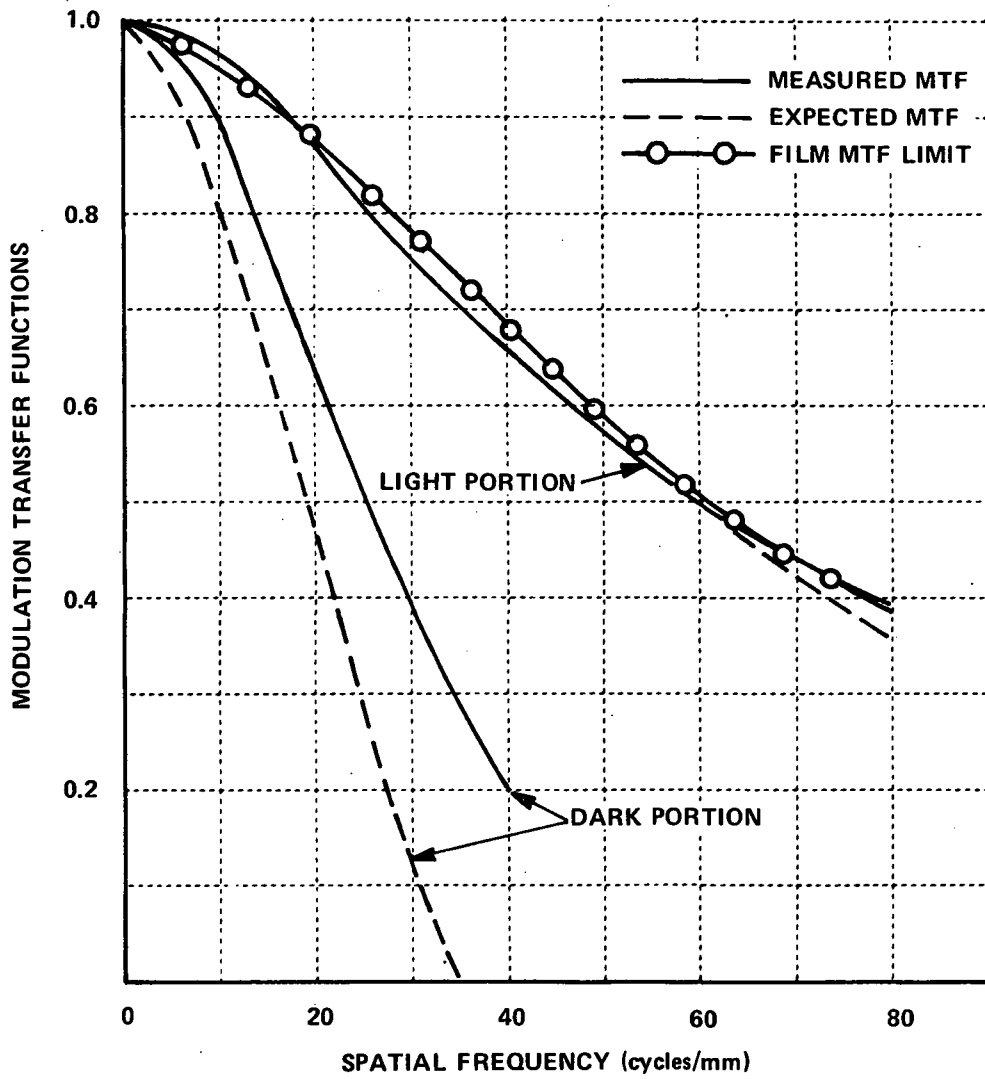


Figure 9 MEASURED AND EXPECTED MTF's FOR APOLLO 15 FRAME 316 WITH V/H ANOMOLY

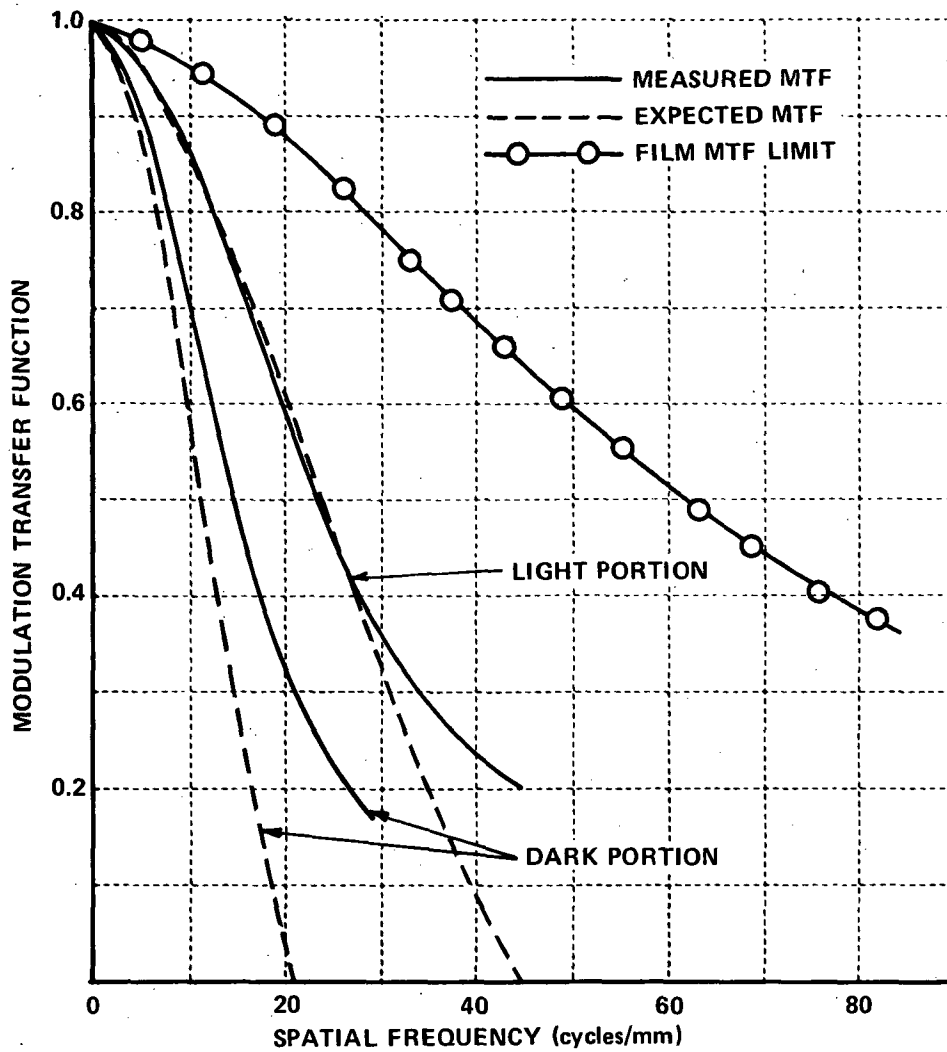


Figure 10 MEASURED AND EXPECTED MTF's FOR APOLLO 15 FRAME 360 WITH V/H ANOMOLY



Also shown in the Figures is the net film MTF limit for the 4th Generation Positive copies employed in the evaluation. We note that there is excellent agreement between the expected and measured MTF values in all four instances. For the light portion of Frame 316 the measured and expected MTF values are essentially identical and equal to the net film MTF limit over the range of spatial frequencies shown. This is a result of the nearly perfect compensation provided in this case. In all the other cases the compensation was poor and the resolution reduced by 1/3 (to about 6 meters on the lunar surface).

Other low sun angle photography known to have V/H discontinuities include Frames 8852 (Rev. 4) and 344 (Rev. 72). When such a discontinuity did not occur the V/H command signal was either at the nominal value (13.0 mrad/sec) similar to the light portions of the frames evaluated or varying about an anomalously high value similar to the dark portions. Telemetry data indicates that the latter situation occurred at least for Frames 345, 346 and 347 (Rev. 72). Only when it is equal to the nominal value can the full "resolution" potential of the panoramic camera be realized; but this may not always occur (refer to the MTF for the light portion of Frame 360). The user of Apollo 15 panoramic data should refer to the telemetry data to determine the V/H command situation for the frames he is exploiting and account for the effects of poorer resolution if necessary.

#### 4. COMPARISON AMONG MULTIPLE GENERATIONS OF APOLLO 16 AND 17 PHOTOGRAPHY

One of the specific tasks accomplished during this study was an assessment of the detailed content of multiple generations of Apollo 16 and 17 photography. The purpose of this assessment was to determine the degradation, if any, in the quality of the photographic products furnished to various users. The original flight film is copied to produce a Master Positive (2P) or Direct Negative (2N) copy. These are the earliest generations which a user may exploit and only a limited number of such copies are generated. The Master Positive is subsequently copied twice to produce a 4th Generation Positive (4P) which most investigators are likely to use. The Direct Negative is also copied once to produce a Third Generation Positive (3P) which is also available to investigators. This latter sequence eliminates one copy step in the hope of improving product quality or reducing production time. Unfortunately the characteristics of the reversal film required to produce the 2N copy may limit the detail content and no actual improvement in product quality obtained. The purpose of this task was to assess the effect of both reproduction sequences on the detail content of Apollo 16 and 17 photography.

An inter-comparison of the total quality and the fine detail content was made for Apollo 16 panoramic photography, Apollo 17 panoramic photography and Apollo 17 metric photography. The frames selected and subsequently evaluated were shown previously in Table 1. Unfortunately 3P and 4P copies of the same type of photography were not available at the Lunar Science Institute thus preventing a direct comparison of the most likely user products. Instead a comparison of preceding generations (2N and 2P) was made. The results of the evaluations are discussed in detail in the subsections below.

4.1 Product Tonal Quality - The methodology used to assess the tonal quality of the Apollo 16 and 17 photography was discussed previously in Section 2. The most common measure of tonal quality is the Hurter-Driffield or D-Log E response curve. It specifies how the apparent scene brightness is reproduced as density in the photograph. The D-Log E response curve was measured for each frame evaluated. The results obtained are presented in

Figures 11 through 13. These curves were generated from microdensitometer scans of step wedges placed on the original flight film and subsequently copied during each duplication step. Consequently, the relative exposure refers to the apparent brightness of scene elements at the original flight film. The exposure of the first step was arbitrarily assigned a value of 1.0. Since there is an increment of 0.15 in the log exposure between the 21 steps, the last step has a relative exposure of 1000.

A software program was written that calculates the gain factors expressed by Eq. (6) using step wedge densities (sensitometric calibration) supplied as input. The input values were obtained from the curves shown in Figures 10 through 13 created by visually passing a smooth curve through the actual measured step wedge densities. Spline interpolation functions are used to compute density values for exposure levels between the individual steps. These interpolation functions yield results equivalent to forcing a flexible straight line (spline) through the data points and tend to avoid the "waviness" often encountered by other curve fitting techniques.

The tone quality evaluation program uses the resulting coefficients of the spline regression to estimate the density difference between the image and the background for various contrast levels identified previously in Table 2. The average exposure levels, i.e. the average of the object and background exposure values, were set equal to the relative exposure levels of each of the steps in the step tablet. The density difference at each average exposure level is divided by  $\Delta$  (c.f. Table 2) to determine the gain.

The gain as a function of the average exposure level was identical for the low and mid-contrast objects for all the cases examined. The gain functions for the second generation photography are presented in Figures 14 through 16. In describing tonal quality the term "dynamic range" is frequently employed. This is loosely defined as the exposure region corresponding to the linear portion of the D-Log E curve. In this study we defined the dynamic

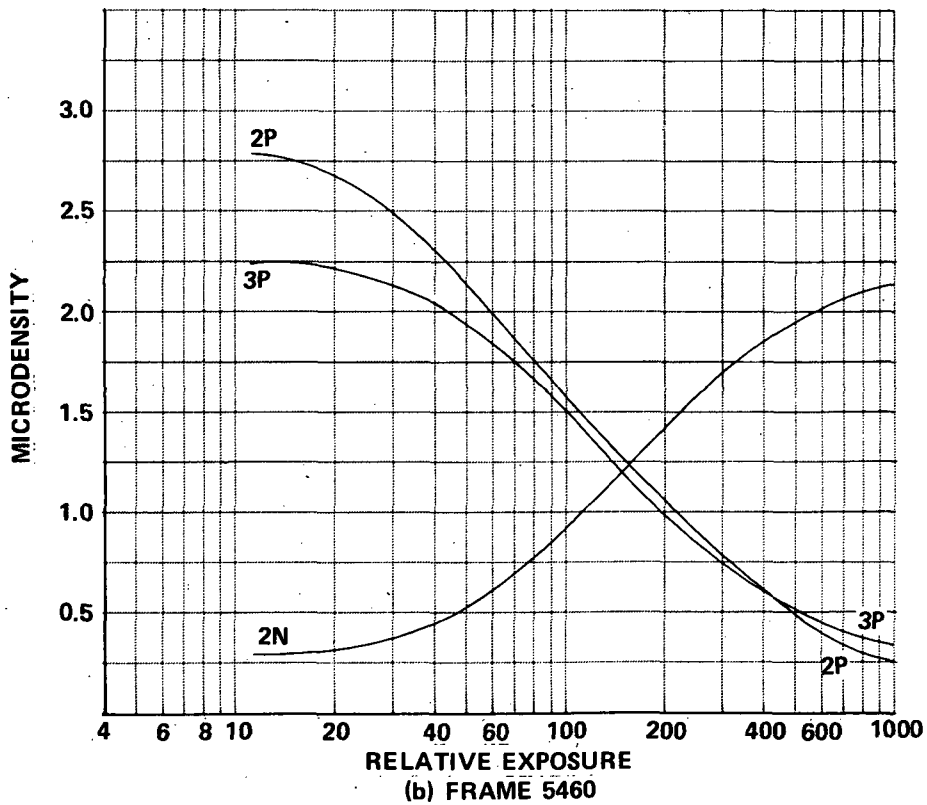
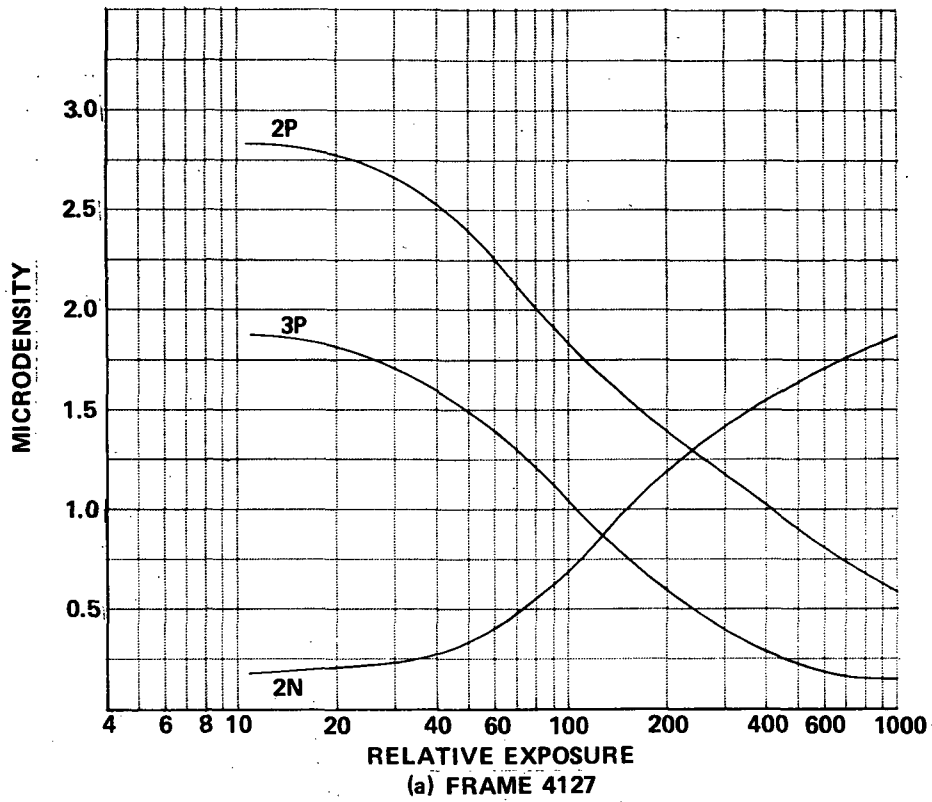


Figure 11 SENSITOMETRIC CALIBRATION - APOLLO 16 PANORAMIC PHOTOGRAPHY

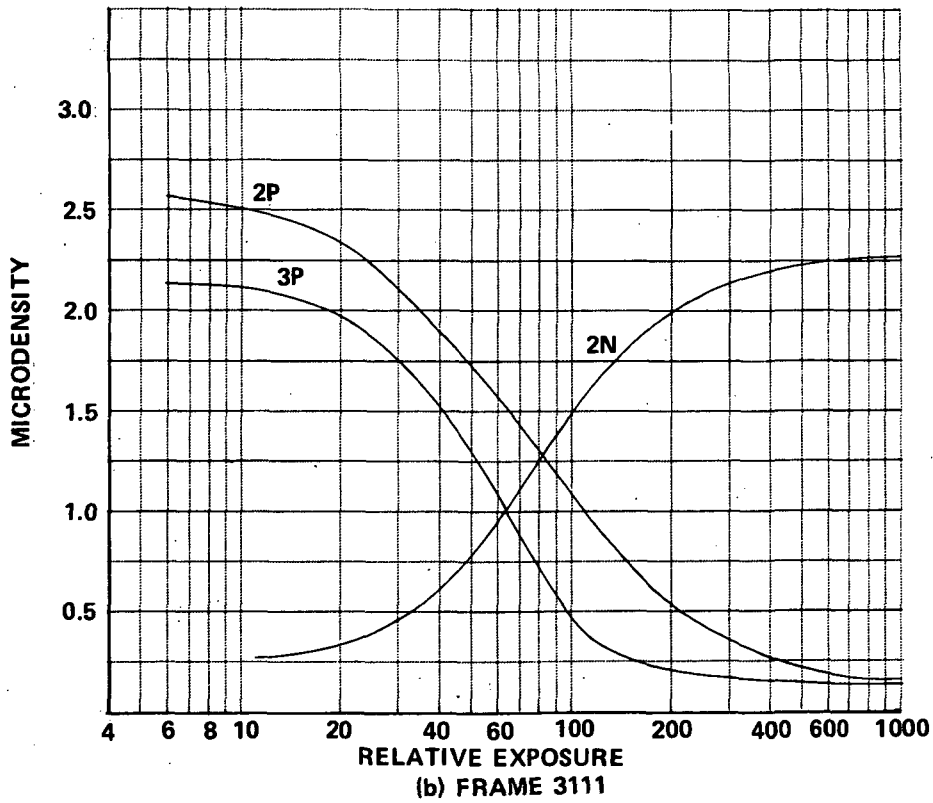
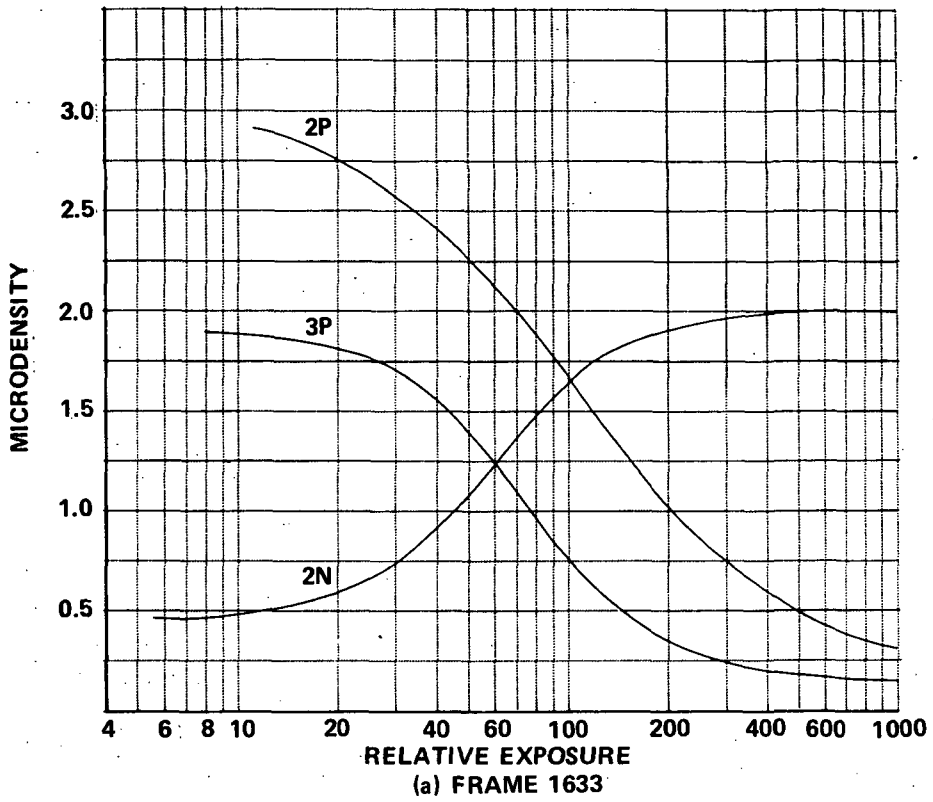


Figure 12 SENSITOMETRIC CALIBRATION - APOLLO 17 PANORAMIC PHOTOGRAPHY

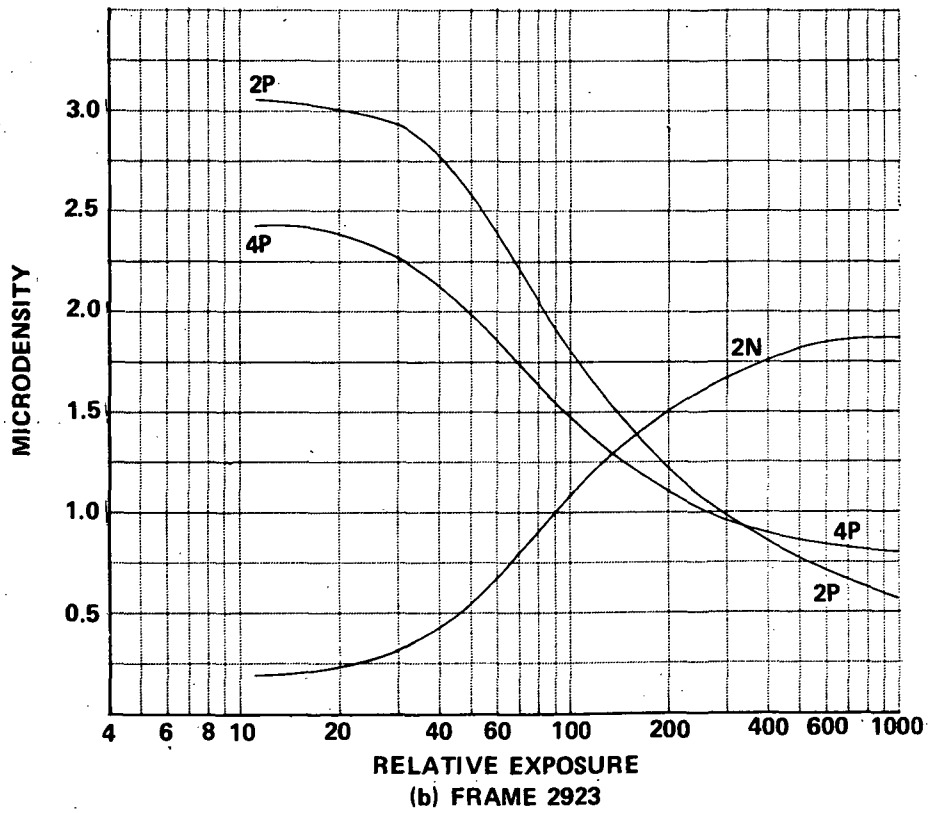
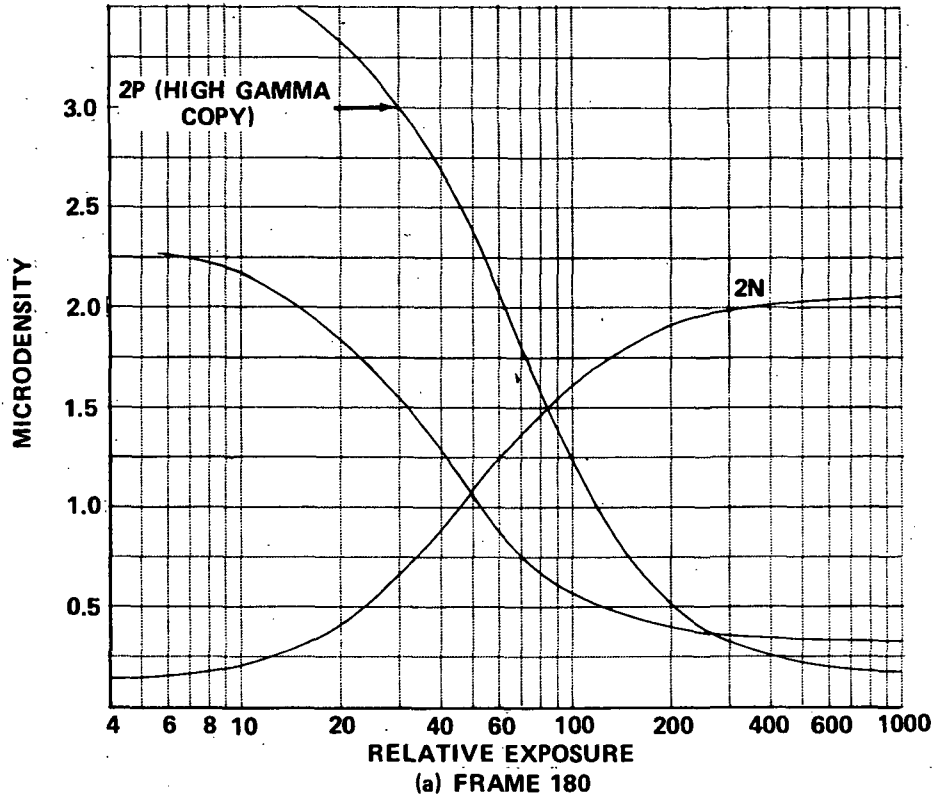


Figure 13 SENSITOMETRIC CALIBRATION - APOLLO 17 METRIC PHOTOGRAPHY

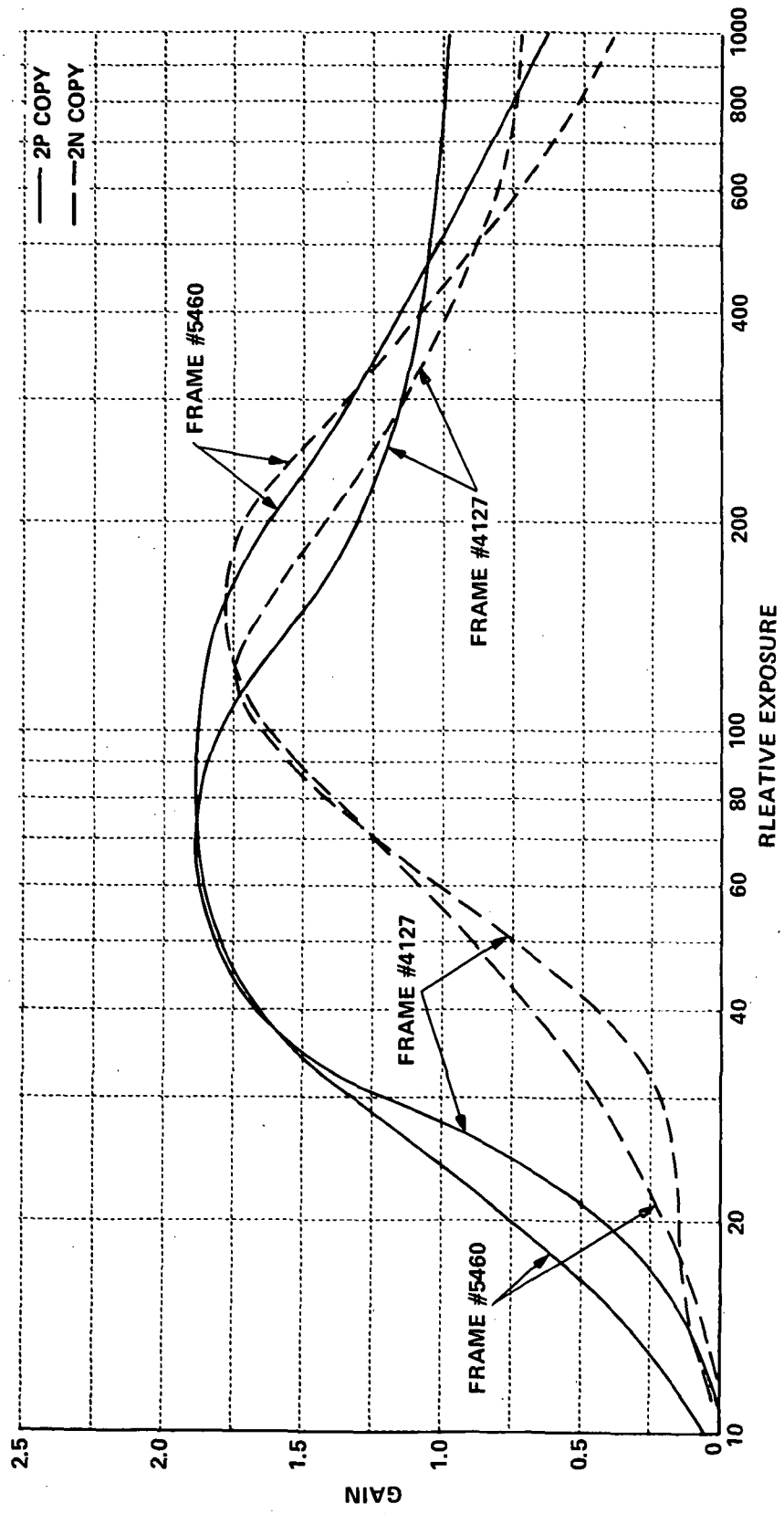


Figure 14 GAIN FOR LOW AND MID-CONTRAST OBJECTS -- APOLLO 16 2nd GENERATION PANORAMIC PHOTOGRAPHY

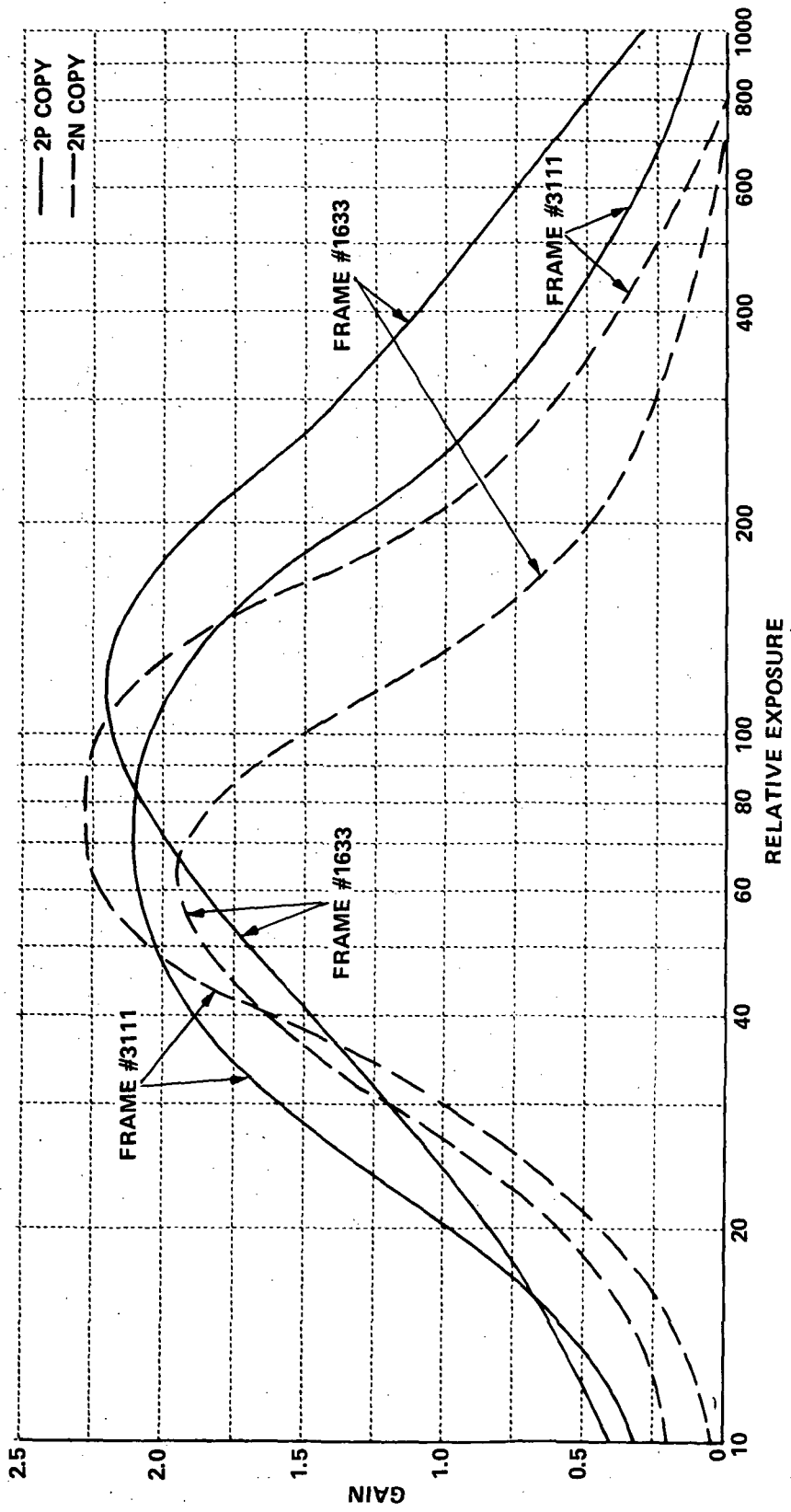


Figure 15 GAIN FOR LOW AND MID-CONTRAST OBJECTS - APOLLO 17 2nd GENERATION PANORAMIC PHOTOGRAPHY



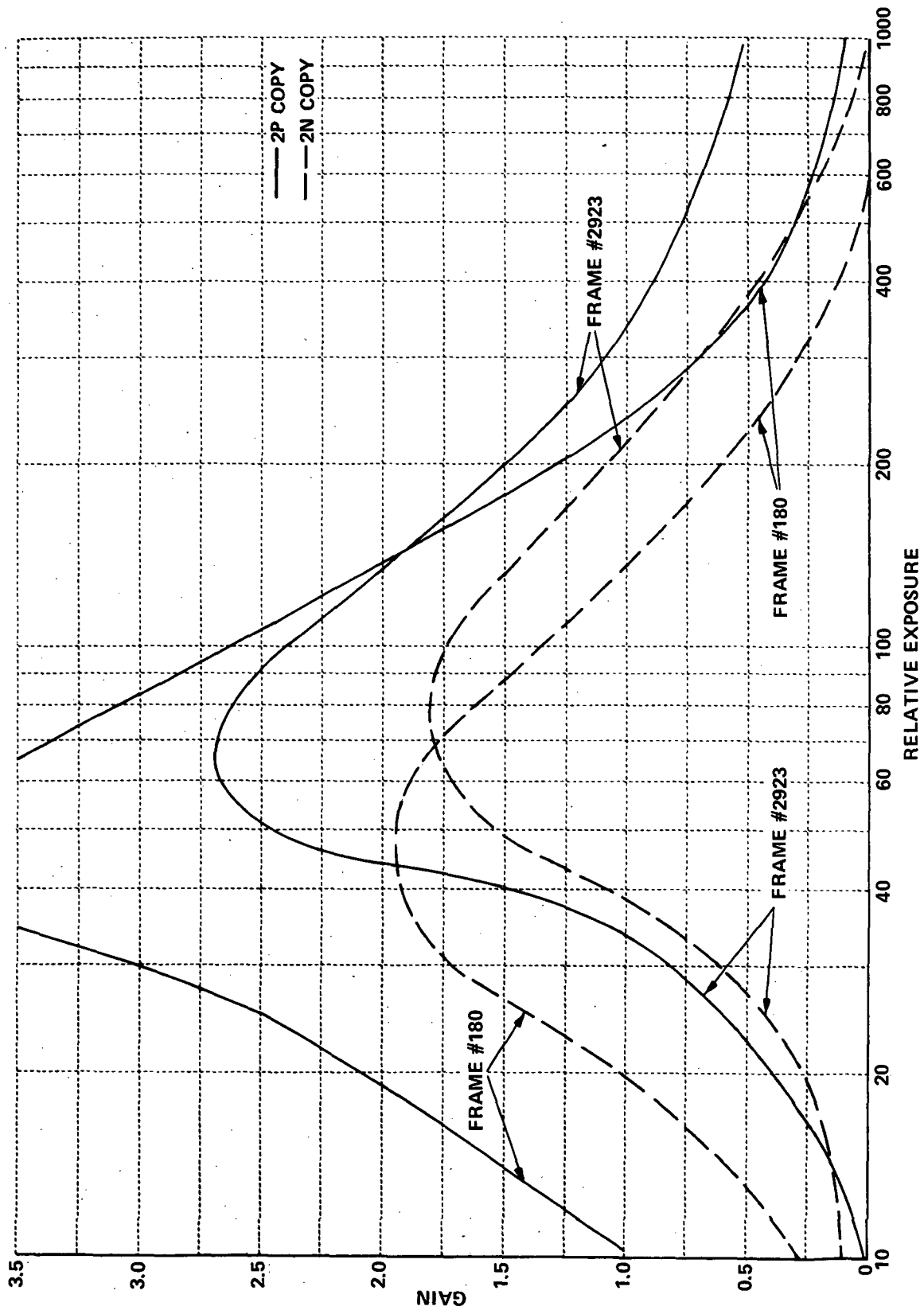


Figure 16 GAIN FOR LOW AND MID-CONTRAST OBJECTS - APOLLO 17 2nd GENERATION METRIC PHOTOGRAPHY

range more quantitatively as the exposure interval between the points where the gain functions dropped to 50% of their peak value. The average value for the peak gain and the dynamic range for each type of photograph evaluated is presented in Table 7. It is clear from examination of Figures 14 and 15 that both the 2P and 2N photography have about the same peak gain but the 2P photography has a much greater dynamic range. This is also evident from the numerical values presented in Table 7. We can conclude, therefore, that the tone quality of the Master Positive is superior to the Direct Negative for the panoramic photography. In the case of the metric photography, it is not clear from Figure 16 that a difference in dynamic range exists and the values in Table 7 show an equivalence of the dynamic range. However, the peak gain of the Master Positive photography is clearly greater. The roll containing Frame 180 was, in fact, processed to yield a "high gamma" copy. In this case we conclude that the Master Positive is superior due to the peak gain rather than any difference in dynamic range.

**Table 7**  
**TONE QUALITY COMPARISON**  
**(LOW AND MID CONTRAST OBJECTS)**

PHOTO TYPE		PEAK GAIN	DYNAMIC RANGE (dB)
APOLLO 16 PAN	2N	1.8	9.9
	2P	1.9	15.5
	3P	1.8	9.6
APOLLO 17 PAN	2N	2.1	7.5
	2P	2.2	11.1
	3P	2.4	6.5
APOLLO 17 METRIC	2N	1.9	8.3
	2P	2.7	8.4
	4P	2.1	7.5

Similar measurements were made on the 3P and 4P copies where they were available. These data were not included in Figures 14 through 16 for the sake of clarity but are presented in Table 7. The quality of these products generally correlates with the corresponding Second Generation photography. There is little change in the peak gain between these generations, but a definite decrease in the dynamic range for the higher generation products. An exception is the 2P to 4P reproduction of the Apollo 17 metric photograph where an apparent drop in the peak gain is noted. Consequently, we cannot infer that the tonal quality differences present in the Second Generations are preserved in the 3P and 4P user products for the metric photography.

The gain functions for a high contrast object (e.g. sunlight-shadow boundary) have lower peak gains and greater dynamic range (c.f. Table 8) but support the conclusions reached above.

**Table 8**  
**tone quality comparison**  
**(HIGH CONTRAST OBJECTS)**

PHOTO TYPE		PEAK GAIN	DYNAMIC RANGE (dB)
APOLLO 16 PAN	2N	1.5	13.0
	2P	1.7	> 15.7
	3P	1.5	12.0
APOLLO 17 PAN	2N	1.7	9.7
	2P	2.0	12.3
	3P	1.9	9.2
APOLLO 17 METRIC	2N	1.6	10.7
	2P	2.6	10.7
	4P	1.6	10.7

4.2 Fine Detail Content - MTF measurements were made in order to compare the detail content of the various generations of photography evaluated. These measurements were made by scanning shadow-to-sunlit edges near the center of each frame using a microdensitometer. The mode in which the instrument was operated was described previously in Section 3.2 in connection with similar measurements on Apollo 15 panoramic photography. The edge data

obtained were processed using the EGSA software as discussed previously in Section 2.2. Table 9 shows the amount of edge data collected and processed for each of the photographs evaluated. The MTFs measured for the Apollo 17 metric photography are presented in Figure 17. Included in the Figure is the MTF limit for the film alone. The significance of the departure of the measured MTFs from the film limit was assessed using the 95% confidence bands calculated by the EGSA main program (see the Appendix). The systematic affect at the low spatial frequencies (0-30 cycles/mm) where the measured functions exceed the limit is a result of the manual smoothing and the noise level. The top and bottom of the edge are masked by the noise and the observer tends to employ small radii of curvature thereby truncating the tails of the spread functions and producing this effect. Consequently the confidence bands are examined only above 30 cycles/mm to assess significance. Both the Direct Negative (a) and Master Positive (b) MTF's are not significantly lower than the film limit except for the 2P copy of Frame 180. The 4th Generation Positive MTF's (c) are both significantly less than the film imposed limit. In these three cases the estimated ground resolution is about 30 meters (versus a nominal 20 meter resolution). Since half of the copies have nominal resolution the loss in fine detail must have occurred during the reproduction processes.

**Table 9**  
**EDGE DATA COLLECTED AND PROPOSED FOR**  
**APOLLO 16 AND 17 PHOTOGRAPHY**

FRAME \ TYPE	DIRECT NEGATIVE	MASTER POSITIVE	3rd GEN. POSITIVE	4th GEN. POSITIVE
180	8	7	-	10
2293	8	8	-	8
1633	10	9	6	-
3111	6	6	3	-
4127	5	10	9	-
5460	10	8	7	-

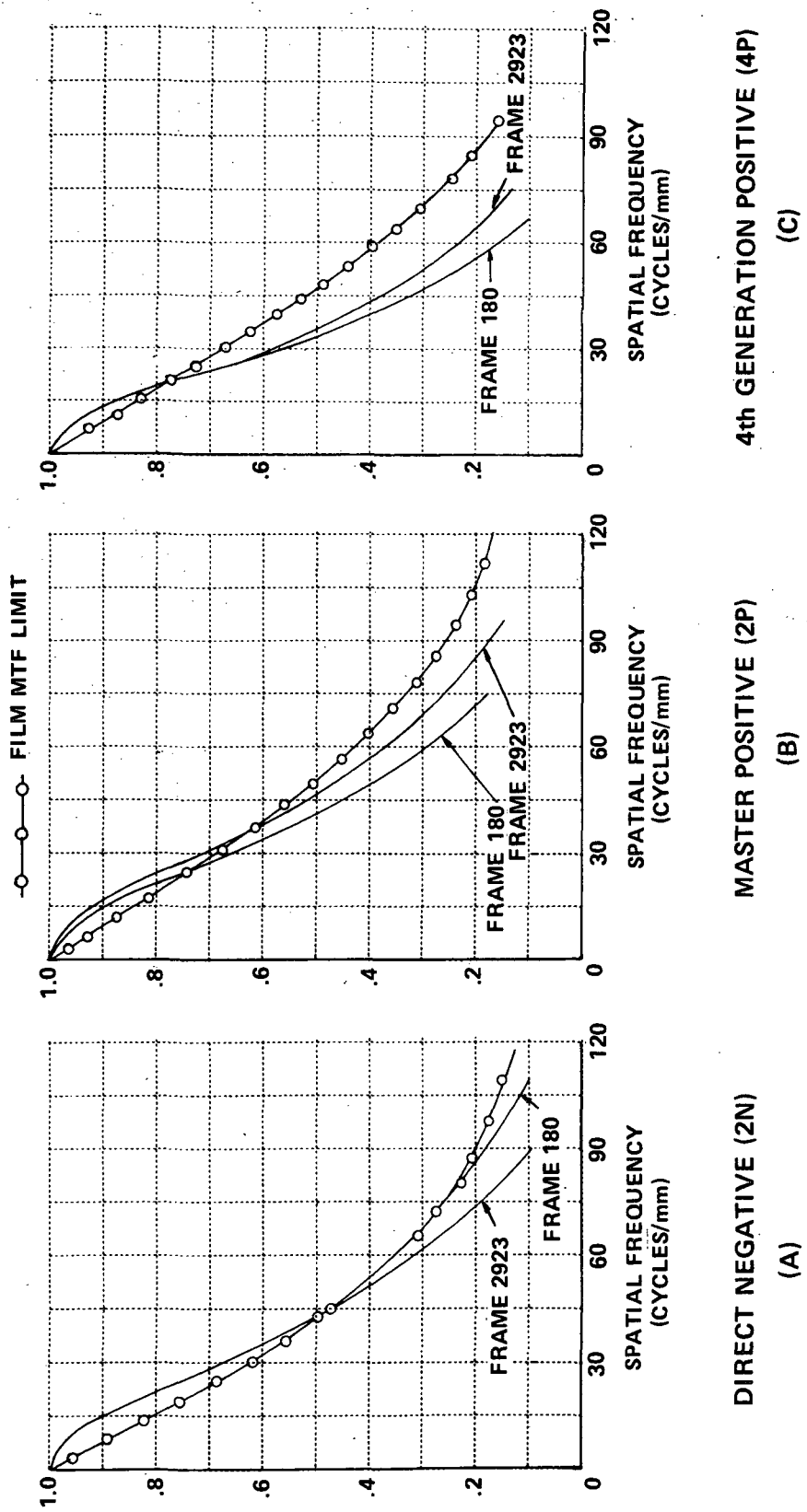


Figure 17 MODULATION TRANSFER FUNCTIONS - APOLLO 17 METRIC PHOTOGRAPHY

Figure 18 presents the MTF results for the Apollo 17 panoramic photography. For both frames the Direct Negative, Master Positive and 3rd Generation Positive MTF's are not significantly different from the respective film limits. This photography has the maximum possible fine detail content or about 2 meter "resolution."

Figure 19 shows the MTFs obtained for the Apollo 16 panoramic photography evaluated. In this case all of the copies examined showed a significantly lower response than that imposed by the photographic films involved. For the Direct Negative copies the ground resolution element is estimated to be 4 meters while the Master Positive and 3rd Generation Positive copies have a 3 meter resolution. Whether this reduced fine detail content is present in the original flight film it is unknown since that photography was not available for evaluation. We note that the Direct Negative copies evaluated are not necessarily those used to produce the 3rd Generation Positive copies (which apparently have better resolution).

Based upon the results presented above it is concluded the reproduction processes may have produced a loss in fine detail. About half the frames evaluated showed some loss. In these cases the ground resolution element increased by a factor of 1.5 to 2.

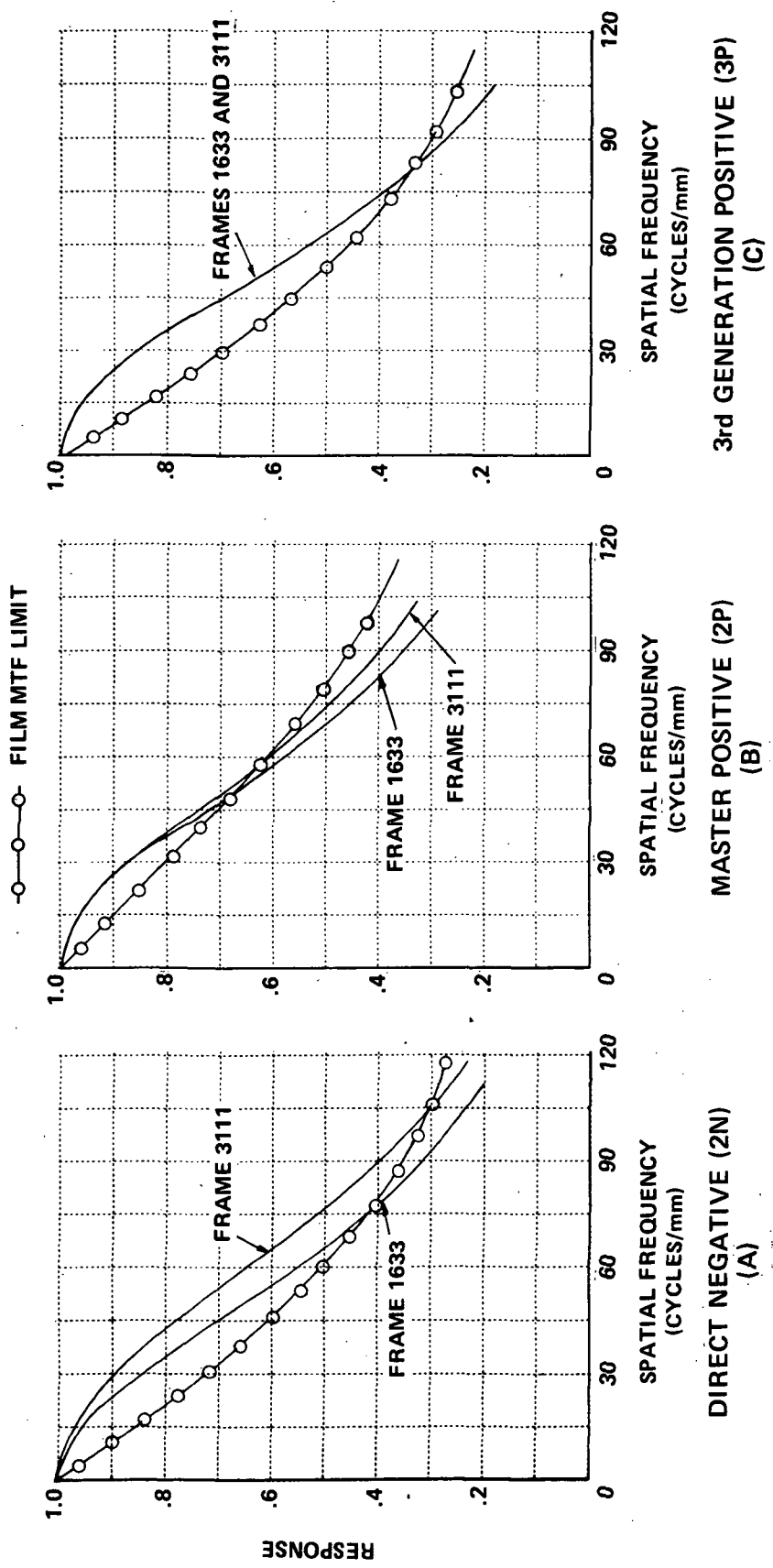


Figure 18 MODULATION TRANSFER FUNCTIONS - APOLLO 17 PANORAMIC PHOTOGRAPHY

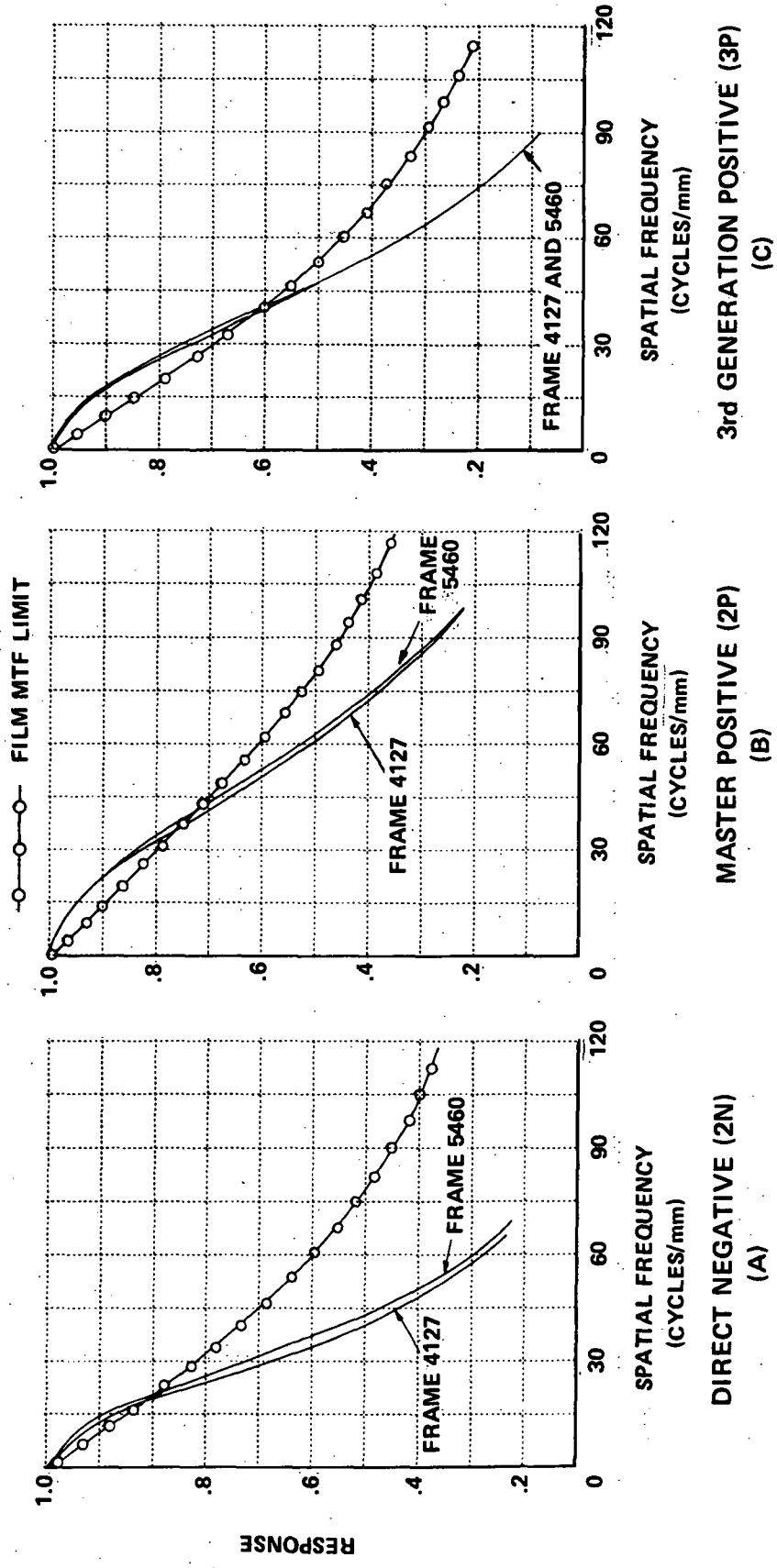


Figure 19 MODULATION TRANSFER FUNCTIONS - APOLLO 16 PANORAMIC PHOTOGRAPHY



## 5. CONCLUSIONS

The development and application of image evaluation methods for assessing the detail content of Apollo Orbital Photography has been demonstrated. Edge analyses using shadow-to-sunlight edges interior to craters was successfully used to evaluate the fine detail content for Apollo 15, 16 and 17 imagery. A method for evaluating tone quality was developed using a gain factor as a function of object contrast and average exposure level that can be related to object detectability.

The anomalous operation of the V/H sensor during the Apollo 15 mission introduced several degrading effects into the panoramic imagery; a loss in resolution due to image motion blur and exposure differences within a frame. The latter effect is present in those frames where an abrupt change in the V/H rate occurs. Two such frames were evaluated and exhibited a 0.4 density difference. It is estimated that this difference would be less in high sun angle photography although no such frames were examined.

The fine detail content was seriously degraded by the anomalous V/H sensor operation. The commanded V/H rate was either anomalously high or equal to the pre-set nominal rate. This resulted in either over or under compensation and a reduction in the resolution by 1/3 (to about 6 meters on the lunar surface). In one instance the nominal V/H rate was sufficiently close to the actual rate to permit nearly perfect compensation. Only when the commanded V/H rate is equal to the nominal value can the full resolution potential of the panoramic camera be realized; but this may not always occur. When the command rate varies about an anomalously high value a loss in resolution can be expected for the full frame. The user of Apollo 15 panoramic imagery should refer to the telemetry data to determine the V/H command situation for the frames he is exploiting and account for the effects of poorer resolution if necessary.

As a result of the comparison among multiple generations of Apollo 16 and 17 photography it was concluded that the tone quality of the Master Positive is superior to that of the Direct Negative for the panoramic photography. This difference is attributed to a greater dynamic range of the 2P photography. This means that lunar objects have a greater contrast over a wider range of average exposure levels in the 2P photography compared to the 2N photography. Unfortunately 3P and 4P copies of the same type of photography were not available thus preventing a direct comparison of the most likely user products. However, the quality of these products generally correlates with the corresponding 2nd Generation Photography, and we can infer that the tonal quality differences are preserved in higher generation user products. Such differences were not evident in the metric photography.

MTF measurements made to compare the detail content of the various generations revealed that half of the imagery examined had a significant loss in fine detail content. These losses were found in both the metric and panoramic photography and are probably introduced during the reproduction process. In the case of the Apollo 16 panoramic imagery all copies showed loss of fine detail and it was not possible to assess whether this loss was present in the flight imagery since it was not available for evaluation. The net effect was an increase in the ground resolution element by an approximate factor of 1.5; 3 meters for the panoramic photography and 30 meters for the metric photography.

The success of the image evaluation methods in assessing the detail content of Apollo orbital photography and the importance of this detail content to potential users suggests that NASA should continue to develop the methods for applications for the future manned and unmanned spacecraft involved in planetary or earth exploration.

## REFERENCES

1. Kinzly, R. E., Study of the Detail Content of Apollo Orbital Photography. Report No. VT-2912-0-1, Calspan Corporation (formerly Cornell Aeronautical Laboratory, Inc.), 29 September 1972.
2. Jensen, N., Optical and Photographic Reconnaissance Systems. J. Wiley and Sons, Inc., 1968.
3. Kawachi, D. A., Image Motion and Its Compensation for the Oblique Frame Camera. Photogrammetric Engineering, Vol. 31, No. 1, January 1965, pp. 154.
4. Kawachi, D. A., Image Motion Due to Camera Rotation. Photogrammetric Engineering, Vol. 31, No. 5, September 1965, pp. 861.

APPENDIX  
SOFTWARE DESCRIPTIONS

This Appendix contains descriptions of eight programs used in the evaluation of the Detail Content of the Apollo Orbital Photography. The purpose, description of inputs, logic and processing, and a sample of the input and output data are included, if appropriate, for each of the programs. All of the programs were written using FORTRAN IV Language. Source and cross reference listings are included for seven of these programs.

Seven of the programs are part of the Edge Gradient Spectral Analysis (EGSA) software package. This package consists of two main programs and five subprograms and is described in Sections 1.0 through 2.0 of this Appendix. Section 8.0 describes the main program used to evaluate the tone quality of Apollo Orbital Photography.

1.0     Main Program DTAPE - This program is part of the Edge Gradient Spectral Analysis software package. It is one of two main programs in the package and is used to create an input data tape for subsequent processing by the main EGSA program. The input to this program is assumed to be edge trace data (i.e., density values at uniform spatial increments) supplied on card input. Sensitometric calibration (step wedge data) is also required for program execution. These data are used by function subprogram EXPOS to convert the density values to relative exposure values which are subsequently written onto an output data tape. No printed output data is furnished by this program.

Figure 20 is a listing of program DTAPE. The function of the major blocks are identified by the comments included in the coding. The program initially reads the sensitometric calibration data supplied by the user in card form. An example of a typical input data set is shown in Figure 21. The initial card of this data deck specifies the number of points, NSW, and the sense of the photographic image (i.e., positive or negative). The variable SENSE is actually a dual purpose variable. It is used to indicate the sense of the image; a positive value corresponds to a positive image and a negative

```

C *****
C ** MAIN PROGRAM - DTAPE (INPUT DATA TAPE CREATION)
C **
C ** THIS PROGRAM IS PART OF THE EDGE GRADIENT SPECTRAL ANALYSIS
C ** SOFTWARE PACKAGE. ITS PURPOSE IS TO CREATE AN INPUT DATA TAPE FOR
C ** THE MAIN EGSA PROGRAM. THIS DATA TAPE CONTAINS THE EDGE DATA TO BE
C ** PROCESSED. VALUES OF DENSITY VERSUS POSITION OBTAINED FROM
C ** MICRODENSITOMETER TRACES ARE READ AND CONVERTED TO RELATIVE
C ** EXPOSURE USING SENSITOMETRIC CALIBRATION DATA ALSO PROVIDED AS
C ** INPUT. FUNCTION 'EXPOS' IS REQUIRED FOR EXECUTION. THE OUTPUT
C ** TAPE WRITTEN CONTAINS TWO TYPES OF RECORDS. THE FIRST SPECIFIES
C ** EDGE IDENTIFICATION PARAMETERS, THE NUMBER OF POINTS AND THE
C ** INCREMENT BETWEEN POINTS. THE SECOND TYPE CONTAINS THE CONVERTED
C ** EDGE DATA.
C **
C ** ** VARIABLE LIST **
C **
C ** INPUT VARIABLES
C **
C ** DX =INCREMENT BETWEEN POINTS IN THE EDGE TRACE IN MM.
C ** E =EDGE TRACE DATA INPUT AS DENSITY VALUES.
C ** NED =OPTIONAL EDGE IDENTIFICATION PARAMETER.
C ** NID =OPTIONAL EDGE IDENTIFICATION PARAMETER.
C ** NP =NUMBER OF POINTS IN THE EDGE TRACE. MUST BE < OR = 500.
C ** NSW =LIMITED BY DIMENSION OF 'E' ARRAY.
C ** =NUMBER OF POINTS IN SENSITOMETRIC CALIBRATION DATA.
C ** MUST BE < OR = 21.
C ** SENSE =A DUAL PURPOSE VARIABLE INDICATING THE SENSE OF THE
C ** OF THE IMAGE: SENSE >0 INDICATES A POSITIVE AND
C ** <0 A NEGATIVE. IF THE DIFFERENCE BETWEEN STEPS IN THE
C ** WEDGE IS 0.15 IN LOG EXPOSURE THE MAGNITUDE OF SENSE
C ** SHOULD BE SET TO 1.0; OTHERWISE IT CAN BE USED AS A
C ** MULTIPLYING FACTOR TO ADJUST THE DIFFERENCE IN LOG
C ** EXPOSURE BETWEEN STEPS.
C ** SWD =SENSITOMETRIC CALIBRATION DENSITY VALUES.
C **
C **
C ** AUTHOR: R.E. KINZLY
C ** DATE: DECEMBER 30, 1971
C ** REVISED: MARCH 13, 1974
C ** APRIL 1, 1974
C **
C *****
C ** DIMENSION E(500),SWD(21)
C ** DATA DUM/0.0/NDUM/G/
C ** 1 FORMAT(3I5,F9.0)
C ** 2 FORMAT(4(I10X,F10.0))
C ** 3 FORMAT(I12,F6.0)
C ** 4 FORMAT(14F5.C,10X)
C **
C **
C ** ISN 0002
C ** ISN 0003
C ** ISN 0004
C ** ISN 0005
C ** ISN 0006
C ** ISN 0007

```

Figure 20 SOURCE AND CROSS REFERENCE LISTINGS FOR MAIN PROGRAM DTAPE (PAGE 1 OF 3)

```

C *****
C * READ SENSITOMETRIC CALIBRATION DATA *
C *
C *
C *****
C
C *****
C * READ(5,3,END=30) NSW,SENSE
C * CALL CLEAR(E(1),SMD(21))
C * READ(5,4) (SMD(1),I=1,NSW)
C *****
C
C *****
C * READ EDGE IDENTIFICATION PARAMETERS,NUMBER OF POINTS AND INCREMENT *
C *
C *
C *****
C
C *****
C * READ(5,1) NED,NID,NP,DX
C * IF(NP.EQ.0) GO TO 20
C *****
C
C *****
C * READ EDGE DATA (DENSITY VERSUS POSITION) *
C *
C *
C *****
C
C *****
C * READ(5,2) (E(I),I=1,NP)
C *****
C
C *****
C * CONVERT DENSITY TO RELATIVE EXPOSURE USING SENSITOMETRIC CALIBRATION *
C *
C *
C *****
C
C *****
C * DO 10 I=1,NP
C * 10 E(I)=EXPOS(E(I),SENSE,SMD,NSW)
C *****
C
C *****
C * WRITE OUTPUT DATA TAPE RECORDS *
C *
C *
C *****
C
C *****
C * WRITE(E(1) NED,NID,NP,DX
C * WRITE(E(1) (E(I),I=1,NP)
C * GO TO 6
C * 20 END FILE 1
C * GO TO 5
C *****
C
C *****
C * WRITE DUMMY OUTPUT RECORD (LAST FILE) AND TERMINATE EXECUTION *
C *
C *
C *****
C
C *****
C * 30 WRITE(1) NDUM,NDUM,NDUM,DUM
C * END FILE 1
C * STOP
C * END
C *****

```

ISN 0008  
ISN 0009  
ISN 0010

ISN 0011  
ISN 0012

ISN 0014

ISN 0015  
ISN 0016

ISN 0017  
ISN 0018  
ISN 0019  
ISN 0020  
ISN 0021

ISN 0022  
ISN 0023  
ISN 0024  
ISN 0025

Figure 20. SOURCE AND CROSS REFERENCE LISTINGS FOR MAIN PROGRAM DTAPE (PAGE 2 OF 3)

\*\*\*\*\*F O R T R A N C R O S S R E F E R E N C E L I S T I N G\*\*\*\*\*

SYMBOL	INTERNAL STATEMENT NUMBERS
E	0022 0009 0014 0016 0017 0018
I	0010 0010 0010 0014 0014 0014 0015 0016 0016 0018 0018 0018
DX	0011 0017
NP	0011 0012 0014 0015 0017 0018
DUM	0003 0022
NED	0011 0017
NTD	0011 0017
NSW	0008 0010 0016
SMD	0032 0009 0010 0016
NDUM	0003 0022 0022 0022
CLEAR	0009
EXPOS	0016
SENSE	0008 0016

LABEL	DEFINED	REFERENCES
1	0004	0011
2	0005	0014
3	0006	0008
4	0007	0010
5	0008	0021
6	0011	0019
10	0016	0015
20	0020	0012
30	0022	0008

Figure 20 SOURCE AND CROSS REFERENCE LISTINGS FOR MAIN PROGRAM DTAPE  
(PAGE 3 OF 3)





value to a negative and to control the difference in log exposure between the points in the sensitometric calibration data. The difference in log exposure between points is computed as  $0.15 * \text{SENSE}$  and consequently if this difference is 0.15, the most likely value, the magnitude of SENSE should be set equal to 1.0. The subsequent cards in this data deck contain density values for each point which are read into the SWD(I) array.

The next two major steps in the program involve reading edge identification parameters, the number of points in the edge data and the increment between points as well as the edge data itself. These data must also be supplied by the user in card deck form. The initial card shown in Figure 21 contains two integer identification parameters, the integer NP equal to the number of points in the edge data and DX, the increment between points. In the Apollo photographic evaluation the identification parameters were set equal to the frame number and a sequential number identifying the edge trace made on that frame of photography. This card is followed by a sequence of cards containing the actual edge data. Provision is made for multiple edge traces in any one edge data set. After the last trace a blank card must be inserted to separate edge data sets. The user is free to add other edge data sets to the input by following this blank card with the new sensitometric calibration data and the associated edge data.

After reading the edge data, the program converts the density values to relative exposure by calling function subprogram EXPOS. The converted edge data are written onto an output tape and the program recycled to read the next edge trace identification parameters and data. This process is repeated until a zero is encountered for the number of points in an edge trace. This identifies the end of the current data set and the program places an end of file on the output data tape. It then recycles to read new sensitometric calibration data for the next data set. If no data is encountered, the program writes a dummy output record as the last file on the output tape and terminates execution.

2.0 Function Subprogram EXPOS - This program is part of the Edge Gradient Spectral Analysis software package. It supports Program DTAPE in the creation of an input data tape for subsequent processing by the main EGSA program. The purpose of this function subprogram is to convert a density value supplied as input into a relative exposure value using sensitometric calibration data. No direct input data must be furnished by the user. The input data is supplied through the calling program. No printed output data is furnished by this program.

Figure 22 is a listing of program EXPOS. The function of the major blocks are identified by the comments included in the coding. The computing path branches depending upon the difference between the input value of density to be converted and the density value of the current point in the sensitometric data. That point is identified by the integer variable I. If these two density values are equal, the exposure for that point is computed and returned to the calling program. If the input density value is greater, the value of I is increased by one and a comparison between the input density and the density value of the next point in the step wedge is made. This process is repeated until the density of the point in the sensitometric calibration is greater than the input density or until the last point of the data is reached. If the latter occurs, the exposure for this last point is computed and returned to the calling program. If a point in the sensitometric calibration data of greater density than the input value is found the program performs a linear interpolation between that point and the previous adjacent point which bracket the value of the input density. If the current point in the sensitometric calibration data has a value which exceeds the input density, a check is made to determine if the density value lies between the current point and the adjacent point and if not, the index I is decreased by one and the comparison made again. This process is repeated until the input density value is bracketed by two points in the sensitometric calibration. Should the input density value be less than the first point in the calibration data (lowest density value) the relative exposure is set equal to one and returned to the calling program.



```

ISN 0010      5 I=I+1
ISN 0011      IF(I.GE.NSW) GO TO 20
ISN 0013      7 IF(D-SWD(I))15,10,5
C
C *****
C * COMPUTE EXPOSURE FOR INPUT DENSITY EQUAL TO DENSITY OF SWD(I) *
C * *****
C
ISN 0014      10 EXPOS=10.**(-DLE*(I-1))
ISN 0015      IF(I.GT.1) I=I-1
ISN 0017      RETURN
C
C *****
C * COMPUTE EXPOSURE FOR INPUT DENSITY BETWEEN SWD(I-1) AND SWD(I) BY *
C * USING LINEAR INTERPOLATION *
C * *****
C
ISN 0018      15 IF(I.EQ.1) GO TO 25
ISN 0020      IF(D.LT.SWD(I-1)) GO TO 30
ISN 0022      EXPOS=10.**(-DLE*(I-1)-(SWD(I)-0)/(SWD(I)-SWD(I-1)))
ISN 0023      I=I-1
ISN 0024      RETURN
C
C *****
C * COMPUTE EXPOSURE FOR INPUT DENSITY BEYOND MAXIMUM WEDGE DENSITY *
C * *****
C
ISN 0025      20 EXPOS=10.**(-DLE*(NSW-1))
ISN 0026      I=I-1
ISN 0027      RETURN
ISN 0028      25 EXPOS=1.0
ISN 0029      RETURN
ISN 0030      30 I=I-1
ISN 0031      GO TO 7
ISN 0032      END

```

Figure 22 SOURCE AND CROSS REFERENCE LISTINGS FOR EXPOS FUNCTION SUBPROGRAM  
(PAGE 2 OF 3)

\*\*\*\*\*FORTRAN CROSS REFERENCE LISTING\*\*\*\*\*

SYMBOL	INTERNAL STATEMENT NUMBERS
D	002 0013 0020 0022
I	0009 0010 0011 0013 0014 0015 0015 0015 0018 0020 0022 0022 0022 0023 0023 0026 0026
DLE	0005 0014 0022 0025
ENT	0004 0004 0006 0008
NSW	0002 0011 0025
SWD	0002 0003 0013 0020 0022 0022 0022
EXPOS	0002 0014 0022 0025 0028
SENSE	0002 0005

LABEL	DEFINED	REFERENCES
5	0010	0013
7	0013	0006 0031
10	0014	0013
15	0018	0013
20	0025	0011
25	0028	0018
30	0030	0020

Figure 22 SOURCE AND CROSS REFERENCE LISTINGS FOR EXPOS FUNCTION SUBPROGRAM  
(PAGE 3 OF 3)

The relative exposures supplied by this program are 1.0 or greater for negative imagery and between 1.0 and 0.0 for positive imagery. The points in the sensitometric calibration data must be provided in order of increasing density.

3.0 Main Program EGSA - This program is part of the Edge Gradient Spectral Analysis software package. It is one of two main programs in the package and is used to compute an Optical Transfer Function (OTF) from edge trace data. The complex OTF is expressed as modulus and phase functions. The edge data is read from an unformatted data tape created by program DTAPE described previously in Section 1.0 of this Appendix. In addition to these data, the user must supply card input which identifies various data options he elects to receive from the program. Both printed and plotted output data are furnished as output options.

Figure 23 is a listing of program EGSA. The function of the major blocks are identified by the comments included in the coding. A macro flow diagram for this program was presented as Figure 3 on page 7 of the main text.

In order to exercise this program, sixteen subprograms are required. Four of these programs are user supplied and are discussed in detail in the following subsections. These include CONVLV which **convolves** an input function with an 11-point differentiating filter, DXSCAL which determines the increment or scale factor (inches/point) for the x-axis of several plots, FORINV which performs an inverse Fourier transform and FOURTR which calculates a Fourier transform of a real input function providing the complex output function as modulus and phase.

Of the twelve remaining subprograms, nine are used to generate graphic output. A brief description of the purpose of each of these programs is presented in Section 2.2 of the main text. Since these programs are peculiar to the data processing facility, no further discussion is provided in this Appendix. Two of the subprograms are IBM supplied FORTRAN IV Library subprograms

```

C *****
C **
C ** MAIN PROGRAM - EGSA (EDGE GRADIENT SPECTRAL ANALYSIS) **
C **
C ** THIS PROGRAM COMPUTES AN OPTICAL TRANSFER FUNCTION (OTF) FROM **
C ** EDGE TRACE DATA. THE COMPLEX OTF IS EXPRESSED AS MODULUS, 'TF', **
C ** AND PHASE, 'PH'. THE EDGE DATA IS READ FROM AN UNFORMATED TAPE, **
C ** DIFFERENTIATED AND FOURIER TRANSFORMED TO COMPUTE THE OTF. INDIVIDUAL **
C ** MODULI CAN BE AVERAGED IF MULTIPLE EDGES ARE CONTAINED IN A SINGLE **
C ** DATA SET. THE INDIVIDUAL EDGES, THEIR DERIVATIVES (OR LINE SPREADS) **
C ** AND RESULTING MODULI ARE PLOTTED IF REQUESTED BY THE USER. OTHER **
C ** OUTPUT OPTIONS INCLUDE PLOTS OF THE AVERAGE MODULUS AND ITS 95% **
C ** CONFIDENCE BAND AND THE AVERAGE LINE SPREAD AND CONFIDENCE BAND AS **
C ** WELL AS PUNCHED CARDS OF THE AVERAGE AND INDIVIDUAL MODULI. **
C **
C **
C ** ** VARIABLE LIST ** **
C **
C ** INPUT VARIABLES **
C **
C ** DX =INCREMENT BETWEEN EDGE DATA POINTS IN MM. MUST REMAIN **
C ** CONSTANT IN ANY ONE DATA SET. **
C ** E =EDGE TRACE DATA (EXPOSURE VALUES). **
C ** FCO =CUTOFF SPATIAL FREQUENCY USED IN SMOOTHING THE LINE **
C ** SPREAD. **
C ** FINV =SPATIAL FREQUENCY INTERVAL REQUESTED BY THE USER IN **
C ** CYCLES/MM. **
C ** FMAX =MAXIMUM SPATIAL FREQUENCY OF OTF DESIRED BY THE USER. **
C ** EXPRESSED IN CYCLES/MM. **
C ** NED =OPTIONAL EDGE TRACE IDENTIFICATION VARIABLE. **
C ** VALUE REPRODUCED ON PLOTTED AND PRINTED OUTPUT. **
C ** NID =OPTIONAL EDGE TRACE IDENTIFICATION VARIABLE. **
C ** NP =NUMBER OF POINTS IN EDGE TRACE DATA; < OR = 900. **
C ** OPTION =ALPHA NUMERIC CHARACTERS IDENTIFYING USER SELECTED **
C ** OUTPUT OPTIONS. **
C **
C ** MAJOR INTERNAL VARIABLES **
C **
C ** ALS =AVERAGE LINE SPREAD FUNCTION. **
C ** ALSM =AVERAGE LINE SPREAD CONFIDENCE BAND (LOWER BOUND). **
C ** ALSP =AVERAGE LINE SPREAD CONFIDENCE BAND (UPPER BOUND). **
C ** ATF =AVERAGE MODULUS OF THE OTF (OR MTF). **
C ** ATFM =AVERAGE MTF CONFIDENCE BAND (LOWER BOUND). **
C ** ATFP =AVERAGE MTF CONFIDENCE BAND (UPPER BOUND). **
C ** DNU =ACTUAL SPATIAL FREQUENCY INTERVAL OF OTF IN CYCLES/MM. **
C ** KNT =COUNTER EQUAL TO THE NUMBER OF EDGE TRACES IN A DATA SET. **
C ** NCF =NUMBER OF POINTS IN DIFFERENTIATED EDGE TRACE. **
C ** NPL =NUMBER OF INDIVIDUAL FUNCTION PLOTS REQUESTED BY USER. **
C ** NPLS =NUMBER OF POINTS IN THE STORED OR UNSMOOTHED LINE SPREAD. **
C ** NPTF =NUMBER OF POINTS IN THE OTF. (=1+NUMBER OF HARMONICS) **
C ** NSL =NUMBER OF POINTS IN THE SMOOTHED LINE SPREAD FUNCTION. **
C ** PH =PHASE OF THE OTF. ON. **
C ** SL =LINE SPREAD FUNCTION (SMOOTHED VALUE IF OPTION REQUESTED). **
C ** SSL ="STORED" OR UNSMOOTHED LINE SPREAD FUNCTION. **
C ** TF =MODULUS OF THE OTF. **

```

Figure 23 SOURCE AND CROSS REFERENCE LISTINGS FOR MAIN PROGRAM EGSA (PAGE 1 OF 12)

```

C **
C **          AUTHORS: R. E. KINZLY
C **                      M. J. MAZUROWSKI
C **          DATE: JULY, 1966
C **          REVISIONS: AUGUST, 1973
C **
C *****
C
ISN 0002      DIMENSION XP(900),ATF(900),ETF(900),SL(900),E(900),CF(900),TF(900)
              *,ATFM(900),ATFP(900),PH(900),DUM(1),XPI(900),XLI(900),OPTION(7),
              *ALS(900),ELS(900),ALSP(900),ALSM(900),XL(900),SSL(900),
              *XS(900),OPT(7),XLE(900)
ISN 0003      LOGICAL LTV(7)/7*.FALSE./
ISN 0004      DATA OPT/4H  E,4H  L,4H  T,4H  SL,4H  AL,4H  AT,4H  PT/
ISN 0005      2000 FORMAT(2F10.0,7A4,F10.0)
ISN 0006      3000 FORMAT(//10X,2I10 / (10X,10F10.3))
ISN 0007      3010 FORMAT(I10)
ISN 0008      3020 FORMAT(F5.3,11F6.3)
ISN 0009      3030 FORMAT(IH1,7X,'--> THE FREQUENCY INTERVAL OF THE OTF HAS BEEN CHA
              *NGED FROM',F6.2,' CYCLES/MM TO', F6.2,' CYCLES/MM,' / 13X,' THE
              *EDGE DATA SET IDENTIFICATION PARAMETERS ARE: NED= ',I10,', NID= ',
              *I10 )
ISN 0010      3032 FORMAT(8X, '--> USER REQUEST FOR AN AVERAGE LINE SPREAD HAS BEEN
              *DELETED.' )
ISN 0011      3034 FORMAT( 8X, '--> USER REQUEST FOR AN AVERAGE MTF HAS BEEN DELEATE
              *D.' )
ISN 0012      CALL PLOTER(1,1,10)
C
C *****
C *
C * READ USER INPUT DATA AND SPECIFIED OPTIONS
C *
C *****
C
ISN 0013      10 READ(5,2000,END=550)FINV,FMAX,(OPTION(I),I=1,7),FCO
ISN 0014      NPL=0
C
C *****
C *
C * INITIALIZE LOGICAL ARRAY 'LTV' DESCRIBING OUTPUT OPTIONS
C *
C *****
C
ISN 0015      DO 16 I=1,7
ISN 0016      16 LTV(I)=.FALSE.
C
C *****
C *
C * SET 'LTV' ARRAY ELEMENTS TO 'TRUE' FOR OPTIONS REQUESTED
C *
C *****
C
ISN 0017      DO 18 I=1,7
ISN 0018      DO 18 J=1,7
ISN 0019      18 IF(OPTION(I).EQ.OPT(J))LTV(J)=.TRUE.

```

Figure 23 SOURCE AND CROSS REFERENCE LISTINGS FOR MAIN PROGRAM EGSA (PAGE 2 OF 12)



```

C *****
C *
C * BEGIN PROCESSING CURRENT EDGE DATA SET
C *
C *****
C
ISN 0021      NPTF=FMAX/FINV+1.5
ISN 0022      DF=FMAX/5.
ISN 0023      20 KNT=0
ISN 0024      CALL CLEAR(ATF(1),ATF(900))
ISN 0025      CALL CLEAR(ETF(1),ETF(900))
ISN 0026      CALL CLEAR(ALS(1),ALS(900))
ISN 0027      CALL CLEAR(ELS(1),ELS(900))
C
C *****
C *
C * READ EDGE DATA PARAMETERS
C *
C *****
C
ISN 0028      50 READ(1,ERR=550,END=400)NED,NID,NP,DX
ISN 0029      IF(NP.EQ.0) GO TO 400
C
C *****
C *
C * READ EDGE DATA FROM TAPE
C *
C *****
C
ISN 0031      NP=NP+12
ISN 0032      READ(1,ERR=550,END=550)(E(I),I=13,NP)
ISN 0033      KNT=KNT+1
C
C *****
C *
C * ADJUST EDGE DATA FOR NUMBER OF POINTS TO BE LOST IN DIFFERENTIATION
C *
C *****
C
ISN 0034      DO 55 I=1,12
ISN 0035      E(I)=E(13)
ISN 0036      55 E(NP+I)=E(NP)
ISN 0037      NP=NP+12
ISN 0038      IF(LTV(I)) CALL SCALE(E,NP,2.,DUMMY,DUMMY,1)
C
C *****
C *
C * DIFFERENTIATE EDGE DATA
C *
C *****
C
ISN 0040      CALL CONVLV(E,NP,DUM,1,CF,NCF,3)

```

Figure 23 SOURCE AND CROSS REFERENCE LISTINGS FOR MAIN PROGRAM EGSA  
(PAGE 3 OF 12)

```

C *****
C *
C * COMPUTE THE NUMBER OF POINTS NEEDED IN LINE SPREAD TO OBTAIN DESIRED *
C * FREQUENCY INTERVAL, 'FINV', FOR OTF *
C *
C *****
ISN 0041      NPLS=1./(FINV*DX)+0.5
C
C *****
C *
C * SET UP X-AXIS INTERVALS AND ARRAYS FOR INDIVIDUAL EDGES AND LINE *
C * SPREADS AND AVERAGE LINE SPREAD IF REQUESTED BY USER *
C *
C *****
ISN 0042      IF(.NOT.(LTV(5).OR.LTV(2).OR.LTV(1))) GO TO 70
ISN 0044      IF(KNT.EQ.1) CALL DXSCAL(2.5,NPLS,DX,DXTI,DXI)
ISN 0046      CALL DXSCAL(2.5,NP,DX,DXTI,DXE)
ISN 0047      DO 60 I=1,NPLS
ISN 0048      XL(I)=(1-I-NPLS/2)*DX
ISN 0049      60 XLE(I)=(I-1)*DXE
ISN 0050      IF(KNT.NE.1) GO TO 62
ISN 0052      DO 61 I=1,NPLS
ISN 0053      61 XLI(I)=(I-1)*DXI
ISN 0054      62 CALL SCALE(XL,NPLS,6.,XM,DI,1)
ISN 0055      70 CALL CLEAR(SL(1),SL(NPLS))
ISN 0056      CALL CLEAR(SSL(1),SSL(NPLS))
C
C *****
C *
C * TEST FOR DECREASING EDGE DATA AND ADJUST IF NECESSARY *
C *
C *****
ISN 0057      IF(E(NP)-E(1).GT.0.) GO TO 72
ISN 0059      DO 71 I=1,NCF
ISN 0060      71 CF(I)=-CF(I)
C
C *****
C *
C * LOCATE THE MAXIMUM VALUE OF THE DERIVATIVE OF THE EDGE DATA *
C *
C *****
ISN 0061      72 BGL=0.0
ISN 0062      DO 80 I=1,NCF
ISN 0063      IF(CF(I).LT.BGL) GO TO 80
ISN 0065      BGL=CF(I)
ISN 0066      LBIG=I
ISN 0067      80 CONTINUE
C
C *****
C *
C * LOCATE AND SMOOTH THE NEGATIVE VALUES IN THE TAILS OF THE *
C * DERIVATIVE, IF ANY *
C *
C *****

```

Figure 23 SOURCE AND CROSS REFERENCE LISTINGS FOR MAIN PROGRAM EGSA (PAGE 4 OF 12)

```

ISN 0068      ITEST=LBIG
ISN 0069      90 ITEST=ITEST+1
ISN 0070      IF(ITEST.GT.NCF-1) GO TO 101
ISN 0072      IF(CF(ITEST).GE.0.) GO TO 90
ISN 0074      CF(ITEST)=(CF(ITEST-1)+CF(ITEST)+CF(ITEST+1))/3.
ISN 0075      IF(CF(ITEST).GE.0.) GO TO 90
ISN 0077      101 IMI=ITEST-1
ISN 0078      ITEST=LBIG
ISN 0079      105 ITEST=ITEST-1
ISN 0080      IF(ITEST.LT.2) GO TO 110
ISN 0082      IF(CF(ITEST).GE.0.) GO TO 105
ISN 0084      CF(ITEST)=(CF(ITEST-1)+CF(ITEST)+CF(ITEST+1))/3.
ISN 0085      IF(CF(ITEST).GE.0.) GO TO 105
ISN 0087      110 ILO=ITEST+1
C
C *****
C *
C * ADJUST THE NUMBER OF POINTS IN THE DERIVATIVE TO INCLUDE THE PORTION *
C * BETWEEN 'ILO' AND 'IMI' AND EQUATE THE LINE SPREADS TO THIS PORTION *
C *
C *****
C
ISN 0088      NCF=IMI-ILO+1
ISN 0089      112 KP=(NPLS+1)/2
ISN 0090      KLO=LBIG-ILO+1
ISN 0091      KHI=IMI-LBIG
ISN 0092      IB=KP-KLO
ISN 0093      IE=ILO-1
ISN 0094      IF((KLO.GT.KP).OR.(KHI.GT.NPLS-KP)) GO TO 114
ISN 0096      DO 113 I=1,NCF
ISN 0097      113 SL(IB+I)=CF(IE+I)
ISN 0098      GO TO 116
ISN 0099      114 IF(KLO.GT.KHI) GO TO 115
ISN 0101      NPLS=2*KHI
ISN 0102      FI=1.0/(FLOAT(NPLS)*DX)
ISN 0103      WRITE(6,3030) FINV,FI,NED,NID
ISN 0104      IF(LTV(5)) WRITE (6,3032)
ISN 0106      LTV(5)=.FALSE.
ISN 0107      IF(LTV(6)) WRITE (6,3034)
ISN 0109      LTV(6)=.FALSE.
ISN 0110      FINV=FI
ISN 0111      GO TO 112
ISN 0112      115 NPLS=2*KLO
ISN 0113      FI=1.0/(FLOAT(NPLS)*DX)
ISN 0114      WRITE(6,3030) FINV,FI,NED,NID
ISN 0115      IF(LTV(5)) WRITE (6,3032)
ISN 0117      LTV(5)=.FALSE.
ISN 0118      IF(LTV(6)) WRITE (6,3034)
ISN 0120      LTV(6)=.FALSE.
ISN 0121      FINV=FI
ISN 0122      GO TO 112
C
C *****
C *
C * NORMALIZE LINE SPREAD AND EQUATE TO "STORED" LINE SPREAD *
C *
C *****

```

Figure 23 SOURCE AND CROSS REFERENCE LISTINGS FOR MAIN PROGRAM EGSA  
(PAGE 5 OF 12)

```

ISN 0123      116 SUM=0.0
ISN 0124      DO 117 I=1,NPLS
ISN 0125      117 SUM=SUM+SL(I)
ISN 0126      DO 118 I=1,NPLS
ISN 0127      SL(I)=SL(I)/SUM
ISN 0128      118 SSL(I)=SL(I)
C
C *****
C *
C * COMPUTE STATISTICS FOR THE AVERAGE LINE SPREAD
C *
C *****
C
ISN 0129      IF(.NOT.LTV(5)) GO TO 130
ISN 0131      DO 120 I=1,NPLS
ISN 0132      ALS(I)=ALS(I)+SL(I)
ISN 0133      120 ELS(I)=ELS(I)+SL(I)*SL(I)
ISN 0134      130 IF(LTV(2))CALL SCALE(SSL,NPLS,2.,DUMMY,DUMMY,1)
ISN 0136      IF(.NOT.(LTV(3).OR.LTV(4).OR.LTV(6))) GO TO 210
C
C *****
C *
C * FOURIER TRANSFORM LINE SPREAD TO OBTAIN THE COMPLEX OPTICAL TRANSFER
C * FUNCTION
C *
C *****
C
ISN 0138      CALL FOURTR(SL,NPLS,DX,TF,PH,DNU,NH)
ISN 0139      IF(.NOT.LTV(4)) GO TO 160
C
C *****
C *
C * COMPUTE THE NUMBER OF HARMONICS FOR THE SMOOTHED LINE SPREAD
C *
C *****
C
ISN 0141      NHM=FCO/FINV
C
C *****
C *
C * APPLY INVERSE TRANSFORM TO OBTAIN THE SMOOTHED LINE SPREAD
C *
C *****
C
ISN 0142      CALL FORINV(TF,PH,NHM,DNU,SL,NSL,DXSLS,1)
ISN 0143      DO 140 I=1,NSL
ISN 0144      140 SL(I)=ABS(SL(I))
ISN 0145      CALL SCALE(SL,NSL,2.,DUMMY,DUMMY,1)
ISN 0146      IF(KNT.NE.1) GO TO 180
ISN 0148      CALL DXSCAL(2.5,NSL,DXSLS,DXSI,DXS)
ISN 0149      DO 150 I=1,NSL
ISN 0150      150 XS(I)=(I-1)*DXS
ISN 0151      160 IF(KNT.NE.1) GO TO 180
ISN 0153      DO 170 I=1,NPTF
ISN 0154      XP(I)=(I-1)*DNU/DF
ISN 0155      170 XPI(I)=2.5*XP(I)*0.5

```

Figure 23 SOURCE AND CROSS REFERENCE LISTINGS FOR MAIN PROGRAM EGSA  
(PAGE 6 OF 12)

```

C *****
C *
C * COMPUTE SUMS RELATED TO THE AVERAGE MTF AND CONFIDENCE BAND
C *
C *****
ISN 0156 180 TF1=TF(1)
ISN 0157 DO 200 I=1,NPTF
ISN 0158 TF(I)=TF(I)/TF1
ISN 0159 ATF(I)=ATF(I)+TF(I)
ISN 0160 200 ETF(I)=ETF(I)+TF(I)**2
C *****
C *
C * PUNCH INDIVIDUAL MTF IF REQUESTED BY USER
C *
C *****
ISN 0161 IF(LTV(7)) WRITE(6,3000)NED,NID,(TF(I),I=1,NPTF)
C *****
C *
C * SCALE INDIVIDUAL MTF FOR PLOTTING
C *
C *****
ISN 0163 DO 205 I=1,NPTF
ISN 0164 205 TF(I)=TF(I)*2.0
C *****
C *
C * PLOT INDIVIDUAL FUNCTIONS AS SPECIFIED BY USER
C *
C *****
ISN 0165 210 IF(MOD(KNT,15).NE.1) GO TO 216
ISN 0167 FNED=NED
ISN 0168 NDS=NED
C *****
C *
C * ESTABLISH THE NUMBER OF INDIVIDUAL FUNCTION PLOTS REQUESTED
C *
C *****
ISN 0169 NPL=0
ISN 0170 DO 212 I=1,4
ISN 0171 212 IF(LTV(I)) NPL=NPL+1
ISN 0173 IF(NPL.EQ.0) GO TO 50
C *****
C *
C * DRAW AXIS FOR EACH TYPE OF INDIVIDUAL FUNCTION PLOT REQUESTED
C *
C *****
ISN 0175 CALL PLOT(0.,0.,0)
ISN 0176 XPL=-8.5

```

Figure 23 SOURCE AND CROSS REFERENCE LISTINGS FOR MAIN PROGRAM EGSA  
(PAGE 7 OF 12)

```

ISN 0177      DO 214 I=1,NPL
ISN 0178      XPL=XPL+8.5
ISN 0179      CALL MGRID(0.5,XPL+5.6,10.,2.5,2.,2.5,1)
ISN 0180      CALL MGRID(0.5,XPL+3.0,10.,2.5,2.,2.5,1)
ISN 0181      CALL MGRID(0.5,XPL+0.4,10.,2.5,2.,2.5,1)
ISN 0182      214 CALL NUMBER(0.15,XPL+4.5,0.14,FMED,-90.,-1)
ISN 0183      XR=0.0
ISN 0184      CALL PLOT(8.5,5.6,-3)
ISN 0185      XOR=0.0
ISN 0186      YOR=0.0
ISN 0187      GO TO 218
ISN 0188      216 IF(NPL.EQ.0) GO TO 50
ISN 0190      YOR=0.0
ISN 0191      XOR=-2.0
ISN 0192      IF(MOD(KNT,5).NE.1) GO TO 218
ISN 0194      XOR=8.0
ISN 0195      YOR=-2.6
ISN 0196      218 CALL PLOT(XOR,YOR+XR,-3)
ISN 0197      XR=0.0
ISN 0198      NPLT=NPL
ISN 0199      IF(LTV(1)) GO TO 230
ISN 0201      221 IF(LTV(2)) GO TO 231
ISN 0203      222 IF(LTV(3)) GO TO 232
ISN 0205      223 IF(LTV(4)) GO TO 233
ISN 0207      230 NPLT=NPLT-1
ISN 0208      CALL LINE(E,XLE,NP,1)
ISN 0209      CALL NUMBER(0.8,2.4,0.07,DXTE,-90.,3)
ISN 0210      KC=1
ISN 0211      GO TO 240
ISN 0212      231 NPLT=NPLT-1
ISN 0213      CALL LINE(SSL,XLI,NPLS,1)
ISN 0214      IF(KNT.EQ.1) CALL NUMBER(0.8,2.4,0.07,DXTI,-90.,3)
ISN 0216      KC=2
ISN 0217      GO TO 240
ISN 0218      232 NPLT=NPLT-1
ISN 0219      CALL LINE(IFS,XPI,NPTF,1)
ISN 0220      IF(KNT.EQ.1) CALL NUMBER(1.8,0.75,.07,FMAX,-90.,1)
ISN 0222      KC=3
ISN 0223      GO TO 240
ISN 0224      233 NPLT=NPLT-1
ISN 0225      CALL LINE(SL,XS,NSL,1)
ISN 0226      IF(KNT.EQ.1) CALL NUMBER(0.8,2.4,.07,DXSI,-90.,3)
ISN 0228      IF(KNT.EQ.1) CALL NUMBER(1.0,2.4,0.07,FCO,-90.,1)
ISN 0230      240 IF(NPLT.EQ.0) GO TO 50
ISN 0232      CALL PLOT(0.,8.5,-3)
ISN 0233      XR=XR-8.5
ISN 0234      GO TO (221,222,223),KC
ISN 0235      400 IF(KNT.EQ.0) GO TO 10
ISN 0237      IF(.NOT.(LTV(5).OR.LTV(6))) GO TO 20

C
C *****
C *
C * CALCULATE AVERAGE MTF AND 95% CONFIDENCE BAND
C *
C *****
C

ISN 0239      IF(.NOT.LTV(6)) GO TO 460
ISN 0241      DO 450 I=1,NPTF

```

Figure 23 SOURCE AND CROSS REFERENCE LISTINGS FOR MAIN PROGRAM EGSA (PAGE 8 OF 12)

```

ISN 0242      ATF(I)=ATF(I)/KNT
ISN 0243      DEV=AMAX1((ETF(I)-KNT*ATF(I)**2),0.0)
ISN 0244      DEV=2*SQRT(DEV/(KNT-1))
ISN 0245      DEV=DEV/SQRT(FLOAT(KNT))
ISN 0246      ATFM(I)=ATF(I)-DEV
ISN 0247      450 ATFP(I)=ATF(I)+DEV
ISN 0248      460 IF(.NOT.LTV(5)) GO TO 490
C *****
C *
C * CALCULATE AVERAGE LINE SPREAD AND 95% CONFIDENCE INTERVAL
C *
C *****
C
ISN 0250      DO 480 I=1,NPLS
ISN 0251      ALS(I)=ALS(I)/KNT
ISN 0252      DEV=AMAX1(ELS(I)-KNT*ALS(I)**2,0.0)
ISN 0253      DEV=2*SQRT(DEV/(KNT-1))
ISN 0254      DEV=DEV/SQRT(FLOAT(KNT))
ISN 0255      ALSPI(I)=ALS(I)+DEV
ISN 0256      480 ALSM(I)=ALS(I)-DEV
ISN 0257      BGL=0.0
ISN 0258      DO 482 I=1,NPLS
ISN 0259      IF(ALSPI(I).LT.BGL) GO TO 482
ISN 0261      BGL=ALSPI(I)
ISN 0262      LBIG=I
ISN 0263      482 CONTINUE
ISN 0264      CALL SCALE(ALSP,NPLS,5.,SLM,DL,1)
ISN 0265      SF=ALSP(LBIG)/BGL
ISN 0266      DO 484 I=1,NPLS
ISN 0267      ALS(I)=ALS(I)*SF
ISN 0268      484 ALSM(I)=ALSM(I)*SF
ISN 0269      IF(.NOT.LTV(6)) GO TO 500
C *****
C *
C * PUNCH AND PRINT AVERAGE MTF IF REQUESTED
C *
C *****
C
ISN 0271      490 IF(LTV(7)) WRITE(6,3000)NDS,KNT,(ATF(I),I=1,NPTF)
ISN 0273      IF(LTV(7)) WRITE(7,3010)NDS
ISN 0275      IF(LTV(7)) WRITE(7,3020)(ATF(I),I=1,NPTF)
C *****
C *
C * PLOT AVERAGE MTF AND CONFIDENCE INTERVAL IF REQUESTED
C *
C *****
C
ISN 0277      DO 495 I=1,NPTF
ISN 0278      ATF(I)=5.0*ATF(I)
ISN 0279      ATFP(I)=5.0*ATFP(I)
ISN 0280      495 ATFM(I)=5.0*ATFM(I)
ISN 0281      CALL PLOT(0.,0.,0)
ISN 0282      CALL PLOT(2.5,6.5,-3)
ISN 0283      CALL AXIS(0.,0.,2*TAU,-2,5.,-90.,0.,DF)
ISN 0284      CALL AXIS(0.,0.,3*TAU,3,5., 0.,0.,0.2)

```

Figure 23 SOURCE AND CROSS REFERENCE LISTINGS FOR MAIN PROGRAM EGSA (PAGE 9 OF 12)

```

ISN 0285      CALL MGRID(0.,-5.,5.,5.,1.,1.,1)
ISN 0286      CALL LINE(ATFP,XP,NPTF,1)
ISN 0287      CALL LINE(ATF,XP,NPTF,1)
ISN 0288      CALL LINE(ATFN,XP,NPTF,1)
ISN 0289      CALL SYMBOL(-1.5,-1.2,0.14,22HAVERAGE OF      SAMPLES,-90.,22)
ISN 0290      CALL NUMBER(-1.5,-2.52,0.14,FLOAT(KNT),-90.,-1)
ISN 0291      CALL NUMBER(5.5,-2.16,0.14,FNED,-90.,-1)
ISN 0292      IF(.NOT.LTV(5)) GO TO 20

C
C *****
C *
C * PLOT AVERAGE LINE SPREAD AND CONFIDENCE INTERVAL IF REQUESTED
C *
C *****
C
ISN 0294      500 CALL PLOT(0.,0.,0)
ISN 0295      CALL PLOT(2.5,7.,-3)
ISN 0296      CALL AXIS(0.,0.,1HX,-1,6.,-90.,XM,DI)
ISN 0297      CALL AXIS(0.,0.,4HL(X),4,5., 0.,SLM,DL)
ISN 0298      CALL PLOT(0.,-6.,-3)
ISN 0299      CALL LINE(ALS,XL,NPLS,1)
ISN 0300      CALL LINE(ALSP,XL,NPLS,1)
ISN 0301      CALL LINE(ALSM,XL,NPLS,1)
ISN 0302      CALL PLOT(0.,6.,-3)
ISN 0303      CALL SYMBOL(-1.5,-1.7,0.14,22HAVERAGE OF      SAMPLES,-90.,22)
ISN 0304      CALL NUMBER(-1.5,-3.02,0.14,FLOAT(KNT),-90.,-1)
ISN 0305      CALL NUMBER(5.5,-2.66,0.14,FNED,-90.,-1)
ISN 0306      GO TO 20

C
C *****
C *
C * TERMINATE EXECUTION
C *
C *****
C
ISN 0307      550 CALL EFPLT
ISN 0308      STOP
ISN 0309      END

```

Figure 23 SOURCE AND CROSS REFERENCE LISTINGS FOR MAIN PROGRAM EGSA (PAGE 10 OF 12)



\*\*\*\*\*FOR TRANSCROSS REFERENCE LISTING\*\*\*\*\*

SYMBOL	INTERNAL STATEMENT NUMBERS	CROSS REFERENCE NUMBERS
E	0002	0032 0035 0036 0036 0038 0040 0057 0057 0208
I	0013	0013 0013 0013 0015 0016 0017 0019 0032 0032 0032 0034 0035 0036 0047 0048 0048 0049 0049 0052
	0053	0053 0059 0060 0060 0062 0063 0065 0066 0096 0097 0097 0124 0125 0126 0127 0127 0128 0128
	0131	0132 0132 0132 0133 0133 0133 0133 0133 0143 0144 0144 0149 0150 0150 0153 0154 0154 0155 0155
	0157	0158 0158 0159 0159 0159 0160 0160 0160 0161 0161 0161 0163 0164 0164 0170 0171 0177 0241
	0242	0242 0243 0243 0246 0246 0247 0247 0250 0251 0251 0252 0252 0255 0255 0256 0256 0258 0259
	0261	0262 0266 0267 0267 0268 0268 0271 0271 0271 0275 0275 0275 0277 0278 0278 0279 0279 0280
J	0018	0019 0019
CF	0002	0040 0060
DF	0022	0154 0283
DI	0054	0296
DL	0264	0297
DX	0028	0041 0044 0046 0048 0102 0113 0138
FI	0102	0103 0110 0113 0114 0121
IB	0092	0097
IE	0093	0097
KC	0210	0216 0222 0234
KP	0089	0092 0094 0094
NH	0138	
NP	0028	0029 0031 0031 0032 0036 0036 0037 0037 0038 0040 0046 0057 0208
PH	0002	0138 0142
SF	0265	0267 0268
SL	0002	0055 0055 0097 0125 0127 0127 0128 0132 0133 0133 0138 0142 0144 0144 0145 0225
TF	0002	0138 0142 0156 0158 0158 0159 0160 0161 0164 0164 0219
XL	0002	0048 0054 0299 0300 0301
XM	0054	0296
XP	0002	0154 0155 0286 0287 0288
XR	0183	0196 0197 0233 0233
XS	0002	0150 0225
ABS	0144	
ALS	0002	0026 0026 0132 0132 0251 0251 0252 0255 0256 0267 0267 0299
ATF	0002	0024 0024 0159 0159 0242 0242 0243 0246 0247 0271 0275 0278 0278 0287
BGL	0061	0063 0065 0257 0259 0261 0265
DEV	0243	0244 0244 0245 0245 0246 0247 0252 0253 0253 0254 0254 0255 0256
DNU	0138	0142 0154
DUM	0002	0040
DXE	0046	0049
OXI	0044	0053
DXS	0148	0150
ELS	0002	0027 0027 0133 0133 0252
ETF	0002	0025 0025 0160 0160 0243
FCO	0013	0141 0228
IHI	0077	0088 0091
ILO	0087	0088 0090 0093
KHI	0091	0094 0099 0101
KLO	0090	0092 0094 0099 0112
KNT	0023	0033 0033 0044 0050 0146 0151 0165 0192 0214 0220 0226 0228 0235 0242 0243 0244 0245 0251
	0252	0253 0254 0271 0290 0304
LTV	0003	0003 0016 0019 0038 0042 0042 0104 0106 0107 0109 0115 0117 0118 0120 0129 0134 0136
	0136	0136 0139 0161 0171 0199 0201 0203 0205 0237 0237 0239 0248 0269 0271 0273 0275 0292
MOD	0165	0192
NCF	0040	0059 0062 0070 0088 0096
NDS	0168	0271 0273
NED	0028	0103 0114 0161 0167 0168
NHM	0141	0142
NID	0028	0103 0114 0161

Figure 23 SOURCE AND CROSS REFERENCE LISTINGS FOR MAIN PROGRAM EGSA (PAGE 11 OF 12)

\*\*\*\*\*FORTRAN CROSS REFERENCE LISTING\*\*\*\*\*

SYMBOL	INTERNAL STATEMENT NUMBERS																			
NPL	0014	0169	0171	0171	0173	0177	0188	0198												
NSL	0142	0143	0145	0148	0149	0225														
DPT	0002	0004	0019																	
SLM	0264	0297																		
SSL	0002	0056	0056	0128	0134	0213														
SUM	0123	0125	0125	0127																
TFI	0156	0158																		
XLE	0002	0049	0208																	
XLI	0002	0053	0213																	
XDR	0185	0191	0194	0196																
XPI	0002	0155	0219																	
XPL	0176	0178	0178	0179	0180	0181	0182													
YOR	0186	0190	0195	0196																
ALSM	0002	0256	0268	0268	0301															
ALSP	0002	0255	0259	0261	0264	0265	0300													
ATFM	0002	0246	0280	0280	0288															
ATFP	0002	0247	0279	0279	0286															
AXIS	0283	0284	0296	0297																
DXSI	0148	0226																		
DXTI	0044	0209																		
DXTI	0044	0214																		
FINV	0013	0021	0041	0103	0110	0114	0121	0141												
FMAX	0013	0021	0022	0220																
FNED	0167	0182	0291	0305																
LBIG	0066	0068	0078	0090	0091	0262	0265													
LINE	0208	0213	0219	0225	0286	0287	0288	0299	0300	0301										
NPLS	0041	0044	0047	0048	0052	0054	0055	0056	0089	0094	0101	0102	0112	0113	0124	0126	0131	0134	0138	
	0213	0250	0258	0264	0266	0299	0300	0301												
NPLT	0198	0207	0207	0212	0212	0218	0218	0224	0224	0230										
NPTF	0021	0153	0157	0161	0163	0219	0241	0271	0275	0277	0286	0287	0288							
PLOT	0175	0184	0196	0232	0281	0282	0294	0295	0298	0302										
SQRT	0244	0245	0253	0254																
AMAXI	0243	0252																		
CLEAR	0024	0025	0026	0027	0055	0056														
DUMMY	0038	0038	0134	0134	0145	0145														
DXSLS	0142	0148																		
FLOAT	0102	0113	0245	0254	0290	0304														
ITEST	0068	0069	0069	0070	0072	0074	0074	0074	0074	0075	0077	0078	0079	0079	0080	0082	0084	0084	0084	
	0084	0085	0087																	
MGR ID	0179	0180	0181	0285																
SCALE	0038	0054	0134	0145	0264															
CONVLY	0040																			
DXSCAL	0044	0046	0148																	
EFPLDT	0307																			
FOR INV	0142																			
FOURTR	0138																			
NUMBER	0182	0209	0214	0220	0226	0228	0290	0291	0304	0305										
OPTION	0002	0013	0019																	
PLOTTER	0012																			
SYMBOL	0289	0303																		

Figure 23 SOURCE AND CROSS REFERENCE LISTINGS FOR MAIN PROGRAM EGSA (PAGE 12 OF 12)

and should be available to most users. The last subprogram, CLEAR, fills a specified block of storage with zeros. If necessary, an equivalent operation can be accomplished by a sequence of do loops in Program EGSA.

The program initially reads user supplied input data on punched cards. The following variables are specified for each data set to be processed:

- FINV - spatial frequency interval desired for output OTF data in cycles/mm
- FMAX - maximum spatial frequency of output OTF data in cycles/mm
- OPTION (7) - alpha-numeric array identifying the types of output data desired by user
- FCO - cutoff spatial frequency in cycles/mm used in smoothing the line spread

Seven output options are available to the user. These are specified by employing one or more of a set of alpha-numeric characters on the punched card input. These characters must be right hand justified in the appropriate field and may be listed in any order. The following characters are allowed:

- E - specifies plots of the individual input edge traces of the data set
- L - specifies plots of the individual line spread data resulting from differentiation of the edge data
- T - specifies plots of the individual MTFs\* resulting from Fourier transformation of the line spread functions
- SL - specifies plots of smooth line spread functions
- AL - specifies a plot of the average line spread and its associated confidence bands
- AT - requests a plot of the average MTF and its confidence bands
- PT - requests the values of the individual and average MTFs

---

\* The Modulation Transfer Function (MTF) is simply the modulus of the complex OTF.

on punched cards and printed values of the average MTF. The values of the average MTF are not punched or printed unless the option for a plot is also specified.

The program sets elements in a logical array, LTV, to true for the options requested if they are properly specified on the input data card. Figure 24 contains an example of this data card where the user has selected plots of the individual MTFs and the average MTF. This input card also specifies the spatial frequency interval as 5 cycles/mm and a maximum spatial frequency of 150 cycles/mm. The cutoff spatial frequency variable is unspecified or equal to zero, indicating that the user has not elected to smooth the line spreads consistent with the deletion of the SL option on the card. The value for the frequency cutoff is, in fact, ignored if this option is not specified.

The next major step in the program is the initialization of parameters and clearing of arrays prior to beginning the actual processing of an edge data set. Identification and data records are then read from an input data tape created using main program DTAPE described previously in Section 1.0. The edge data are then adjusted for the number of points that will be lost due to differentiation. The differentiation is accomplished by subroutine CONVLV described in the next section. Although the current version contains an 11-point, internally specified differentiating filter the dimensions allow a maximum of a 25-point filter. The adjustment in the edge data is commensurate with the maximum size filter.

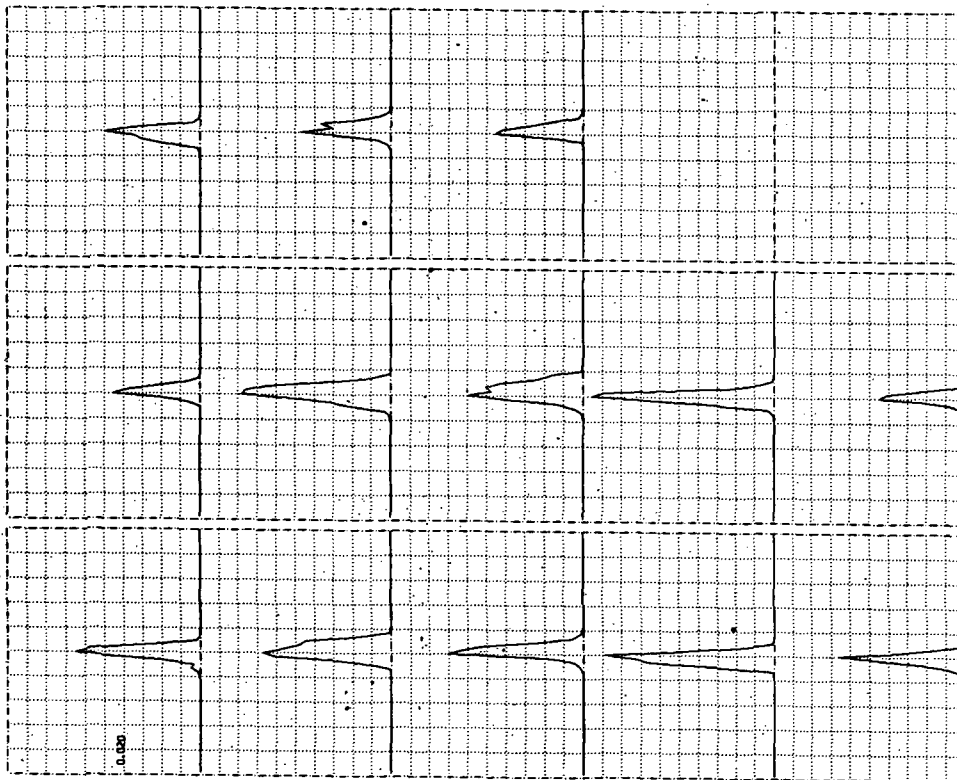
After differentiation the next major step in the execution involves the set-up of x-axis arrays for the output plots of several of the individual functions. This is followed by manipulation of the differentiated edge data including a non-stationary 3-point smoothing of negative values in its tails. Only the non-negative portion of the edge data is retained and equated to the smoothed and unsmoothed line spread functions. The line spread function is then Fourier transformed by calling FOURTR to obtain the modulus and phase functions of the OTF. If the user has requested a smooth line spread, this is computed by truncation of the OTF and subsequent inverse Fourier transformation. The



inverse transformation is accomplished by subroutine FORINV. This calculation is primarily a cosmetic operation and produces no new information about the optical system performance that is not contained in the unsmoothed line spread or the complex OTF.

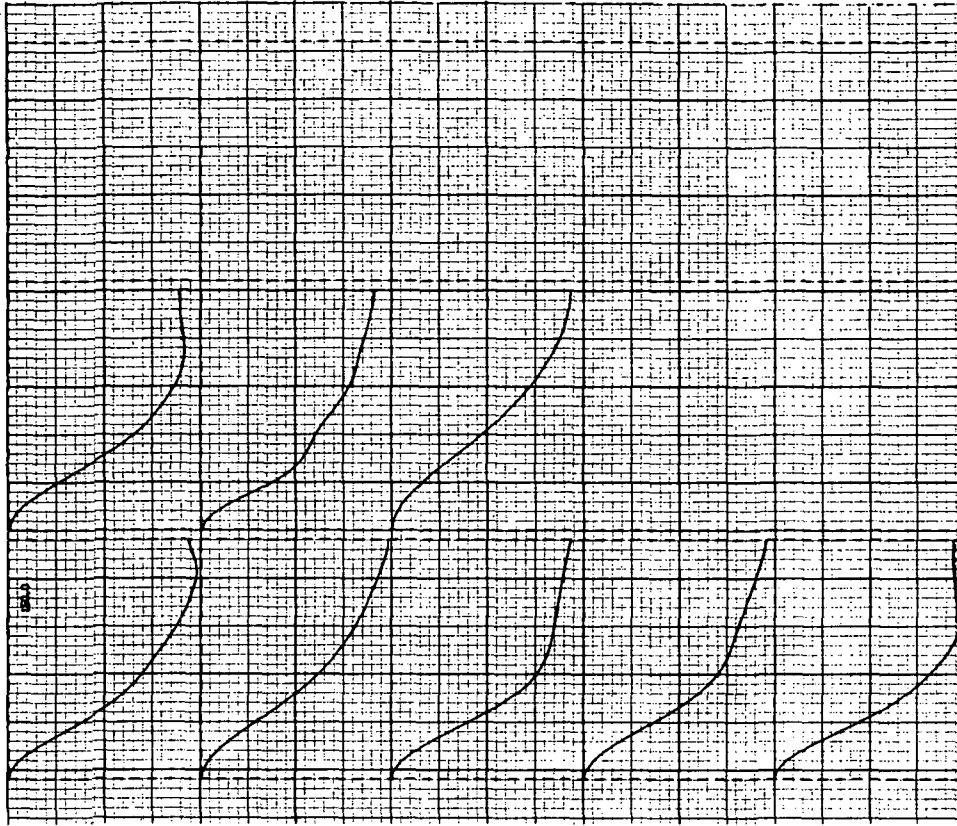
The next steps in the program involve the production of output data as requested by the user. These include punched cards of the individual MTF and plots of the individual edges, line spreads, smoothed line spreads or MTF. The program then recycles to read the next edge trace in the current edge data set and repeats the processing cycle. If no additional edge data exists, the calculation and plotting of the average line spread and a 95% confidence band and the average MTF and its confidence band are accomplished if these options were requested by the user. The program recycles to process the next edge data set, if any, in the same manner. If no additional data sets are identified the program terminates.

Examples of the plots of individual function data generated by the program are presented in Figure 25. Part (a) shows individual line spread functions which resulted during an analysis of the reproduction of Apollo 15 photography and Part (b) shows individual MTF data resulting during a similar analysis of Apollo 17 photography. The original plots fill an 8 x 11 1/2 inch page and were reduced for reproduction here. Similar plots are generated for the individual edges and smoothed line spreads if requested. A number is placed at the bottom of each page which corresponds to the identification number NED specified by the user. In the examples shown this is the number of the frame from which the edge data was acquired. The top left hand plot in both cases also contains a number specifying the total length of the x-axis. In the case of edges, line spreads or smoothed line spreads, this length is expressed in millimeters and for MTFs as spatial frequency in cycles/millimeters. Figure 26 contains an example of an average MTF plot generated from the individual MTFs in Figure 25(b) as part of the evaluation of Apollo 17 photography. The upper and lower curves define the 95% confidence band. The number placed at the top of a plot corresponds to the user specified variable NED and



2219

(a) LINE SPREAD FUNCTIONS



2923

(b) MTFs

Figure 25 EXAMPLE OF INDIVIDUAL FUNCTION PLOTS FROM THE EGSA PROGRAM

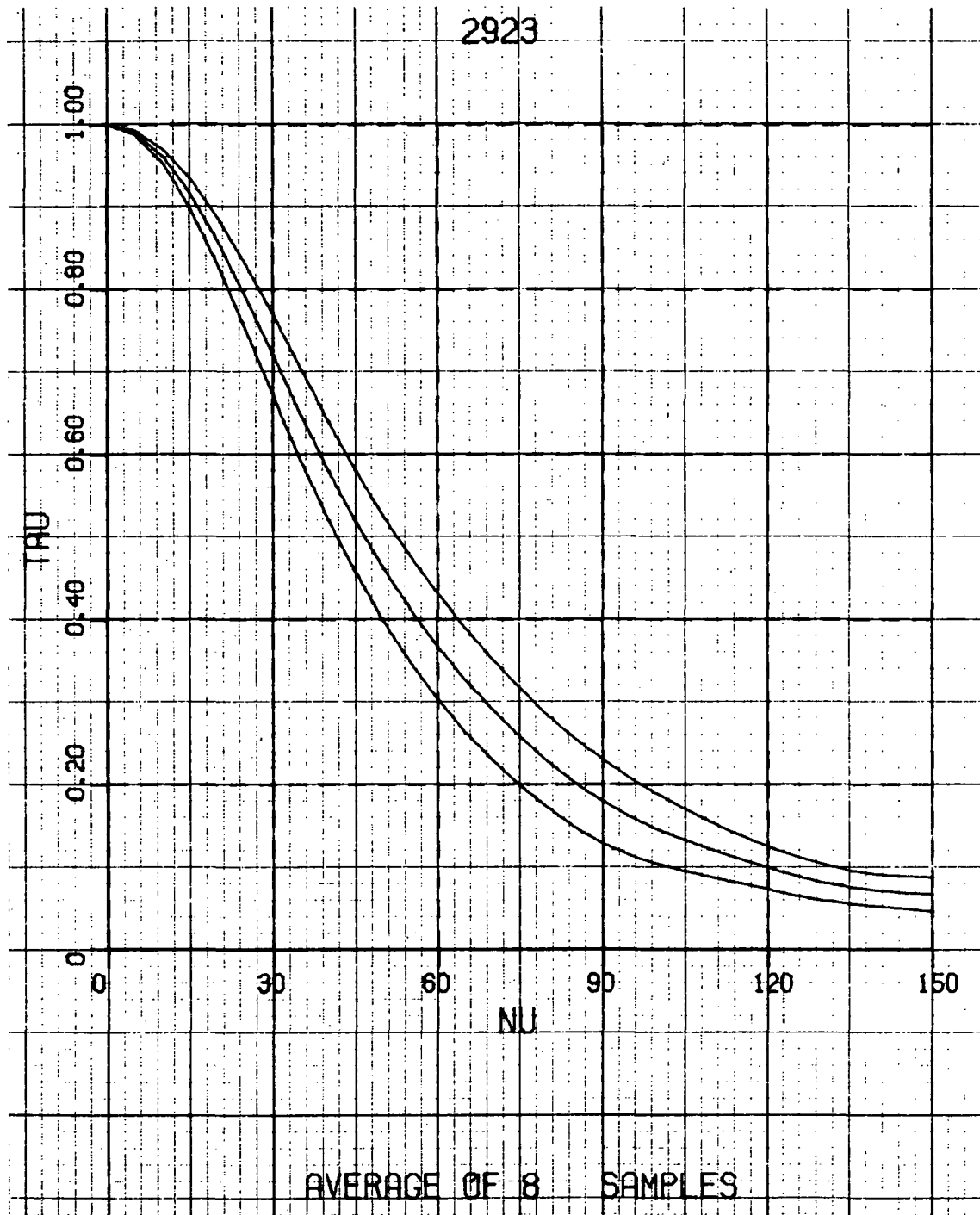


Figure 26 EXAMPLE OF AN AVERAGE MTF PLOT FROM THE EGSA PROGRAM



in this case is equal to the corresponding frame number. The number of individual edge traces which were used to compute the average MTF is indicated on the bottom of the plot. A plot with a similar format is generated for the average line spread function if that output option is requested.

4.0      Subroutine CONVLV - This program is part of the Edge Gradient Spectral Analysis software package. It supports Program EGSA in the calculation of an OTF from edge trace data. The purpose of this subroutine is to differentiate the edge trace data using an internally specified differentiation filter. No direct input data must be furnished by the user. The input data is supplied through the calling program. No printed output data is furnished by this program.

Figure 27 is a listing of subroutine CONVLV. The function of the major blocks are identified by the comments included in the coding. This subroutine has capabilities that are not exploited by the EGSA main program. It can perform the convolution between two input functions or an input function and an internally stored filter. The internal filter options include an 11-point smoothing filter and an 11-point differentiating filter. A maximum of 25-point filters are permitted by the dimension statement and can be inserted by changing the appropriate data statement. The options available in the convolving operation are controlled by the variable KCNTRL as follows:

- 1 - specifies the convolution between two input functions
- 2 - causes the primary input function to be smoothed by the internal filter
- 3 - specifies differentiation of the primary input function by the appropriate internal filter
- 4 - indicates smoothing of the primary input function followed by differentiation.

The computing task branches depending upon the value of the variable KCNTRL. When the specified option involves the convolution between two input functions

```

C *****
C ** SUBROUTINE CONVLV
C **
C ** THIS SUBROUTINE IS PART OF THE EDGE GRADIENT SPECTRAL ANALYSIS
C ** (EGSA) SOFTWARE PACKAGE. THIS PACKAGE ESTIMATES THE OPTICAL
C ** TRANSFER FUNCTION (OTF) FOR ANY OPTICAL SYSTEM USING A SET OF EDGE
C ** DATA MEASURED AT THE OUTPUT OF THE SYSTEM. THIS SUBROUTINE
C ** PERFORMS THE CONVOLUTION BETWEEN TWO INPUT FUNCTIONS OR AN INPUT
C ** FUNCTION AND AN INTERNALLY STORED FUNCTION. THE INTERNAL FUNCTION
C ** OPTIONS INCLUDE AN 11-POINT SMOOTHING FILTER AND AN 11-POINT
C ** DIFFERENTIATING FILTER. UP TO 25-POINT FILTERS CAN BE INSERTED BY
C ** CHANGING THE APPROPRIATE DATA STATEMENTS. THE CONVOLVING OPERATION IS
C ** SPECIFIED BY THE VARIABLE "KCNTRL" AS FOLLOWS:
C **      =1 SMOOTHING OF TWO INPUT FUNCTIONS
C **      =2 SMOOTHING OF INPUT FUNCTION BY INTERNAL FILTER
C **      =3 DIFFERENTIATION OF INPUT FUNCTION BY INTERNAL FILTER
C **      =4 SMOOTHING FOLLOWED BY DIFFERENTIATION
C **
C **      ** VARIABLE LIST **
C **
C ** INPUT VARIABLES
C **      FUN1 =PRIMARY INPUT FUNCTION. RETURNED TO THE CALLING
C **            PROGRAM UNCHANGED. MUST BE DIMENSIONED IN THE CALLING
C **            PROGRAM.
C **      FUN2 =SECONDARY INPUT FUNCTION. MUST HAVE FEWER POINTS THAN
C **            THE PRIMARY INPUT FUNCTION. RETURNED TO THE CALLING
C **            PROGRAM UNCHANGED. MUST BE DIMENSIONED IN THE CALLING
C **            PROGRAM.
C **      KCNTRL =INTEGER FLAG IDENTIFYING THE EXECUTION OPTION SELECTED
C **              BY THE USER.
C **      N1    =NUMBER OF POINTS IN FUN1.
C **      N2    =NUMBER OF POINTS IN FUN2.
C **
C ** OUTPUT VARIABLES
C **      CFUN  =CONVOLVED FUNCTION. MUST BE DIMENSIONED IN THE CALLING
C **            PROGRAM.
C **      NC    =NUMBER OF POINTS IN CFUN.
C **
C **      AUTHORS: R. E. KINZLY
C **              M. J. MAZUROWSKI
C **      DATE:  APRIL, 1966
C **
C *****
C ** SUBROUTINE CONVLV(FUN1,N1,FUN2,N2,CFUN,NC,KCNTRL)
C ** DIMENSION FUN1(1), FUN2(1), CFUN(1), FIL(25), SMF(25), DIF(25)

```

```

ISN 0002
ISN 0003

```

Figure 27 SOURCE AND CROSS REFERENCE LISTINGS FOR SUBROUTINE CONVLV (PAGE 1 OF 4)

```

C *****
C * SMOOTHING FILTER DEFINITION (DATA STATEMENT) *
C *****
ISN 0004 DATA SMF(1),SMF(2),SMF(3),SMF(4),SMF(5),SMF(6),SMF(7),SMF(8),
*SMF(9),SMF(10),SMF(11)/-0.0005616,-0.0005366,C.02395,-0.1049,
*0.2266,0.72108,0.2266,-0.1049,0.02395,-0.0005366,-0.0005616/,
*NSM/11/
C *****
C * DIFFERENTIATING FILTER DEFINITION (DATA STATEMENT) *
C *****
ISN 0005 DATA DIF(1),DIF(2),DIF(3),DIF(4),DIF(5),DIF(6),DIF(7),DIF(8),
*DIF(9),DIF(10),DIF(11)/0.00079365,-0.0099206,0.059524,-0.2381,
*0.833333,0.0,-0.833333,0.2381,-0.059524,0.0099206,-0.00079365/,
*NDF/11/
C *****
C * TRANSFER CONTROL TO THE APPROPRIATE PROGRAM SECTION BASED UPON THE *
C * VALUE OF "KCNTRL" *
C *****
ISN 0006 GO TO (1,20,30,20),KCNTRL
C *****
C * CONVOLVE TWO INPUT FUNCTIONS "FUN1" AND "FUN2" *
C *****
ISN 0007 1 NC=N1+N2+1
ISN 0008 DO 3 I=1,NC
ISN 0009 3 CFUN(I)=0.0
ISN 0010 IF(N1.LT.N2) RETURN
ISN 0011 NCF1 = NC-1
ISN 0012 DO 8 I=2,NCF1
ISN 0013 CFUN(I) = 0.0
ISN 0014 KK = 1
ISN 0015 IF(I.GT.N2+1) KK=I-N2
ISN 0016 KKK = I-1
ISN 0017 IF(I.GT.N1+1) KKK=N1
ISN 0018 DO 7 J = KK,KKK
ISN 0019 L=I-J
ISN 0020 7 CFUN(I) = CFUN(I) + FUN1(J)* FUN2(L)
ISN 0021 8 CONTINUE
ISN 0022 8 RETURN
ISN 0023
ISN 0024
ISN 0025

```

Figure 27 SOURCE AND CROSS REFERENCE LISTINGS FOR SUBROUTINE CONVLV  
(PAGE 2 OF 4)

```

ISN 0026
ISN 0027
ISN 0028
ISN 0029
ISN 0030
ISN 0031
ISN 0032
ISN 0033

C *****
C * SMOOTH INPUT FUNCTION "FUN1" USING THE INTERNAL FILTER "SMF"
C *
C *****
C
20 NFP = NSM
   DO 21 I=1,NFP
21   FIL(I) = SMF(I)
22   LOSS = (NFP-1)/2
   NFM1 = N1-LOSS
   NC = N1
   LP1=LOSS+1
   GO TO 40

C *****
C * DIFFERENTIATE THE INPUT FUNCTION "FUN1" USING THE INTERNAL FILTER "DIF"
C *
C *****
C
30 NFP=NDF
   DO 31 I=1,NFP
31   FIL(I) = -DIF(I)
   IF(KCNTRL.EQ.3) GO TO 22
   DO 33 I=1,N1
33   FUN1(I)=CFUN(I)
   KCNTRL=3
   GO TO 22

C *****
C * PERFORM THE CONVOLUTION OF THE INPUT FUNCTION AND EITHER INTERNAL
C * FILTER
C *
C *****
C
40 DO 48 I=LP1,NFM1
   CFUN(I) = 0.0
   KK = I-LOSS
   KL = I +LOSS
   JI=0
   DO 47 J=KK,KL
   JI=JI+1
47   CFUN(I) = CFUN(I)+FUN1(J)*FIL(JI)
48   CONTINUE
   DO 49 I=1,LOSS
   II=NC-LOSS+I
   CFUN(I)=CFUN(LOSS+I)
+9   CFUN(II) = CFUN(II-1)
   IF(KCNTRL.EQ.4) GO TO 30
   RETURN
   END
ISN 0043
ISN 0044
ISN 0045
ISN 0046
ISN 0047
ISN 0048
ISN 0049
ISN 0050
ISN 0051
ISN 0052
ISN 0053
ISN 0054
ISN 0055
ISN 0056
ISN 0058
ISN 0059

C *****
C * SMOOTH INPUT FUNCTION "FUN1" USING THE INTERNAL FILTER "SMF"
C *
C *****
C
20 NFP = NSM
   DO 21 I=1,NFP
21   FIL(I) = SMF(I)
22   LOSS = (NFP-1)/2
   NFM1 = N1-LOSS
   NC = N1
   LP1=LOSS+1
   GO TO 40

C *****
C * DIFFERENTIATE THE INPUT FUNCTION "FUN1" USING THE INTERNAL FILTER "DIF"
C *
C *****
C
30 NFP=NDF
   DO 31 I=1,NFP
31   FIL(I) = -DIF(I)
   IF(KCNTRL.EQ.3) GO TO 22
   DO 33 I=1,N1
33   FUN1(I)=CFUN(I)
   KCNTRL=3
   GO TO 22

C *****
C * PERFORM THE CONVOLUTION OF THE INPUT FUNCTION AND EITHER INTERNAL
C * FILTER
C *
C *****
C
40 DO 48 I=LP1,NFM1
   CFUN(I) = 0.0
   KK = I-LOSS
   KL = I +LOSS
   JI=0
   DO 47 J=KK,KL
   JI=JI+1
47   CFUN(I) = CFUN(I)+FUN1(J)*FIL(JI)
48   CONTINUE
   DO 49 I=1,LOSS
   II=NC-LOSS+I
   CFUN(I)=CFUN(LOSS+I)
+9   CFUN(II) = CFUN(II-1)
   IF(KCNTRL.EQ.4) GO TO 30
   RETURN
   END

```

Figure 27 SOURCE AND CROSS REFERENCE LISTINGS FOR SUBROUTINE CONVLV  
(PAGE 3 OF 4)



expressed mathematically as

$$f_c(x) = \int_{D_g} f(y) g(x-y) dy \quad (28)$$

the first or primary function in the calling list must contain more points than the second function. If this is not the case the program returns zeros for all points in the convolved function. Equation 28 is implemented as

$$f_{c,i} = \sum_{n=1}^{n_g} f_{i-n_g+n-1} \cdot g_{n_g-n+1}; \quad i=1, \dots, n_f+n_g+1 \quad (29)$$

where  $f_n = 0.0$  for  $n \leq 0$  or  $n \geq n_f+1$  and  $f_c, n_f+n_g+1$   
 $f_{c,1} = 0.0$ . The assumption that the primary function is zero outside of the range of its input should be compensated for in the calling program if it is not valid. This is accomplished by deleting points at the beginning and/or the end of the convolved function array returned to the calling program. Note that the total number of points in the returned function is one more than the sum of the number of points in each individual input function.

When either the differentiation or smoothing operations have been specified Equation 28 is implemented as

$$f_{c,i} = \sum_{n=1}^{n_g} f_{i-n_g+n-1} \cdot g_n; \quad i = \frac{n_g+1}{2}, \dots, n_f - \frac{n_g-1}{2}$$

and

(30)

$$f_{c,1} = f_{c,2} = \dots = f_{c, \frac{n_g+1}{2}}$$

$$f_{c, n_f} = f_{c, n_f-1} = \dots = f_{c, n_f - \frac{n_g-1}{2}}$$

where  $g_n$  is set equal to the appropriate internally stored filter and  $n_g$  is the number of points in the filter array. Note that  $n_g-1$  points, divided equally between the beginning and the end of the convolved function

are not computed by Equation 30 but arbitrarily set to the nearest computable point. Therefore, although  $n_f$  points are returned in the convolved function array, some of these points contain artificial information and may require special treatment in the calling program.

The major difference between Equations 29 and 30, beside the method of treatment of the points at the beginning and end of the convolved function array, is the folding of the secondary function  $g$ . In Equation 29 this folding is accomplished through manipulation of the index while this is not required in Equation 30 because of symmetry properties of the internally stored smoothing and differentiating filters. The secondary function is actually set equal to the negative of the stored differentiating filter in order to accomplish the required folding.

Note that both Equation 29 and Equation 30 do not account for the effect of the differential,  $d_y$ , present in Equation 28. This must be accomplished in the calling program if required.

5.0 Subroutine DXSCAL - This program is part of the Edge Gradient Spectral Analysis software package. It supports Program EGSA in the calculation of the OTF from edge trace data. The purpose of this subroutine is to determine the best scale factor for the x-axis for plots of individual functions requested by the user as an output option. No direct input data must be furnished by the user. The input data is supplied through the calling program. No printed output data is furnished by this program.

No explicit listing of this program is provided since its requirements may depend upon the user's computing facility similar to the other plotting subroutines. Its operation, however, is straightforward and will permit a user to code an equivalent program.

Three calls to DXSCAL are made by Program EGSA. The calling sequence is DXSCAL (XL, NP, DX, DXT, DXI) where

XL = the length of the x-axis in inches (input variable)  
 NP = the number of points in the array to be plotted (input variable)  
 DX = the increment between points (input variable)  
 DXT = the total length of the x-axis in units of DX (output variable)  
 DXI = the scale for plotting in inches/point (output variable)

The purpose of the subrouting is to compute "convenient" values for DXT and DXI. DXI is chosen so that DX/DXI is the smallest number in the set  $(10^m, 1.5 \cdot 10^m, 2 \cdot 10^m, 2.5 \cdot 10^m, 4 \cdot 10^m, 5 \cdot 10^m, 8 \cdot 10^m, m \text{ an integer})$  that makes the data fit an axis of length XL, i.e. subject to the restriction that  $(NP-1) \cdot DXI \leq XL$ . This scaling ensures that the plotted function will fill at least half of the XL inches.

DXI is used directly by Program EGSA to compute an x-axis array for the plots of individual edges, line spreads or smoothed line spreads. The DXT variable is placed on the plots so that the axis can be labeled by user if desired. The units of DX and hence DXT in these cases are mm.

6.0 Subroutine FORINV - This program is part of the Edge Gradient Spectral Analysis software package. It supports Program EGSA in the calculation of an OTF from edge trace data. The purpose of this subroutine is to Fourier transform complex spectra (modulus and phase) to obtain a real output function. Specifically it is used by Program EGSA to compute the smooth line spread function from the truncated OTF. No direct input data must be furnished by the user. The input data is supplied through the calling program. No printed output data is furnished by this program.

Figure 28 is a listing of subroutine FORINV. The function of the major blocks are identified by the comments included in the coding. The algorithm employed in this program is specifically designed for transforming a complex to a real function. The function to be transformed is expressed as modulus and phase functions. Consequently the inverse Fourier transform can be written as

$$I(x) = \int \tau(\nu) e^{-i(2\pi\nu x - \phi(\nu))} d\nu \quad (31a)$$



```

C *****
C SUBROUTINE FORINV
C
C THIS SUBROUTINE IS PART OF THE EDGE GRADIENT SPECTRAL ANALYSIS
C (EGSA) SOFTWARE PACKAGE. THIS PACKAGE ESTIMATES THE OPTICAL
C TRANSFER FUNCTION (OTF) FOR ANY OPTICAL SYSTEM USING A SET OF EDGE
C DATA MEASURED AT THE OUTPUT OF THE SYSTEM. THIS SUBROUTINE
C COMPUTES THE INVERSE FOURIER TRANSFORM USING AN ALGORITHM FOR
C TRANSFORMING A COMPLEX FUNCTION TO A REAL FUNCTION. AN OPTION FOR
C SMOOTHING THE MODULUS OF THE FUNCTION TO BE TRANSFORMED PRIOR TO
C TRANSFORMATION CAN BE SELECTED BY SETTING "KLIP" TO NON-ZERO INTEGER.
C THE FUNCTION TO BE TRANSFORMED IS ASSUMED TO BE COMPLEX AND INPUTED
C AS MODULUS, "TAU", AND PHASE, "PHI", ARRAYS. IF A REAL FUNCTION IS
C SUPPLIED IT IS ASSUMED TO BE SYMMETRIC ABOUT THE FIRST ELEMENT IN THE
C ARRAY. A MAXIMUM OF 500 POINTS IN EACH OF THE INPUT ARRAYS IS
C PERMITTED DUE TO THE DIMENSIONS OF THE INTERNAL WORKING ARRAYS "A,
C B, VCOS AND V SIN".
C
C *****
C ** VARIABLE LIST **
C
C INPUT VARIABLES
C
C TAU =MODULUS OF FUNCTION TO BE TRANSFORMED. RETURNED TO THE
C CALLING PROGRAM UNCHANGED. MUST BE DIMENSIONED IN THE
C CALLING PROGRAM.
C PHI =PHASE OF THE FUNCTION TO BE TRANSFORMED. RETURNED TO
C THE CALLING PROGRAM UNCHANGED. MUST BE DIMENSIONED IN
C THE CALLING PROGRAM.
C NHARM =NUMBER OF "HARMONICS" IN THE FUNCTION TO BE TRANSFORMED.
C MUST BE < OR = 500. THE ACTUAL NUMBER OF POINTS IN
C THE "TAU" AND "PHI" ARRAYS IS ASSUMED TO BE NHARM+1.
C RETURNED TO THE CALLING PROGRAM UNCHANGED.
C UELNU =INTERVAL BETWEEN THE POINTS OF THE FUNCTION ARRAYS.
C USUALLY EXPRESSED IN SPATIAL FREQUENCY AS CYCLES/MM.
C RETURNED TO THE CALLING PROGRAM UNCHANGED.
C KLIP =CONTROL INTEGER FOR MODULUS SMOOTHING FACTOR. IF KLIP=0
C NO SMOOTHING IS EMPLOYED. RETURNED TO THE CALLING
C PROGRAM UNCHANGED.
C
C OUTPUT VARIABLES
C
C FUNC =REAL TRANSFORMED FUNCTION. MUST BE DIMENSIONED IN THE
C CALLING PROGRAM.
C MFUN =NUMBER OF POINTS IN THE TRANSFORMED FUNCTION; EQUAL TO
C 2*NHARM. ( < OR = 1000 )
C DELF =THE INCREMENT BETWEEN POINTS IN THE TRANSFORMED FUNCTION.
C USUALLY EXPRESSED IN MM. CALCULATED AS 1/(2*NHARM*DELFNU).
C
C AUTHORS: R. E. KINZLY
C M. J. HAZUROWSKI
C DATE: JULY, 1966
C *****

```

Figure 28 SOURCE AND CROSS REFERENCE LISTINGS FOR SUBROUTINE FORINV (PAGE 1 OF 4)

```

ISN 0002      SUBROUTINE FORINV(TAU,PHI,NHARM,DELNU,FUNC,NFUN,DELF,KLIP)
ISN 0003      DIMENSION TAU(1),PHI(1),FUNC(1),A(501),B(501),VCOS(251),VSIN(251),
*SIGF(501)
ISN 0004      DATA PI/3.14159265/
ISN 0005      DELF=0.0
ISN 0006      NFUN=0
C
C *****
C *
C * DELETE EXECUTION IF "NHARM" > 500
C *
C *****
ISN 0007      IF(NHARM.GT.500) RETURN
ISN 0009      NHPI = NHARM +1
ISN 0010      HNO = NHARM
ISN 0011      IF(KLIP.EQ.0) GO TO 41
C
C *****
C *
C * DEFINE SINC FUNCTION "SMOOTHING" FACTORS IF REQUESTED BY USER
C *
C *****
ISN 0013      SIGF(1)=1.0
ISN 0014      DO 10 I=2,NHPI
ISN 0015      FI = I-1
ISN 0016      10 SIGF(I)=SIN(PI*FI/HNO)/(PI*FI/HNO)
C
C *****
C *
C * CALCULATE COEFFICIENTS, A(I) AND B(I), FOR THE SINE AND COSINE TERMS
C *
C * OF THE INVERSE TRANSFORM.
C *
C *****
ISN 0017      DO 40 I=1,NHPI
ISN 0018      A(I) = 2.*TAU(I)*COS(PHI(I))*SIGF(I)
ISN 0019      B(I) = 2.*TAU(I)*SIN(PHI(I))*SIGF(I)
ISN 0020      GO TO 43
ISN 0021      41 DO 42 I=1,NHPI
ISN 0022      A(I) = 2.*TAU(I)*COS(PHI(I))
ISN 0023      B(I) = 2.*TAU(I)*SIN(PHI(I))
ISN 0024      43 A(I) = A(I)/2.0
C
C *****
C *
C * SET UP COSINE AND SINE ARRAYS OVER FIRST QUADRANT TO BE USED TO
C * COMPUTE THE INVERSE TRANSFORM.
C *
C *****
ISN 0025      NHCS=NHARM/2 +1
ISN 0026      DO 50 M = 1,NHCS
ISN 0027      VCOS(M) = COS(PI*FLOAT(M-1)/HNO)
ISN 0028      VSIN(M) = SIN(PI*FLOAT(M-1)/HNO)
C

```

Figure 28 SOURCE AND CROSS REFERENCE LISTINGS FOR SUBROUTINE FORINV (PAGE 2 OF 4)



\*\*\*\*\* O R T R A N C R O S S R E F E R E N C E L I S T I N G \*\*\*\*\*

SYMBOL	INTERNAL STATEMENT NUMBERS	CROSS REFERENCE	LISTING
A	0003 0018 0022 0024 0041 0044 0047 0050		
B	0003 0019 0023 0041 0044 0047 0050		
I	0014 0015 0016 0017 0018 0018 0018 0019 0019 0021 0022 0022 0022 0023 0023 0023 0023		
J	0030 0032 0052		
L	0037 0038 0041 0041 0043 0043 0044 0044 0046 0046 0047 0047 0049 0049 0049 0050 0050		
M	0026 0027 0027 0028 0028		
FI	0015 0016 0016		
MO	0036 0037		
NN	0032 0033 0039		
PI	0004 0016 0016 0027 0028		
SN	0039 0041 0044 0047 0050		
CDS	0018 0022 0027		
MND	0010 0016 0016 0027 0028 0053		
NNA	0033 0035		
NMH	0035 0036 0037		
PHI	0002 0003 0018 0019 0022 0023		
SIN	0016 0019 0023 0028		
SUM	0031 0041 0041 0044 0044 0047 0050 0050 0052		
TAU	0002 0003 0018 0019 0022 0023		
DEL	0002 0005 0053		
FUNC	0002 0003 0052		
IABS	0033 0037		
KLIP	0002 0011		
NRUN	0032 0006 0029 0030		
NHCS	0025 0026		
NMP1	0009 0014 0017 0021 0034		
SIGF	0003 0013 0016 0018 0019		
VCS	0003 0027 0041 0044 0047 0050		
VSIN	0003 0028 0041 0044 0047 0050		
DELNU	0002 0053		
FLOAT	0027 0028		
ISIGN	0039		
KSIGN	0038 0040		
NHARM	0002 0007 0009 0010 0025 0029 0032 0036 0037 0038 0043 0046 0049		
FORINV	0002		

LABEL	DEFINED	REFERENCES
10	0016	0014
40	0019	0017
41	0021	0011
42	0023	0021
43	0024	0020
50	0028	0026
51	0041	0040
52	0043	0040
53	0046	0040
54	0049	0040
80	0051	0034 0042 0045 0048
100	0052	0030

Figure 28 SOURCE AND CORSS REFERENCE LISTINGS FOR SUBROUTINE FORINV (PAGE 4 OF 4)

and the discrete representation as

$$I(x) = \sum_{n=-n^*}^{n^*} \tau_n e^{-i(2\pi\nu_n x - \phi_n)} \quad (31b)$$

where  $\tau_n = \tau(\nu_n)$ ,  $\phi_n = \phi(\nu_n)$ , and  $\nu_n = -\nu_{-n}$ . Note that the effect of the differential,  $d\nu$ , in Equation 31a has been suppressed in Equation 31b.

Since  $I(x)$  is real the following conditions must be met

$$\begin{aligned} \tau_n &= \tau_{-n} \\ \phi_n &= -\phi_{-n} \\ \phi_0 &= 0.0 \end{aligned} \quad (32)$$

Expanding Equation 31b and using these conditions we can write the discrete form of the inverse transform as

$$I(x) = \sum_{n=0}^{n^*} A_n \cos(2\pi\nu_n x) + \sum_{n=0}^{n^*} B_n \sin(2\pi\nu_n x) \quad (33)$$

where  $A_0 = \tau_0$ ,  $A_n = 2\tau_n \cos \phi_n$ ,  $B_0 = 0.0$ ,  $B_n = 2\tau_n \sin \phi_n$  and the factor of 2 accounts for the summation over the negative values of  $n$ . For coding purposes this equation is rewritten with summation over positive indices by letting  $i = n+1$ , namely

$$I(x) = \sum_{i=1}^{n^*+1} A_i \cos(2\pi\nu_i x) + \sum_{i=1}^{n^*+1} B_i \sin(2\pi\nu_i x) \quad (34)$$

and the coefficients  $A_i$  and  $B_i$  are appropriately redefined. Letting

$$x_j = (-n^* + j) \Delta_x ; j = 1, \dots, 2n^* \quad (35a)$$

$$\nu_i = (i-1) \Delta_\nu ; i = 1, \dots, n^* + 1 \quad (35b)$$

and requiring that

$$\Delta_x = \frac{1}{2n^* \Delta_\nu} \quad (35c)$$

we can write

$$2\pi V_i X_j = \frac{\pi(i-1)(-n^*+j)}{n^*} \quad (35d)$$

Setting  $m_{ij} = (i-1)(-n^*+j)$  in Equation 35d, the expression for the inverse transform can be written

$$I(X_j) = \sum_{i=1}^{n^*+1} A_i \cos\left(\frac{\pi m_{ij}}{n^*}\right) + \sum_{i=1}^{n^*+1} B_i \sin\left(\frac{\pi m_{ij}}{n^*}\right) \quad (36)$$

The sine and cosine terms need only be computed over the first quadrant, i.e.  $0 \leq m_{ij} \leq \frac{n^*}{2}$  and an appropriate algorithm developed for selecting the appropriate element from this array when the argument lies in another quadrant. Note that  $m_{ij}$  can be less than zero and is accounted for in the coding by changing the sign of the second summation in Equation 36. In order to select the appropriate sine or cosine term and identify the quadrant the initial step involves a transformation of  $m_{ij}$  from the range  $[0, n^{*2}]$  to  $[0, 2n^*]$  through the expression

$$L = m_{ij} - 2n^* \left\lfloor \frac{m_{ij}}{2n^*} \right\rfloor \quad (37)$$

where  $\left\lfloor \quad \right\rfloor$  represents the greatest integer which is less than the enclosed argument. The quadrant can then be subsequently specified by the expression

$$K = \left\lfloor \frac{2L}{n^*} \right\rfloor + 1; \quad 0 \leq K \leq 4 \quad (38)$$

and the value of  $L$  given by Equation 37 appropriately modified depending upon the quadrant to select the appropriate sine and cosine terms to perform the summations indicated by Equation 36.

The restriction of performing an inverse transform from a complex to a real function, i.e. conditions of Equation 32 and the required relationship between the spatial and frequency increments, Equation 35c, permit the development of this algorithm which results in a considerable savings in computation

time. As the listing in Figure 28 indicates the user has an option of smoothing the modulus prior to inverse transformation. If this option is elected the initial step in the program is the setup of the smoothing factors SIGF(I). This is followed by the calculation of the coefficients A(I) and B(I) identified at Equation 33. The sine and cosine factors appearing in Equation 36 are then computed for argument values in the first quadrant and the calculation of both sum terms of the inverse transform of Equation 36 completed. In calculating the sums the program branches depending upon the value of KSIGN which is equivalent to Equation 38. After all the sum terms are computed, the spatial increment is defined using Equation 35c and execution is returned to the calling program.

7.0 Subroutine FOURTR - This program is part of the Edge Gradient Spectral Analysis software package. It supports Program EGSA in the calculation of an OTF from edge trace data. The purpose of this subroutine is to Fourier transform a real input function to obtain a complex spectrum expressed by modulus and phase functions. It is specifically employed by Program EGSA to calculate individual OTF from differentiated edge trace data. No direct input data must be furnished by the user. The input data is supplied through the calling program. No printed output data is furnished by this program.

Figure 29 is a listing of subroutine FOURTR. The function of the major blocks are identified by the comments included in the coding. The algorithm employed in this program is specifically designed for transforming a real to a complex function and results in considerable savings in execution time compared to a more direct implementation. If we assume that the transformed function will be written in terms of a modulus function  $\tau(\nu)$  and a phase function  $\phi(\nu)$  the Fourier transform can be expressed by the equation

$$\tau(\nu) e^{i\phi(\nu)} = \int_{-\infty}^{\infty} I(x) e^{2\pi i \nu x} dx \quad (39a)$$

The corresponding discrete representation is

$$\tau(\nu) e^{i\phi(\nu)} = \Delta x \sum_{n=-n^*}^{n^*} I(x_n) e^{2\pi i \nu x_n} \quad (39b)$$

```

C *****
C ** SUBROUTINE FOURTR
C **
C ** THIS SUBROUTINE IS PART OF THE EDGE GRADIENT SPECTRAL ANALYSIS
C ** (EGSA) SOFTWARE PACKAGE. THIS PACKAGE ESTIMATES THE OPTICAL
C ** TRANSFER FUNCTION (OTF) FOR ANY OPTICAL SYSTEM USING A SET OF EDGE
C ** DATA MEASURED AT THE OUTPUT OF THE SYSTEM. THIS SUBROUTINE
C ** COMPUTES THE FOURIER TRANSFORM OF A REAL FUNCTION USING A SPECIAL
C ** ALGORITHM. THE FUNCTION IS INPUTTED THROUGH THE ARRAY "DATA". A
C ** MAXIMUM OF 1000 POINTS IS PERMITTED DUE TO THE DIMENSION OF THE
C ** INTERNAL WORKING ARRAYS "F, G, A, B, VCOS, AND VSIN".
C **
C ** ** VARIABLE LIST **
C **
C ** INPUT VARIABLES
C **
C ** DATA =FUNCTION TO BE TRANSFORMED. RETURNED TO THE CALLING
C ** PROGRAM WITH EXTRA POINT ADDED IF FURNISHED WITH AN
C ** ODD NUMBER OF POINTS. MUST BE DIMENSIONED IN THE
C ** CALLING PROGRAM.
C ** DX =INCREMENT BETWEEN POINTS IN THE FUNCTION ARRAY. RETURNED
C ** TO THE CALLING PROGRAM UNCHANGED.
C ** NDATA =NUMBER OF POINTS IN DATA ARRAY. RETURNED TO THE CALLING
C ** PROGRAM INCREASED BY ONE IF ORIGINALLY ODD.
C **
C ** OUTPUT VARIABLES
C **
C ** DELNU =INCREMENT BETWEEN POINTS OF THE TRANSFORMED FUNCTION.
C ** USUALLY EXPRESSED AS SPATIAL FREQUENCY IN CYCLES/MM.
C ** CALCULATED AS 1/(2*NHARM*DX) = 1/(NDATA*DX).
C ** NHARM =NUMBER OF "HARMONICS" IN TRANSFORM. CALCULATED AS
C ** NDATA/2. THE NUMBER OF POINTS IN THE TRANSFORM IS
C ** ACTUALLY NHARM*1.
C ** PHI =PHASE OF THE TRANSFORM. MUST BE DIMENSIONED IN THE
C ** CALLING PROGRAM.
C ** TAU =MODULUS OF THE TRANSFORM. MUST BE DIMENSIONED IN THE
C ** CALLING PROGRAM.
C **
C ** AUTHORS: R. E. KINZLY
C ** M. J. MAZURONSKI
C ** DATE: JULY, 1966
C **
C *****
C ** SUBROUTINE FOURTR(DATA,NDATA,DX,TAU,PHI,DELNU,NHARM)
C ** DIMENSION DATA(1),TAU(1),PHI(1),F(501),G(501),A(501),B(501),
C ** *VCOS(251),VSIN(251)
C ** DATA PI/3.14159265/
C ** DELNU=0.0
C ** NHARM=0

```

```

ISN 0002
ISN 0003
ISN 0004
ISN 0005
ISN 0006

```

Figure 29 SOURCE AND CROSS REFERENCE LISTINGS FOR SUBROUTINE FOURTR (PAGE 1 OF 4)





```

ISN 0029 HND = 2*NHARM
ISN 0030 SUM = 0.0
ISN 0031 DO 30 J=1,NHPI
ISN 0032   SUM = SUM + F(J)
ISN 0033   A(I) = SUM/HND
ISN 0034   B(I) = 0.0
ISN 0035 DO 50 I=2,NHARM
ISN 0036   SUMA = 0.0
ISN 0037   SUMB = 0.0
ISN 0038 DO 40 J=1,NHPI
ISN 0039   MD = (I-1)*(J-1)/(2*NHARM)
ISN 0040   L = (I-1)*(J-1)-2*MD*NHARM
ISN 0041   KSIGN = 2*L/NHARM + 1
*****
C *
C * BRANCH ACCORDING TO THE QUADRANT OF THE ARGUMENT
C *
C *
C *
*****
30 GO TO (31,32,33,34),KSIGN
31 SUMA = SUMA+F(J)*VCOS(L+1)
   SUMB = SUMB+G(J)*VSIN(L+1)
   GO TO 40
32 L = NHARM-L
   SUMA = SUMA-F(J)*VCOS(L+1)
   SUMB = SUMB+G(J)*VSIN(L+1)
   GO TO 40
33 L = L-NHARM
   SUMA = SUMA-F(J)*VCOS(L+1)
   SUMB = SUMB-G(J)*VSIN(L+1)
   GO TO 40
34 L = 2*NHARM-L
   SUMA = SUMA+F(J)*VCOS(L+1)
   SUMB = SUMB-G(J)*VSIN(L+1)
40 CONTINUE
50 CONTINUE
   B(I) = SUMA/HND
   C(I) = SUMB/HND
   SUM = 0.0
   DO 60 J=1,NHPI
     SUM = SUM+F(J)*(-1)**(J-1)
     A(NHPI) = SUM/(2.*HND)
     B(NHPI) = 0.C
*****
C *
C * CALCULATE THE MODULUS AND PHASE FUNCTIONS FROM THE REAL AND IMAGINARY
C *
C * TERMS.
C *
C *
*****
DO 70 I=1,NHPI
  TAU(I) = SQRT(A(I)**2+B(I)**2)
  IF(B(I).EQ.0.) GO TO 61
  PHI(I) = ATAN2(B(I),A(I))+PI*(1.-SIGN(1.,B(I)))
  GO TO 70
61 PHI(I)=(1.-SIGN(1.,A(I)))*PI/2.

```

Figure 29 SOURCE AND CROSS REFERENCE LISTINGS FOR SUBROUTINE FOURTR (PAGE 3 OF 4)

ISN 0073.  
ISN 0074  
ISN 0075  
ISN 0076

7C CONTINUE  
DELNU = 1./((FLOAT(NDATA)\*DX)  
RETURN  
END

```

***** F O U R T R A N   C R O S S   R E F E R E N C E   L I S T I N G *****

SYMBOL  INTERNAL STATEMENT NUMBERS
A      0003 0033 0058 0064 0067 0070 0072
B      0003 0034 0059 0065 0067 0068 0070 0070
F      0003 0015 0020 0032 0043 0047 0051 0055 0063
C      0003 0016 0021 0023 0044 0048 0052 0056
I      0035 0039 0040 0058 0059 0066 0067 0067 0067 0070 0070 0070 0072 0072 0072
J      0017 0018 0019 0020 0021 0031 0032 0038 0039 0040 0043 0044 0047 0048 0051 0052 0055 0056 0062
L      0040 0041 0043 0044 0046 0047 0048 0050 0050 0051 0052 0054 0054 0055 0056
M      0026 0027 0027 0028 0028
DX     0002 0074
MD     0004 0027 0028 0070 0072
PI     0004 0027 0028 0070 0072
COS    0025 0027 0028 0029 0033 0058 0059 0064
HND    0019 0020 0021
NHP    0018 0020 0021
PHI    0002 0003 0070 0072
SIN    0028
SUM    0030 0032 0033 0061 0063 0063 0064
TAU    0002 0003 0067
DATA   0002 0003 0012 0012 0015 0020 0020 0021 0021 0022
NHCS   0024 0026
NHPI   0014 0022 0023 0031 0038 0062 0064 0065 0066
SIGN   0070 0072
SQRT   0067
SUMA   0036 0043 0047 0047 0051 0051 0055 0058
SUMB   0037 0044 0048 0048 0052 0052 0056 0056 0059
VCDS   0003 0027 0043 0047 0051 0055
VSIN   0003 0028 0044 0048 0052 0056
ATANZ  0070
DELNU  0002 0005 0074
FLOAT  0027 0028 0074
KSIGN  0041 0042
NDATA  0002 0007 0009 0009 0011 0011 0012 0012 0013 0022 0074
NHARM  0002 0006 0013 0014 0015 0017 0018 0019 0019 0025 0029 0035 0039 0040 0041 0046 0050 0054
FOURTR 0002

```

```

LABEL  DEFINED  REFERENCES
8      0013 0009
10     0021 0017
20     0028 0026
30     0032 0031
31     0043 0042
32     0046 0042
33     0050 0042
34     0054 0042
40     0057 0038 0045 0049 0053
50     0060 0035
60     0063 0062
61     0072 0068
70     0073 0066 0071

```

Figure 29. SOURCE AND CROSS REFERENCE LISTINGS FOR SUBROUTINE FOURTR (PAGE 4 OF 4)

where  $x_0 = 0.0$ ,  $x_{-n} = -x_n$ , and  $\Delta x$  is the increment between points. Note that the effect of the differential,  $d_x$ , is included in the discrete representation. Since  $I(x)$  is real, the summation can be divided into real and imaginary terms, namely

$$\tau(\nu) e^{i\phi(\nu)} = A(\nu) + i B(\nu) \quad (40a)$$

where

$$A(\nu) = \Delta x \sum_{n=-n^*}^{n^*} I(x_n) \cos(2\pi\nu x_n) \quad (40b)$$

and

$$B(\nu) = \Delta x \sum_{n=-n^*}^{n^*} I(x_n) \sin(2\pi\nu x_n) \quad (40c)$$

Through algebraic manipulation the sum over the negative and positive indices can be combined and for coding purposes the summation rewritten using positive indices by letting  $j = n+1$ ;  $j = 1, \dots, n^*+1$ . Equations 40b and 40c become

$$A(\nu) = \Delta x \sum_{j=1}^{n^*+1} F_j \cos(2\pi\nu x_j) \quad (41)$$

$$B(\nu) = \Delta x \sum_{j=1}^{n^*+1} G_j \sin(2\pi\nu x_j) \quad (42)$$

where

$$F_j = \begin{cases} I(0); & j=1 \\ I(x_j) + I(-x_j); & j \geq 2 \end{cases} \quad (43)$$

$$G_j = \begin{cases} 0.0; & j=1 \\ I(x_j) - I(-x_j); & j \geq 2 \end{cases} \quad (44)$$

The modulus and phase of the Fourier transform can be written in terms of the real and imaginary terms by referring to Equation 40a, namely

$$\tau(\nu) = (A(\nu)^2 + B(\nu)^2)^{1/2} \quad (45)$$

$$\phi(\nu) = \tan^{-1} \frac{B(\nu)}{A(\nu)} \quad (46)$$

The arguments of the sine and cosine factors appearing in Equations 41 and 42 are treated in the same fashion described in the previous section, namely setting

$$x_j = (j-1) \Delta x ; j = 1, \dots, n^*+1 \quad (47a)$$

$$\nu_i = (i-1) \Delta \nu ; i = 1, \dots, n^*+1 \quad (47b)$$

and requiring that

$$\Delta x = \frac{1}{2 n^* \Delta \nu} \quad (47c)$$

we can write the argument of the sine and cosine terms as

$$2 \pi \nu_i x_j = \frac{\pi (i-1)(j-1)}{n^*} = \frac{\pi m_{ij}}{n^*} \quad (47d)$$

In this case, however,  $m_{ij}$  is not negative and has values in the range  $[0, n^{*2}]$ . The equations for the real and imaginary terms become

$$A'_i = A_i \Delta \nu = \frac{1}{2n^*} \sum_{j=1}^{n^*+1} F_j \cos\left(\frac{\pi m_{ij}}{n^*}\right) \quad (48)$$

$$B'_i = B_i \Delta \nu = \frac{1}{2n^*} \sum_{j=1}^{n^*+1} G_j \sin\left(\frac{\pi m_{ij}}{n^*}\right) \quad (49)$$

The sine and cosine terms need only be computed over the first quadrant, i.e.  $0 \leq m_{ij} \leq \frac{n^*}{2}$ , and an appropriate algorithm developed for selecting the correct element from this array when the argument lies in another quadrant.

We define

$$L = m_{ij} - 2\pi^* \left[ \left\lfloor \frac{m_{ij}}{2\pi^*} \right\rfloor \right] \quad (50)$$

where  $\left[ \right]$  represents the greatest integer which is less than the enclosed argument. The quadrant is then specified by the expression

$$K = \left[ \left\lfloor \frac{2L}{\pi^*} \right\rfloor + 1 \right] ; \quad 0 \leq K \leq 4 \quad (51)$$

and the value of  $L$  from Equation 50 appropriately modified depending upon the quadrant to select the correct sine and cosine terms from the stored arrays.

The restriction of Fourier transforming a real function to obtain a complex spectrum and the required relationship between spatial and frequency increments, Equation 47c, are required to develop the algorithm described and permit a considerable savings in computation time. The elements of the modulus and phase arrays are calculated using a modified form of Equations 45 and 46, namely

$$\tau_i = (A_i'^2 + B_i'^2)^{1/2} = \Delta_\nu (A_i^2 + B_i^2)^{1/2} \quad (52)$$

$$\phi_i = \tan^{-1} B_i'/A_i' = \tan^{-1} B_i/A_i \quad (53)$$

Note that the phase array is equivalent to that described by Equation 46. However, the modulus has been multiplied by the spatial frequency increment  $\Delta_\nu$  and appropriate action should be taken in the calling program if required.

The first step in the program is to adjust the number of points in the input function array to be even. This is not a requirement of the mathematics but executed only as an interface convenience with subroutine FOUINV described in the previous section. The origin of the spatial axis,

i.e.  $\lambda=0$ , is assumed to be located at the midpoint of the array. The next step in the program is the establishment of the sum and difference arrays expressed by Equations 43 and 44 and subsequently used to calculate the real and imaginary parts of the Fourier transform. This is followed by the computation of the sine and cosine terms within the first quadrant. The real and imaginary terms can then be computed from Equations 48 and 49 and subsequent branching depending upon the quadrant number specified by the variable KSIGN calculated using Equation 51. The sign of the sine and cosine terms are adjusted in accordance with the quadrant number and selected from the corresponding array using the transformed value of  $L$  (c.f. Equation 50). The final step in the program is the calculation of the modulus and phase arrays using Equations 52 and 53 and the definition of the spatial frequency increment based upon Equation 47c. Execution is then returned to the calling program.

8.0 Main Program TONEQ - This program provides data which can be used to evaluate the tone quality of a photograph. It computes the gain achieved as a function of object contrast and average exposure level. Input data on punched cards must be supplied by the user. Printed values of the gain factors are furnished in tabular form by the program.

Figure 30 is a listing of TONEQ. The function of the major blocks are identified by the comments included in the coding. In order to exercise this program two subprograms that are part of the Calspan Corporation Program Library are required. Detailed descriptions of these programs will not be furnished in this Appendix, however, the user is likely to have equivalent programs available in the library at his computing facility. CLEAR fills each byte of a specified block of storage with zeros. This operation can be accomplished by substituting a sequence of do loops in the TONEQ program. SPLN46 calculates a set of interpolation functions for a set of input points. These interpolation functions produce a continuous function that has a continuous first and second derivative over the interval spanned by the input data. The function tends to avoid waviness often encountered by other curve fitting techniques. The input data points must be reasonably accurate or







```

C *****
C *
C * OBTAIN SPLINE INTERPOLATION FUNCTIONS FOR SENSITOMETRIC CALIBRATION
C * DATA AND PRINT OUT COEFFICIENTS IN TABULAR FORM
C *
C *****
C
ISN 0023
ISN 0024
ISN 0025
C *****
C *
C * CALL SPLN46(J,X1,DUM,DUM,DUM,X,D,NSW,C1,C2,C3)
C * WRITE(6,1) (TITLE(N),N=1,17)
C * WRITE(6,5) (X(J),D(J),C1(J),C2(J),C3(J),J=1,NSW)
C *****
C *
C * COMPUTE GAIN FACTORS AT AVERAGE EXPOSURE LEVELS EQUAL TO EACH POINT
C * IN THE CALIBRATION DATA AND THREE OBJECT CONTRAST LEVELS
C *
C *****
C
ISN 0026
ISN 0027
ISN 0028
ISN 0029
ISN 0030
ISN 0031
ISN 0032
ISN 0033
ISN 0034
ISN 0035
ISN 0036
ISN 0037
ISN 0038
ISN 0039
ISN 0040
ISN 0041
ISN 0042
ISN 0043
C *****
C *
C * PRINT OUT GAIN FUNCTIONS IN TABULAR FORM
C *
C *****
C
ISN 0044
ISN 0045
ISN 0046
ISN 0047
ISN 0048
C *****
C *
C * TERMINATE EXECUTION
C *
C *****
C
ISN 0049
ISN 0050
C *****
C *
C * 50 STOP
C * END
C *****

```

Figure 30 SOURCE AND CROSS REFERENCE LISTINGS FOR MAIN PROGRAM TONEO (PAGE 3 OF 4)

\*\*\*\*\* F O R T R A N C R O S S R E F E R E N C E L I S T I N G \*\*\*\*\*

SYMBOL	INTERNAL STATEMENT NUMBERS	CROSS REFERENCE LISTING
U	0002 0003 0015 0023 0025 0037 0042	
I	0044 0044 0044 0045 0046 0047	
J	0025 0025 0025 0025 0025 0025	0025 0027 0028 0043 0043 0044 0044 0044 0044 0044 0047 0047 0047 0047
N	0011 0011 0011 0015 0015 0015	0021 0022 0022 0024 0024 0036 0036 0041 0041 0046
X	0002 0003 0012 0022 0023 0025 0037 0042	
C1	0002 0003 0023 0025 0037 0042	
C2	0002 0003 0023 0025 0037 0042	
C3	0002 0003 0023 0025 0037 0042	
DD	0002 0003 0012 0043 0047	
DH	0037 0043	
DL	0042 0043	
DX	0019 0020 0022 0026 0026 0029	
NH	0033 0034 0034 0036 0037 0037	0037 0037
NI	0029 0033 0038	
NL	0038 0039 0039 0041 0042 0042	0042 0042
M1	0011 0013 0013 0020 0020	
XD	0028 0029 0030 0030 0036 0041	
XM	0036 0037 0037 0037	
XL	0041 0042 0042 0042	
XX	0046 0047	
X1	0016 0017 0020 0020 0022 0023	
ABS	0026	
DEL	0003 0004 0028 0043 0044	
DUM	0023 0023 0023	
NSW	0011 0015 0021 0023 0025 0032 0034 0034 0045	
CLEAR	0012	
SENSE	0011 0013 0017 0017 0019 0030	
TITLE	0003 0011 0024 0044	
SPLN#6	0023	

Figure 30 SOURCE AND CROSS REFERENCE LISTINGS FOR MAIN PROGRAM TONEQ (PAGE 4 OF 4)

smooth since the subroutine forces the function to pass through these points and consequently cannot perform any smoothing of the input data. The interpolation functions are piecewise cubic and yield about the same curve one would obtain by forcing a flexible straight edge (a spline) through the set of input points. For additional information about spline interpolation procedures the reader is referred to DeBoor, Carl; Bicubic Spline Interpolation Journal of Mathematics and Physics, Vol. 41, No. 3, March 1962, pp. 212. Subroutine SPLN46 is used by this program to obtain interpolation functions for the sensitometric calibration data.

The initial step in the program is to read user input data which specifies the number of points in the sensitometric calibration data, the sense of the imagery (i.e. positive or negative) and the number from 1 to 21 of the first step in the calibration data. The user may also include a title to identify the photograph under evaluation if he so desires. Figure 31 shows a typical input data set. This example is taken from that used in the evaluation of the Apollo 17 panoramic photography. The first two cards compose the initial data block and the first card indicates that there are 14 points in the sensitometric calibration data measured on a negative image. The number of the step for the first data point is 8. The fact that the magnitude of the variable SENSE is 1.0 indicates that the difference in relative log exposure between points in the sensitometric calibration is equal to 0.15. The optional identification label indicates that the data were obtained from a Direct Negative roll of Apollo 17 panoramic photography that contains Frame 3111. An optional identification tag can be placed in columns 73 through 80 to aid in data set identification. The figure shows a second data block for another photograph; in this case a Third Generation Positive copy of the same frame. This can be followed by additional data blocks for each photograph under evaluation.

The next step in the program is the input of the sensitometric calibration value (density values). This data is contained on the second card of the first data block and the second and third cards in the second data



block. The program then calculates an array of relative log exposure values  $X(N)$  in the range 0.0 to 3.0 that correspond to the input density values. By calling subroutine SPLN46 the coefficients of the spline interpolation functions for the sensitometric calibration data are obtained and subsequently printed out in tabular form. Figure 32 shows the printout generated for the first data block of Figure 31. The next step in the program involves the computation of the gain factors at an average exposure level equal to that of each point in the calibration data and three different object contrast levels. The levels of object contrast are specified by a data statement at the beginning of the program. Once the calculations have been completed the gain factors are printed out in tabular form. An example of this printout is included in Figure 32 for the first data block identified in Figure 31. The program then recycles to process the next data block if one is supplied by the user. If not, the program terminates execution.

D-LOGE RESPONSE CURVE SPLINE REGRESSION

APOLLO 17 PAN - FRAME 3111 - DIRECT NEG (2N)

F31112N

LOGE	DENSITY	*****	COEFFICIENTS	*****
1.05	0.28	0.0832	0.0000	2.2274
1.20	0.30	0.2336	1.0023	0.7149
1.35	0.36	0.5825	1.3241	0.8384
1.50	0.48	1.0363	1.7014	4.8206
1.65	0.69	1.8721	3.8707	-11.2321
1.80	1.02	2.2752	-1.1837	4.5509
1.95	1.35	2.2272	0.8642	-6.9708
2.10	1.68	2.0160	-2.2726	-0.3734
2.25	1.93	1.3090	-2.4406	2.5386
2.40	2.08	0.7482	-1.2982	2.0702
2.55	2.17	0.4984	-0.3666	-1.9309
2.70	2.23	0.2581	-1.2355	2.6912
2.85	2.25	0.0691	-0.0245	0.0544
3.00	2.26	0.0654	0.0	0.0

TONE QUALITY EVALUATION PROGRAM

APOLLO 17 PAN - FRAME 3111 - DIRECT NEG (2N)

F31112N

RELATIVE EXPOSURE (DELTA LOGE =)	LOW CONTRAST (0.0414)	MID CONTRAST (0.1139)	HIGH CONTRAST (0.7782)
11.220	0.08	0.09	0.39
15.849	0.23	0.24	0.46
22.387	0.58	0.59	0.78
31.623	1.04	1.05	1.20
44.668	1.87	1.86	1.58
63.095	2.27	2.26	1.85
89.125	2.23	2.22	1.90
125.892	2.01	2.00	1.70
177.827	1.31	1.31	1.36
251.187	0.75	0.76	0.97
354.812	0.50	0.50	0.59
501.185	0.26	0.26	0.34
707.942	0.07	0.07	0.20
999.994	0.07	0.07	0.11

Figure 32 EXAMPLE OF TONEQ PROGRAM PRINTED OUTPUT